HIV-1 GP120 MEDIATED NEURONAL DEREGULATION: UNRAVELING THE MOLECULAR MECHANISMS INVOLVED

A Dissertation
Submitted to
the Temple University Graduate Board

In Partial Fulfillment
of the Requirements for the Degree
DOCTOR OF PHILOSOPHY

---

by
Jenny Shrestha
July 2016

Examining Committee Members:

Bassel E. Sawaya PhD, Advisory Chair, Department of Neurology, Pharmacology and Fels Institute of Cancer Research and Molecular Biology
Thomas Rogers PhD, Examining Chair, Center for Inflammation, Translational and Clinical Lung Research, Pharmacology and Fels Institute for Cancer Research and Molecular Biology
George Smith PhD, Department of Neuroscience and Shriners Hospitals Pediatric Research Center
Jonathan Soboloff PhD, Medical Genetics and Molecular Biology and Fels Institute of Cancer Research and Molecular Biology
Lynn Kirby PhD, External Member, Department of Anatomy and Cell Biology and Center for Substance Abuse Research

ABSTRACT

The advancement in combinatory antiretroviral therapy (cART) has granted people with HIV-1 an improved lifespan by decreasing the likelihood of AIDS-defining illnesses. People diagnosed early in their infection and undergo cART can keep the virus suppressed and live as long as their HIV-negative peers. As of 2015, more than 50% of people living with HIV in the United States are aged 50 and older. With improved life expectancy, individuals living with long-term HIV infection exhibit many clinical characteristics commonly observed in aging such as: cardiovascular disease, lung disease, certain cancers, HIV-Associated Neurocognitive Disorders (HAND), and liver disease (including hepatitis B and hepatitis C), among others. Regarding neurocognitive disorders, HIV/AIDS patients seem to have **learning deficits** and **working memory impairment** such as easy forgetfulness and slowness in action, difficulties in concentration, planning, and multitasking in the condition of having a relatively uneventful and well-controlled clinical course with low HIV viral titers. Neuropsychological studies have disclosed cognitive impairment in a substantial (15–50%) proportion of patients, including learning and working memory deficits which may affect their quality of life, adherence to treatment and ultimately result in increased comorbidity.

Studies have described cAMP responsive-element binding **(CREB)-1** protein - involved in mitochondrial biogenesis, long-term memory and synaptic plasticity - as a key player in protecting neurons and preventing neurodegeneration. However, loss of CREB protein expression and phosphorylation leads to the development of neurocognitive impairments such as learning deficit and working memory alteration. CREB performs its functions by regulating several genes such, PGC-1α and BDNF being the few (key

regulators of mitochondrial bioenergetics, synaptic plasticity and long-term memory, respectively). In here, we have shown that exposure of neuronal cells and animals to HIV-1 gp120 protein decreases expression level of phosphorylated CREB and inhibits its function. Therefore, it will lead to altered neuronal communication and mitochondrial functions. Using pharmacological reagent – rolipram (activates cAMP by inhibiting PDE-4), we were able to reverse the effect of Gp120. Rolipram treatment restored CREB expression and functions altered by gp120.

During my graduate years, using *in vitro* and *in vivo* studies, I was able to determine the mechanisms used by gp120 leading to the loss of; i – energy metabolism; ii – synaptic plasticity; and iii – long-term memory. We partially determined the relation between gp120, CREB and downstream targets of CREB (PGC-1α and/or BDNF). This approach allowed me to further understand the relation between gp120 and mitochondria as well as between gp120 and neuronal communication.

Overall, our study has marked a milestone with regards to understanding the role of gp120 and learning deficiency. Our study mechanistically unravels for the first time the relation between HIV-gp120 protein and development of cognitive disorders such as declarative memory impairment that is commonly observed in HIV-1 patients as well as in aged people. Using an intervention (rolipram) approach, to prevent CREB loss of functions, will help establish new therapeutic strategy (high throughput screening) to mitigate cognitive impairments associated with HIV-1 infection in HIV/AIDS patients.

ACKNOWLEDGMENTS

I would like to thank my mentor Dr. Bassel E. Sawaya who gave me the opportunity to work in his laboratory and directed this work. I thank him for his guidance throughout my Ph.D. career. His words of wisdom and encouragement have helped me become a better individual. He always gave me the sense of independence by allowing me to design my own experiments and explore the field and guided me as needed to become a better scientist.

I am grateful towards my committee members: Drs. Thomas Rogers, Jonathan Soboloff and George Smith who have helped me with my project with their questions and suggestions.

I would like to thank Dr. Lynn Kirby who honored me by accepting to be the external examiner for my thesis committee.

I would also like to thank all former and current members from the Sawaya lab who have helped me with their suggestions and ideas especially Dr. Asen Bagashev who was always there to answer my questions and cheer my moral. I would also like to thank Dr. Ruma Mukherjee who helped me establish my research.

A special thanks to all our collaborators for their contributions (ideas, data, materials) especially Dr. Jeannie Chin (Baylor School of Medicine); Dr. Marcus Kaul (UCSD), Dr. Italo Mocchetti (Georgetown University), Dr. Robert Hooper (Temple University – Soboloff Lab) and Dr. Saul Villeda (UCSF).

I am very thankful towards my parents who believed in me and supported me all my life with all my decisions. They have always encouraged me to achieve my goals. To my sister and her family, I cannot thank you enough. You were always there for me and your kids bring me such joy and happiness.

Finally, I am thankful to Jeff, my other half, who despite all my complaints and long commute, was there to support me, listen to me and encourage me throughout this graduate school journey.

TABLE OF CONTENTS

Page

LIST OF TABLES

LIST OF FIGURES

Figures Page

LIST OF ABBREVIATIONS

3’UTR	3’untranslated region
ADP	Adenosine diphosphate
AIDS	Acquired immunodeficiency syndrome
ANI	Asymptomatic neurocognitive impairment
ATP	Adenosine triphosphate
BBB	Blood brain barrier
BDNF	Brain derived neurotrophic factor
BMEC	Brain microvascular endothelial cell
BSA	Bovine serum albumin
CA	Capsid
CaMK	Calmodulin Kinase
CaN	Calcineurin
cART	Combinatory antiretroviral therapy
CCCP	carbonyl cyanide m-chlorophenylhydrazone
CCR5	C-C chemokine receptor type 5
cDNA	Complementary DNA
CDK	Cyclin dependent kinase
CNS	Central nervous system
COX	Cytochrome c oxidase
CR	Caloric restriction
CREB	cAMP response element binding protein
CXCR4	C-X-C chemokine receptor type 4
DAPI	4',6-diamidino-2-phenylindole
DNA	Deoxyribonucleic acid
DNMT	DNA methyltransferase
Drp-1	Dynamin related protein 1

E2F3	E box factor 3
EAAT	Excitatory amino acid transporter 2
EMRE	Essential MCU regulator
EPSP	Excitatory post synaptic potential
ER	Endoplasmic reticulum
ETC	Electron transport chain
FIS-1	Mitochondrial fission 1
FPLC	Fast performance liquid chromatography
GAPDH	Glyceraldehyde 3-phosphate dehydrogenase
GFAP	Glial fibrillary acidic protein
Gp120	Glycoprotein 120
HAD	HIV associated dementia
HAND	HIV associated neurodegenerative disease
HIV	Human immunodeficiency virus
HIVE	HIV encephalitis
IL	Interleukin
IMM	Inner mitochondrial membrane
KIF	Kinesin family
LD	Learning deficiency
LTD	Long term depression
LTP	Long term potentiation
MA	Matrix
MAP-2	Microtubule-Associated Protein 2
MeCP2	Methyl CPG binding protein 2
MCU	Mitochondrial calcium uniporter
MCUR	Mitochondrial calcium uniporter receptor

Mfn	Mitofusin
MHC	Major histocompatibility complex
MICU	Mitochondrial calcium uptake
MIP	Macrophage inflammatory protein
MIRO	Mitochondrial Rho GTPase
miRNA	Micro RNA
MMP	Mitochondrial membrane potential
MND	Mild neurocognitive disorder
MnSOD	Manganese superoxide dismutase
MOI	Multiplicity of infection
MRI	Magnetic resonance imaging
mRNA	Messenger RNA
mtDNA	Mitochondrial DNA
NAD	Nicotinamide adenine dinucleotide
NC	Nucleocapsid
ND5	NADH dehydrogenase 5
NLS	Nuclear localization signal
NMDAR	N-methyl-D-aspartate receptor
NOS	Nitric oxide synthase
NPC	Neural progenitor cells
NTR	Neurotrophin receptor
OMM	Outer mitochondrial membrane
OPA	Optic atrophy
PAGE	Polyacrylamide gel electrophoresis
PBS	Phosphate buffered saline
PD	Parkinson's disease
PDE	Phosphodiesterase

PGC-1α	Peroxisome proliferator-activated receptor-γ coactivator – 1 alpha
PIC	Pre-integration complex
PKA	Phosphokinase A
PKC	Phosphokinase C
PNS	Peripheral nervous system
PRO	Protease
PSD-95	Postsynaptic density protein 95
RA	Retinoic acid
RFP	Red fluorescent protein
RNA	Ribonucleic acid
ROS	Reactive oxygen species
RRE	Rev Response element
RSV	Rous sarcoma virus
RT	Reverse transcriptase
RT-PCR	Reverse transcription- polymerase chain reaction
RyR	Ryanodine receptor
SDF-1α	Stromal cell derived factor 1 alpha
SDS	Sodium dodecyl sulfate
SOCe	Store operated calcium entry
SIRT	Sirtuin
Tg	Thapsigargin
TJ	Tight junction
TNF	Tumor necrosis factor
TRAK	Trafficking kinesin protein
WMI	Working memory impairment

CHAPTER 1

BACKGROUND

HIV-1

Officially identified in 1982, the human immunodeficiency virus type 1 (HIV-1) is a lentivirus that belongs to the family of retroviruses. HIV-1 has been shown to claim the lives of millions of people. According to the world health organization, 36.9 million people live with HIV/AIDS worldwide. HIV has been characterized into two subtypes: HIV-1 and HIV-2 based on their origin, prevalence, infectivity and virulence. HIV-1 is the most common infection found in the world which could lead to progressive failure of immune system and cause AIDS (Donnelly, Leisenring, Kanki, Awerbuch, & Sandberg, 1993; Kanki, Hopper, & Essex, 1987). HIV-2 exist only in western Africa and has low infectivity (Kannangai, David, & Sridharan, 2012).

HIV-1 Structure and Genome

HIV is relatively a small virus (9.8 kb in size) and contains nine genes (Figure 1): gag, *pol*, and *env* (common genes); *tat* and *rev* (structural genes); and *vif, vpr, vpu and nef* (accessory genes).

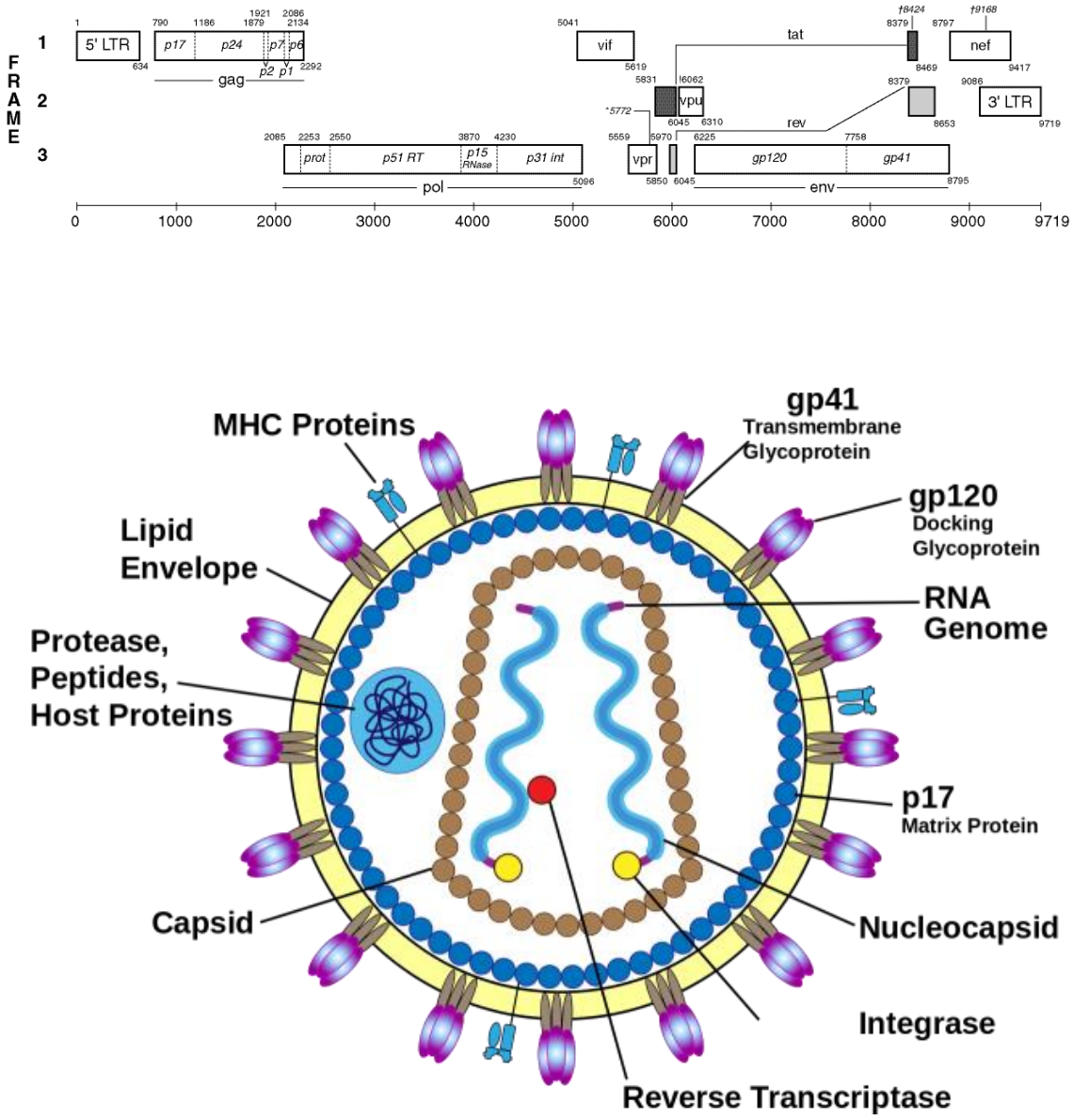

Figure 1. Representation of the HIV structure and genes (Sources: HIV sequence database and Wikimedia common)

A. Common Genes - These genes are involved in the viral-cell association, viral entry, viral assembly and maturation.

A (1) Gag (Group specific antigen): The *gag* gene is first transcribed to a 55kDa precursor polypeptide (p55) that is required for the viral assembly. With the help of the HIV-1 protease (PR), Gag precursor is then cleaved into four small mature proteins: p17 matrix (MA), p24 capsid (CA), p7 nucleocapsid (NC) and p6. The gag precursor and the major Gag proteins are highly conserved in all the retroviruses. P1 and P2 are the small spacer proteins also generated from the cleavage of Gag precursor but their roles are not well defined (Freed, 1998; Gottlinger, Sodroski, & Haseltine, 1989).

MA – MA molecules facilitate the nuclear transport of the viral genome.

CA – forms the conical core of viral particles which can interact with cyclophilin A and enhance viral replication.

NC – its role is to recognize a specific stem loop at 5' end of the HIV-RNA molecule that facilitates the incorporation of newly synthesized nucleic acids into the new virus.

P6 – mediates interaction with Vpr and virion budding

(Freed, 1998).

A (2) Env (envelope): The *env* gene encodes for 160 kDa precursor (gp160), which is first synthesized in the endoplasmic reticulum then migrated to the Golgi where it is glycosylated by the host machinery prior to its activation. In the golgi, gp160 is cleaved into gp120 (surface subunit) and gp41 (transmembrane subunit) by furin or furin-like protease followed by trafficking to the plasma membrane where both gp120 and gp41 are

bound by non-covalent bond and function as a trimeric structure. (Checkley, Luttge, & Freed, 2011; Wyatt et al., 1998). Gp120 and gp41 play an important role in viral entry into the target cells by mediating fusion between the virus and the target cell through interaction of gp120 with CD4 and co-receptors CCR5/CXCR4 (Capon & Ward, 1991). Binding of gp120 to the CD4 receptor causes a change in the conformation thus facilitating the binding of gp120 to the co-receptor CCR5/CXCR4 followed by conformation change in gp41 as well. These changes lead to a fusion of the viral and the host cell membrane and the release of the viral particles into the cell (Wilen, Tilton, & Doms, 2012). Gp120 is one of the viral proteins released by the infected cells and play an important role in neurodegeneration.

A (3) Pol (Polymerase): Pol initially exists as a fusion protein forming the complex Gag-Pol which is then cleaved by a viral protease into Gag and Pol during viral maturation. The *pol* gene encodes for the following proteins: protease (PRO), reverse transcriptase (RT), integrase (IN), and RNaseH.

PRO - is involved in the cleavage of the precursor peptide into the mature viral proteins.

RT - is important for a reverse transcription of HIV RNA into a DNA.

IN - is important for integration of viral DNA into a host genome.

RNase H – plays a role in the priming of the (+)- strand, but not in the conventional method of synthesizing a new primer sequence. Rather RNase H creates a “primer” from the purine-rich polypurine tract (PPT) that is resistant to RNase H cleavage. By removing all bases but the PPT, the PPT is used as a marker for the end of the U3 region of its long terminal repeat.

B. Regulatory and accessory proteins

B (1) Tat (transactivator of transcription): Tat is a 13-kDa protein encoded by *tat* gene. It is a key activator of HIV transcription by activating HIV replication. Tat binds to trans-activator response element (TAR) region on the 5'-LTR of the HIV RNA and promotes initiation and elongation. (Aboul-ela & Varani, 1998; Taube, Fujinaga, Wimmer, Barboric, & Peterlin, 1999). There are two isoforms of Tat: Tat-1 exon (minor form) with 72 amino acids and Tat-2 exon (major form) with 86 amino acids. Tat is primarily localized in the nucleolus/nucleus. Tat has also been shown to play a role in neuronal deregulation (J. R. Chang et al., 2011).

B (2) Rev (Regulator of virion expression): Rev is a 19-kDa phosphoprotein encoded by *rev* gene and binds to the rev response element (RRE). It is primarily localized in the nucleus and regulates nuclear export of the incompletely spliced HIV-1 RNAs containing RRE in a sequence specific manner (Malim, Hauber, Le, Maizel, & Cullen, 1989; Meyer & Malim, 1994)

B (3) Nef (Negative factor): The *nef* gene encodes for myristylated Nef protein that is 27-kDa. It is highly expressed during the early stages of the HIV infection. It activates T-cells and establishes the persistent state of infection based on 10-fold difference between HIV-1 strains with HIV +/- Nef. Nef performs its function by down-regulating MHC I, MHC II, CD4, and CD20 on antigen presenting cells and by targeting cells and helper T-cells respectively (Das & Jameel, 2005; Miller, Warmerdam, Gaston, Greene, & Feinberg, 1994).

B (4) Vpu (Viral protein U): It is a 16-kDa type I integral membrane protein that is HIV-1 specific. It is involved in degradation of CD4 in the ER and the release of the virion from the infected cells (Opella et al., 2005).

B (5) Vif (Viral infectivity factor): It is a 23-kDa protein and promotes the infectivity of the virus. It can interfere with the natural antiviral defense of the infected cells by inactivating APOBEC3G protein and preventing its integration into the virus (Jaeger et al., 2012)

B (6) Vpr (Viral protein R): It is a 14-kDa protein that is incorporated into the virion. Vpr mediates the ability of HIV to infect non-dividing cells productively by enhancing the NLS (Nuclear Localization Signal) of the PIC (Pre-integration Complex) (Heinzinger et al., 1994).

Mechanism of Infection

HIV life cycle can be categorized into: (i) binding, (ii) fusion, (iii) reverse transcription, (iv) integration, (v) replication, (vi) assembly, and (vii) budding. HIV initially targets lymphoid cells such as CD4+ T cells and binds to its CD4 receptor and then to the co-receptors, either CCR5 (M tropic) or CXCR4 (T tropic). This interaction is mediated by the envelope protein gp120 which leads to a conformation change in gp41 thus, causing a fusion of the virus to the host cell membrane and its entry (Arrildt, Joseph, & Swanstrom, 2012). During the initial infection, HIV-1 infection is M-tropic (Wolinsky et al., 1996) which can evolve to a T-tropic later in the infection (Connor, Sheridan, Ceradini, Choe, & Landau, 1997). Once inside the host cell, the nucleocapsid containing the viral RNA disintegrates and releases viral RNA along with other factors

present in the reverse transcription complex (RT, NC, MA, IN, Vpr, Nef, Vif). This is followed by the reverse transcription of the HIV-RNA into a DNA and translocation into the nucleus followed by integration into the host genome (Levin, Hayouka, Friedler, & Loyter, 2010). Next, the assembly of the new HIV RNA and proteins (Gag and Gag-pol polyproteins, envelope proteins and viral RNA genome) made by the host cells that are released from the host cells as an immature HIV. They become mature after the cleavage of long protein chains by a protease (Ghafouri, Amini, Khalili, & Sawaya, 2006). HIV-1 infected lymphocytes, monocytes and macrophages could be in either of the three infection stages: productive infection (actively producing new viruses), latent infection (contains pro-viral DNA but does not produce virus, remains dormant and have the capability to produce virus in future), and non-productive infection (contains either integrated or un-integrated viral DNA but will not produce any infection) (Bissel & Wiley, 2004).

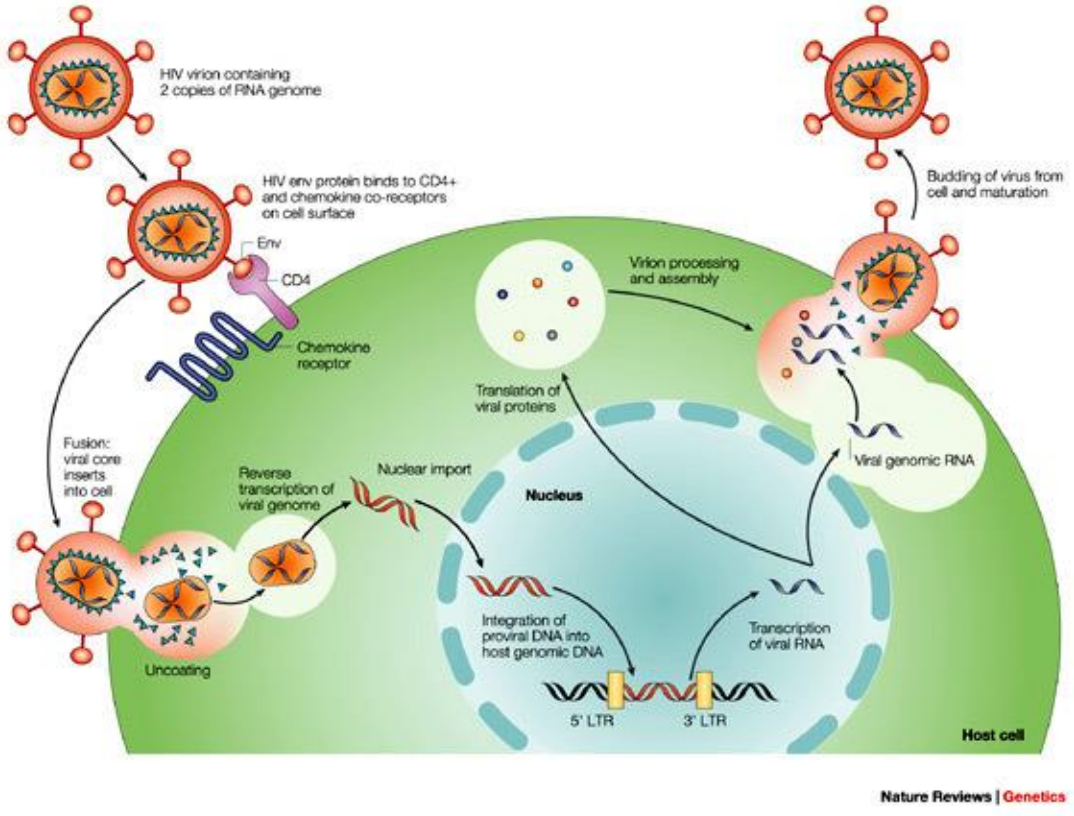

Figure 2. HIV life cycle (Rambaut, Posada, Crandall, & Holmes, 2004)

Infected immune cells such as CD4+ T-cells and monocytes circulate in the blood and migrate to kidney, muscle, bone marrow, brain, and other organs earlier during the infection and could form a viral reservoir. Viral reservoir could be established as early as three days post infection (Whitney et al., 2014).

CNS penetration

CNS is separated from the peripheral nervous system (PNS) by the blood brain barrier (BBB). The BBB is composed of highly specialized brain microvascular endothelial cells (BMEC) present on the thick layer of basal lamina. Underneath the basal

lamina, the presence of other brain cells such as: astrocytes, pericytes, perivascular macrophages, parenchymal microglia and neurons form a micro-environment.

Astrocytes are able to form a perivascular feet and has been shown to be involved in forming tight junction (TJ). BBB is selectively permeable allowing the permeability of small hydrophobic molecules such as O_2, CO_2 and hormones and preventing the entry of large molecules such as: viruses and bacteria (Abbott, 2002; Strazza, Pirrone, Wigdahl, & Nonnemacher, 2011). However, during an infection the integrity of the BBB may be compromised. In the case of HIV infection, the specific mechanism of viral entry into the CNS remains unclear. A Trojan horse model was proposed and is one of the widely accepted theories to explain the HIV-1 entry into the CNS via the infected cells such as monocytes and macrophages (Fischer-Smith & Rappaport, 2005; Ghafouri et al., 2006).

Infiltrating monocytes are then able to infect perivascular macrophages, microglia and astrocytes that release viral particles (such as gp120, tat, nef, vpr) and pro-inflammatory cytokines such as TNF alpha, IL-1Beta (Ghafouri et al., 2006). These released factors have been shown to deregulate neurons. As mentioned earlier, based on the co-receptor binding HIV-1 could be either T tropic or M tropic. In the case of CNS most of the HIV strains isolated are M trophic using CCR5 for entry into macrophages and microglia (Gorry et al., 2001; Joseph, Arrildt, Sturdevant, & Swanstrom, 2015) however few cases on dual tropic strains (R5X4) have been reported in the CNS (Mefford, Gorry, Kunstman, Wolinsky, & Gabuzda, 2008; Ohagen et al., 2003). Additional proposed mechanisms for viral entry are- the direct crossing of the virus particle by compromising the integrity of the BBB (Moses & Nelson, 1994); endocytosis

(Banks, Akerstrom, & Kastin, 1998); or, by modifying the permeability of the BBB by the viral proteins (Arese, Ferrandi, Primo, Camussi, & Bussolino, 2001).

HIV Associated Neurocognitive Disorder (HAND)

In the early years of the AIDS epidemic, being infected with the HIV was considered as a virtual death sentence. Now, with the introduction of combinatory antiretroviral therapy (cART), life expectancy of HIV-1 infected individuals has improved however, the incidence exhibiting illnesses and clinical conditions commonly associated with older people such as cardiovascular, liver, lungs, bone and neurocognitive impairment have been observed (Cardoso et al., 2013; Deeks, 2011; Nasi et al., 2014). Furthermore, the eradication of latent virus remains ineffective and studies have shown the persistence of HIV-1 in the brain cells and the presence of viral proteins in the CSF (Desplats et al., 2013; Siliciano & Siliciano, 2010).

Neurocognitive impairment associated with HIV-1 infection is called HIV-1 associated neurocognitive disorder (HAND). HAND has been divided into three categories as indicated in Table 1 (Heaton et al., 2011; Valcour, Sithinamsuwan, Letendre, & Ances, 2011):

1. Asymptomatic neurocognitive impairment (ANI)
2. Mild neurocognitive disorder (MND)
3. HIV associated dementia (HAD).

Severity is determined based on the neuropsychological testing conducted in the following categories (Figure 3) (Woods, Moore, Weber, & Grant, 2009):

1. Verbal
2. Speed of information processing
3. Learning
4. Recalling information
5. Attention/working memory
6. Executive functioning and
7. Motor speed

Table 1: HAND (Valcour et al., 2011)

Diagnostic Entity	**Cognitive Performance**	**Functional Performance**
Normal cognition	Normal	Normal
Asymptomatic neurocognitive impairment	Acquired impairment in at least two cognitive domain (<1 SD)	Does not impact daily function
Mild neurocognitive disorder	Acquired impairment in at least two cognitive domains (<1 SD)	Interferes with daily function to at least a mild degree (e.g., work inefficiency, reduced mental acuity)
HIV-associated dementia	Acquired impairment in at least two domains, typically in multiple domains with at least two domains with severe impairment (<2 SD)	Marked impact on daily function

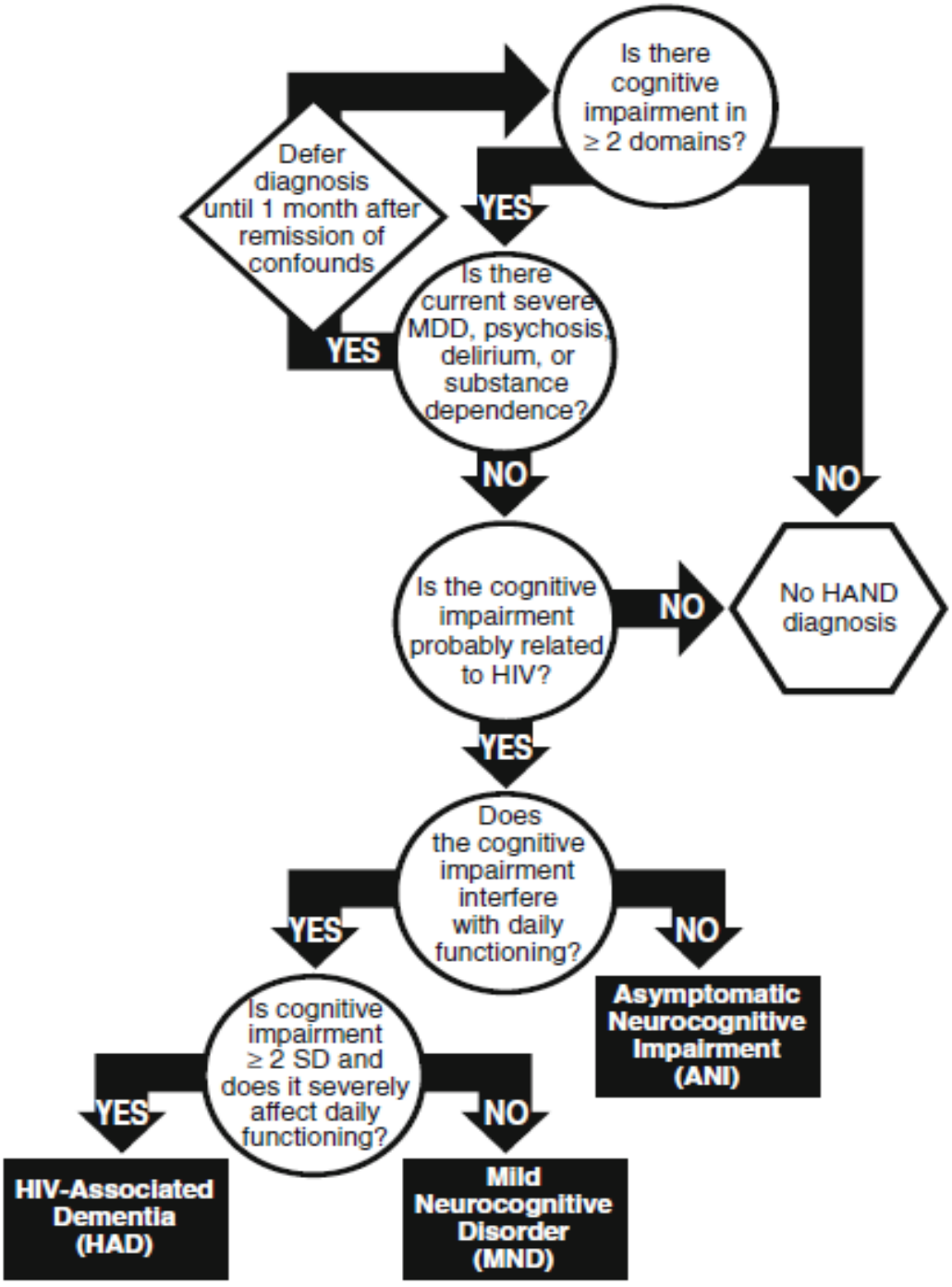

Figure 3. Flow chart for diagnostic criteria to diagnose HAND (Woods et al., 2009)

A decrease in the incidence of HIV associated dementia (HAD) has been observed in the cART era however, the prevalence of milder forms in particular mild or asymptomatic neurocognitive impairment has increased (Gelman et al., 2012; Ghafouri et al., 2006; Gomes da Silva, 2012; Heaton et al., 2011; Zhang, Shi, et al., 2012). Currently, 40-70% of HIV infected patients are living with HAND (Williams et al., 2013). Therefore, cognitive impairment, particularly learning, working memory and executive functioning are the major deregulated brain functions even during the cART era (Heaton et al., 2011). This has been clinically proven when analysis of postmortem brain of cART-treated, HAND patients was performed. These studies showed that cART reduces morbidity and mortality, but HAND persisted despite treatments (Borjabad et al., 2011; Fellows, Byrd, & Morgello, 2014; Heaton et al., 2011).

Furthermore, decreased brain density (Mukerjee et al., 2011) and 15% thinning of primary sensor, motor and premotor cortices in AIDS brain have been observed when compared to the normal brain using three dimensional map as revealed by high resolution brain MRI (magnetic resonance imaging) scan (Thompson et al., 2005). The observed decrease in brain volume and density could be due to the loss of dendritic structure and changes in neuronal size and not necessarily neuronal loss (Freeman et al., 2008). Similar pattern of cortical thinning has also been observed in the milder forms of other neurodegenerative disease such as Alzheimer's (Frisoni, Fox, Jack, Scheltens, & Thompson, 2010), Parkinson's (Segura et al., 2014) and Huntington's (Rosas et al., 2008).

The prevalence of neurocognitive impairment during the age of cART is not completely understood and remains a challenge in neuro-AIDS. Various factors have

been suggested to explain this phenomenon such as, the early entry of the virus into the central nervous system and also could be due to poor penetration of anti-retroviral drugs into the CNS (Heaton et al., 2011). Although HIV-1 does not infect neurons, it is able to deregulate their function through released viral proteins and other neurotoxins (cytokines and chemokines). Therefore, one may ask: why and how are neurons deregulated? Neurons lack the CD4 receptor required for the HIV-1 infection but, the neurotoxins released by the infected cells could lead to it deregulation. In my thesis I have focused on the HIV-1 protein gp120 and investigated its role leading to neuronal deregulation in order to understand learning deficiency and working memory impairment.

HIV-1 gp120 and HAND

gp120 structure: HIV-1 gp120 is a surface glycoprotein encoded by *env* gene of the virus (Ghafouri et al., 2006). It is obtained along with gp41 as a byproduct from a cleavage of gp160 (a precursor) by furin or furin like protease in the golgi apparatus (Checkley et al., 2011). This cleavage is important for the viral infectivity. Post cleavage, mature gp120 (surface subunit) and gp41 (transmembrane subunit) are trafficked into the plasma membrane where both function as a trimeric structure (Figure 4) (Checkley et al., 2011; Wyatt et al., 1998). They play an important role in viral entry into the target cells by mediating fusion between the virus and the target cell. Gp120 consist of five variable regions (V1, V2, V3, V4 and V5) that are interspersed and five constant domains (C1, C2, C3, C4 and C5). These subunits are able to undergo constant trafficking to and from the plasma membrane (Checkley et al., 2011). V3 loop has been extensively studied for its ability to harbor mutations to overcome the effect of anti-retroviral drugs (Xiang et al., 2010; Yuan et al., 2013).

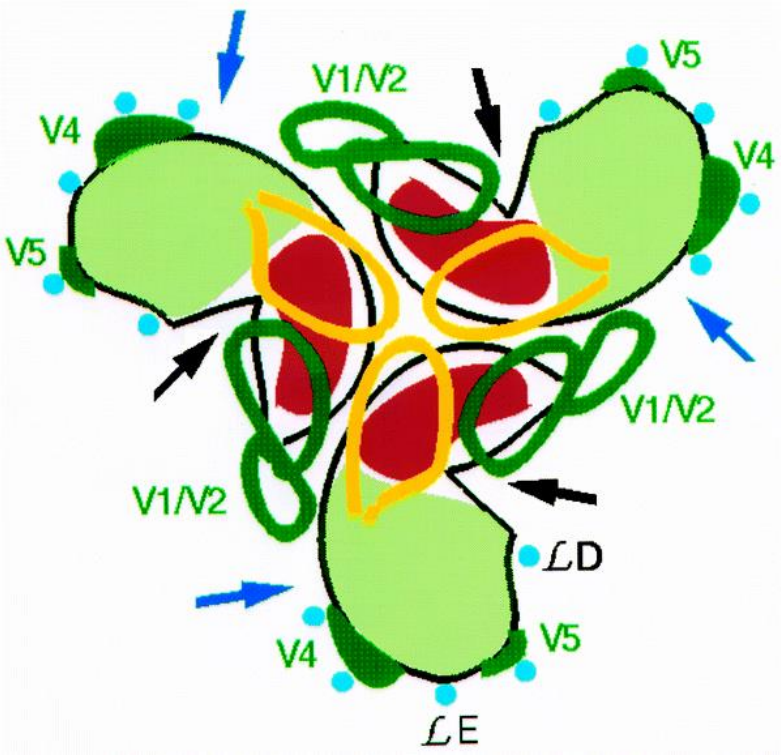

Figure 4. Arrangement of HIV-1 gp120 in a trimeric structure (Wyatt et al., 1998) Black arrows indicate the CD4 binding pockets and chemokine binding areas are indicated in red and V3 loops are indicated in yellow.

gp120 entry to neurons: This soluble viral protein plays a major role in viral entry to the host cells such as microglia, lymphocytes, dendritic cells and macrophages by binding to CD4 receptor and the co-receptors CXCR4 or CCR5 (Kaul, Ma, Medders, Desai, & Lipton, 2007; Wyatt et al., 1998). HIV-1 does not infect neurons due to the lack of CD4 receptor but the released gp120 from the infected cells can bind to either of these co-receptors to produce neurotoxic effects. Their natural ligands such as MIP1α, RANTES and SDF1α could inhibit their effect (Catani et al., 2000).

CXCR4 mediated effect could be attenuated by using its direct inhibitor AMD3100 (Mocchetti, Bachis, & Avdoshina, 2012). Some studies have also shown that CCR5 binding might have some neuro-protective effect via Akt/PKA pathway. The neuroprotective effect occurs by inhibiting CXCR4 and preventing intracellular calcium influx. Therefore, CCR5 could lead to heterologous desensitization of CXCR4 and could provide a partial neuroprotection to the cells (Kaul et al., 2007).

Gp120 has been detected in the cerebrospinal fluid of the AIDS patients at early stages (Walter Reed stages I and II) and has been identified to be neurotoxic. Its picomolar concentration was enough to cause mouse hippocampal neuronal death which was attenuated by peptide T treatment (Brenneman, McCune, Mervis, & Hill, 1994; Glowa et al., 1992). Additional studies have shown that gp120 is internalized by the neurons of the CNS thus increasing its toxicity (A. Bachis, Major, & Mocchetti, 2003) and is transported in the retrograde manner from the axon to the nerve cell body (Ahmed, MacArthur, De Bernardi, & Mocchetti, 2009; A. Bachis, Aden, Nosheny, Andrews, & Mocchetti, 2006). Recently, it was also shown that HIV-1 gp120 internalization occurs through cholesterol dependent lipid raft and pinocytosis in neuroblastoma cell and cultured dorsal root ganglion neurons (Berth, Caicedo, Sarma, Morfini, & Brady, 2015) and micropinocytosis of CXCR4 receptor in HeLa cells (Tanaka et al., 2012). It is possible that gp120 is able to carry its effect via multiple mechanisms and suggest its effect via receptor independent mechanism.

Gp120 and neuronal dysfunction: Neurons have a dynamic shape and their processes such as dendrites and axons play a critical role in information processing and synapse formation. *Hill et al*., showed that a neonatal rat systemically injected with purified

gp120 suffer a morphological aberration of the dendrites with decreased dendritic branching, shorter dendrites, aberrant spine morphology and thick processes in the pyramidal neurons (Hill, Mervis, Avidor, Moody, & Brenneman, 1993) which resembled the cortical pyramidal neurons of HIV encephalopathy (Brenneman et al., 1994). Rodents injected radio labeled gp120 showed that gp120 broke into toxic fragments in the rodent brain as detected by fast performance liquid chromatography (FPLC) and suggested that these fragments are probably more toxic than the full length protein (Hill et al., 1993). Electrophysiology experiments have shown that gp120 causes a decrease in excitatory post synaptic potential (EPSP) in CA1 region of rat hippocampus (Dong & Xiong, 2006) which is involved in long term potentiation (LTP) – responsible for learning and memory. Loss of neurons or change in neuronal architecture could be one of the leading factors for dementia in HIV patients however, the mechanisms that lead to neuronal deregulation are still elusive. Any damage could alter the neuronal communication thus, affecting synaptic plasticity in the long run.

Gp120 and cellular factors:

A- NMDAR and calcium:

N-Methyl-D-Aspartate Receptor (NMDAR) is a type of a glutamate receptor that plays a critical role in LTP that is associated with synaptic plasticity and memory formation. Its deregulation has been reported in several neurodegenerative disease models (Ferreira et al., 2012; Warmus et al., 2014). Proper functioning of NMDAR is dependent on a membrane depolarization to release Mg^{2+} present in the pore and a binding of L-glutamine on the NMDA receptor (Bliss & Collingridge, 1993). At the resting membrane polarization, Mg^{2+} ions enter the NMDAR pore and bind tightly but,

the membrane depolarization leads to the release of Mg^{2+} from the pore and thus activating the NMDAR which then leads to calcium (Ca^{2+}) influx from its pore and activation the calcium store in the endoplasmic reticulum (ER) ("Biology of the NMDA Receptor," 2009; Bliss & Collingridge, 1993) which mediates synapse formation. Calcium is a ubiquitously expressed molecule and it plays an important role in various life processes causing short term and long term effects, for example muscle contraction and secretion as short term effects; and gene transcription, memory formation as the long term effects. Alteration in calcium homeostasis could alter cellular functions. In the case of neurons, one of the role of calcium entry in the pre-synaptic zone is in facilitating the release of neurotransmitters from a pre-synaptic neurons (Haughey & Mattson, 2002; Suedhof, 2012). However, accumulation of excess intracellular calcium can activate cell death pathway causing neuronal dysfunction and leading to programmed cell death. HIV-1 gp120 is able to cause an influx of calcium in neurons by hyper activating NMDA receptor and also release of calcium from the ER leading to an activation of inositol 1,4,5-triphosphate (InsP3) receptor (Haughey & Mattson, 2002). Gp120 increases the intracellular calcium in a dose dependent manner in the hippocampal neurons in vitro in a picomolar concentration. This increase is greatly contributed by the intracellular calcium stores as well (Dreyer, Kaiser, Offermann, & Lipton, 1990). Deregulation of calcium homeostasis has been attributed to the hyper activation of NMDAR caused by excessive release of glutamate, a neurotransmitter, which then binds to NMDAR. This mechanism is often known as glutamate excitotoxicity. Another mechanism leading to it is the reduce expression levels of excitatory amino acid transporter 2 (EAAT2) in the astrocytes by gp120 which would prevent the uptake of extracellular glutamate from the synapse thus

leading to hyper activation of NMDAR (Z. Y. Wang et al., 2003) and increased Ca^{2+} entry into the neurons and deregulating its homeostasis.

Additionally, gp120 is able to cause a release of pro inflammatory cytokine IL-1β that can lead to phosphorylation of NR2B (NMDAR receptor) at tyrosine 1472 causing its hyper-activation thus leading to increased intracellular calcium (Viviani et al., 2006). Furthermore, gp120 has been described to promote phosphorylation of NR2 (glycine binding site of NMDAR, NR1 (glutamate binding site) on serine residue 897 by PKA (phosoho kinase A) and 896 by PKC (phospho kinase C) which causes the forward trafficking of NR1 on the lipid raft present on the plasma membrane causing the clustering of NMDAR on the membrane . The forward trafficking, in which the receptors are trafficked from the ER to the post synaptic membrane, was made possible due to the stabilization and enlargement of the lipid raft by gp120 treatment on hippocampal cells and the alteration on the lipid raft could have interfered with NMDAR trafficking (Xu et al., 2011). HIV-1 gp120 induced neurotoxicity can be prevented by NMDAR inhibitors such as dixocelpine (MK-801), a non-competitive antagonist, and mimentine (Haughey & Mattson, 2002).

Finally, hyperactivity of NMDAR seems to affect the golgi apparatus, which is involved in trafficking of various proteins in the cells, by causing its fragmentation in the cultured hippocampal neurons. The fragmentation is due to the activation of calmodulin kinase (CaMK) caused by increased intracellular calcium (Thayer, Jan, & Jan, 2013). Studies regarding gp120 and its effect on golgi are scarce and could be an interesting area to be considered for future studies. Therefore, gp120 is able to deregulate calcium homeostasis in neurons through various mechanisms and lead to cascade of events among

which superoxide formation by activating NOS, nitric oxide synthase, and altering mitochondrial function (Halliwell, 2006) are the additional factors affected which contributes towards oxidative stress.

B- Mitochondria, oxidative stress and transport

Mitochondria are the powerhouse of the cells and are the critical organelle in a high energy expenditure cells like neurons (Cheng, Hou, & Mattson, 2010) and muscles (Peterson, Johannsen, & Ravussin, 2012). Efficient mitochondrial function and integrity are critical for neuronal well-being. Mitochondrial defects have been associated with several neurodegenerative diseases such as Parkinson's (Exner, Lutz, Haass, & Winklhofer, 2012; Gautier, Corti, & Brice, 2014), Alzheimer's (Sheng et al., 2012), amyotrophic lateral sclerosis (Shi, Gal, Kwinter, Liu, & Zhu, 2010) Huntington's (Quintanilla & Johnson, 2009) and HIV-1 (Huang, Chiang, Lin, Chiou, & Chow, 2012; Thomas, Mayer, & Sperber, 2009). Major functions of the mitochondria in neurons are to regulate Ca^{2+} homeostasis, generate energy in the form of ATP (through electron transport chain and oxidative phosphorylation) and synapse formation (Mattson, Gleichmann, & Cheng, 2008). Along with the energy production, mitochondria also generate ROS (reactive oxygen species) as a byproduct leading to oxidative stress and mtDNA deregulation (Indo et al., 2007). Deregulation of mtDNA could lead to altered nuclear gene transcription and mitochondrial biogenesis thus affecting mitochondrial bioenergetics. This complex loop is often known as a vicious cycle.

Oxidative Stress: Among other mitochondrial factors, oxidative stress has been described to be one of the major causes for neurocognitive impairment (Federico et al.,

2012) and neuropathology of HIV-1 (Zhang, Wang, et al., 2012). HIV-1 gp120 treatment increased ROS and decreased manganese superoxide dismutase (MnSOD) in neurons. Furthermore, NF-κB p65 pathway is involved in maintaining optimal level of MnSOD in astrocytes but, in neurons due to low level of NFkB p65, they fail to produce adequate amount of MnSOD which increases their susceptibility to oxidative stress and leads to neuronal degeneration (Saha & Pahan, 2007). Therefore, inability to produce optimal level of superoxide dismutase increases the production of ROS. Additionally, gp120 treatment on SH-SY5Y neuroblastoma cell line has also been shown to cause an increase in mitochondrial pro-apoptotic proteins, caspase-8 along with increased Fas/FADD which were down regulated when treated with a caspase-8 and caspase-9 inhibitors, Z-IETD-FMK and Z-LEHD-FMK respectively (Thomas et al., 2009).

Furthermore, autopsy of prefrontal cortex from HAND patient and non-HAND patient showed the increase in DNA oxidative marker 8-oxoG compared to the control (an individual without HIV) in the nuclear and mtDNA. Using dihydroethidium (HE), a superoxide indicator, and flow cytometry showed an increase in super oxide ion levels in patients infected with HIV-1 and suffering from HAND compared to the control. These data suggest that HIV-1 triggers production of ROS components. The presence of sub optimal MnSOD dosage is responsible for neurons inability to combat the ROS formation compared to glial cells (astrocytes) that contain optimal dosage of MnSOD (Zhang, Wang, et al., 2012).

Mitochondrial Calcium: Increased ROS has been linked to compromised mitochondrial morphology and glutamate excitotoxicity (Nguyen et al., 2011). These suggest the important role played by HIV-1 gp120 in mitochondrial deregulation.

Increased intracellular Ca^{2+} could lead to influx of Ca^{2+} into the mitochondria facilitated by the MCU complex. MCU complex is a macromolecular structure present in the inner mitochondrial membrane and is composed of proteins involved in mitochondrial Ca^{2+} uptake machinery. It is categorized as, core components of the membrane pore (MCU, MCUb and EMRE) and MCU- associated regulators (the MICU's family, MCUR1 and SLC25A23) (De Stefani, Patron, & Rizzuto, 2015). The influx of mitochondrial calcium could trigger increased ROS (Goerlach, Bertram, Hudecova, & Krizanova, 2015) which could then alter mitochondrial morphology (Ahmad et al., 2013) by deregulating the expression and function of mitochondrial fission and fusion genes and proteins (Drp-1, Fis-1, Mfn-1, Mfn-2 and Opa1). In neurons, MCU overexpression could lead to NMDAR mediated excitotoxicity and the knockdown of MCU has been shown to be neuroprotective (Qiu et al., 2013).

Mitochondrial transport: Mitochondrial movement along the axon and dendrite of neurons is the other important function of mitochondria. Their transport facilitates localization and distribution of mitochondria based on high energy demand of neurons at the nerve terminal. Their transport also help them undergo fission and fusion to maintain balance. Mitochondrial transport deficiency has been reported in several neurodegenerative diseases – Alzheimer's (Stokin et al., 2005) and Huntington's (D. T. W. Chang, Rintoula, Pandipati, & Reynolds, 2006). It is possible that due to increased ROS and oxidative stress with HIV, mitochondrial transport along the neuronal processes is altered. These alterations could be triggered by loss of mitochondrial integrity. Peroxisome proliferator-activated receptor-γ coactivator (PGC-1α) is a transcriptional co-activator that can regulate transcription of genes involved in cellular energy metabolism.

Its activity could be regulated by other key proteins such as CREB and SIRT1 (Amat et al., 2009; Herzig et al., 2001).

Studies regarding mitochondrial functions such as membrane potential, glutathione have been done on CD4+T Lymphocytes (Roggero et al., 2001), microglial (Samikkannu et al., 2015) and the endothelial cells (Price, Ercal, Nakaoke, & Banks, 2005) and these studies on neuronal cells are lacking. There is enough evidence regarding deregulation of factors associated with mitochondrial function to pursue the study more in depth on neurons to better understand the role of mitochondria in neuronal deregulation that could alter learning and working memory. Our lab is currently studying the effect of HIV-1 viral proteins in the neuronal mitochondrial biogenesis and bioenergetics to further understand the mechanisms involved and have evidence showing that HIV-1 gp120 and HIV-1 Vpr is able to deregulate several mitochondrial factors and functions (unpublished data).

C- cAMP response element binding protein (CREB):

CREB is a transcription factor that is able to regulate the gene expression by binding to the CRE site in the promoter and its activity dependent on its phosphorylation status at S133 (Mayr & Montminy, 2001). CREB plays an important role in memory and learning particularly associated with the establishment of a long term memory in the hippocampus (J. J. Brightwell, Smith, Countryman, Neve, & Colombo, 2005; Jennifer J. Brightwell, Smith, Neve, & Colombo, 2007; Yin & Tully, 1996). CREB expression and function has been shown to be altered in aged brain and neurodegeneration (Mantamadiotis et al., 2002). Decreased CREB expression and pCREB activity was

observed in the hippocampus and amygdala of aged mice (24 month old) vs. young mice (3 month old) (Morris & Gold, 2012). Exposing the old mice with new mice blood via heterochronic parabiosis and transfusion of plasma led to enhanced dendritic spine density and synaptic plasticity in the old mice. This improvement is mediated by activation of CREB in the aged hippocampus (Villeda et al., 2014). Furthermore, caloric restriction (CR) is known to delay brain senescence and prevent neurodegeneration (Sohal & Forster, 2014) but, in the CREB deficient mice the CR was unable to restore neuronal plasticity, memory and social behavior (Fusco et al., 2012). This shows the importance of CREB in learning and memory.

Decreased CREB and phospho-CREB expressions have already been shown in several neurodegenerative diseases such as Alzheimer's (Saura & Valero, 2011), Parkinson's , Huntington's (Giralt et al., 2013) and ALS (Rouaux et al., 2007). Although CREB is an important player in learning and memory and more than 50% of HIV-1 infected individuals struggle with some form of HAND, studies regarding HIV and CREB are scarce. Our lab has been focusing on the effect of HIV-1 proteins in CREB and have been able to show it's deregulated with Tat (J. R. Chang et al., 2011) , gp120 and Vpr treatment (unpublished data). CREB has several downstream targets that are related to mitochondrial biogenesis and energetics such as: PGC-1α (Cheng et al., 2012), SIRT1 (Fusco et al., 2012), ND5 and other mitochondrial genes (De Rasmo, Signorile, Roca, & Papa, 2009) and neuronal markers such as BDNF (L.-C. Ou & Gean, 2007; Tao, Finkbeiner, Arnold, Shaywitz, & Greenberg, 1998; Zheng, Zhou, Moon, & Wang, 2012). CREB could regulate PGC-1α directly by affecting its promoter or indirectly via miR-132 and DNMT3b (to methylate its promoter) (Lv, Xin, Zhou, & Qiu, 2013).

It is possible that deregulation of pCREB and CREB affect the downstream targets leading to altered mitochondrial functioning and neuronal communication. Likewise, upstream regulators of CREB are also important to consider. Our lab has shown miR-34a to be one of the upstream regulators of CREB (J. R. Chang et. al., 2011). We have data showing that miR-34a is able to deregulate CREB via E3F3. Therefore, studies regarding HIV and CREB are important to understand the mechanism and to develop a treatment strategy to delay leaning deficiency.

D – Brain derived neurotrophic factor (BDNF):

Neurotrophic factors, such as brain derived neurotrophic factor (BDNF), play an important role in brain development, neuronal survival, differentiation, morphology and synapse formation (Cohen-Cory, Kidane, Shirkey, & Marshak, 2010; Horch & Katz, 2002). Human BDNF gene is composed of 11 exons and 9 functional promoters (D. T. W. Chang et al., 2006). Multiple promoters are regulated by different factors. BDNF promoter IV has been shown to be regulated by CREB and is induced during neuronal activity (Tao et al., 1998; Zheng et al., 2012). BDNF promoter IV is also regulated epigenetically via MeCP2 (Zhou et al., 2006). BDNF is first synthesized as pro-BDNF, a larger precursor, which is then cleaved into a mature BDNF (mBDNF) by enzymes such as furin in the endoplasmic reticulum (Fayard, Loeffler, Weis, Vogelin, & Kruttgen, 2005) and plasmin in the extracellular space (B. Lu, Pang, & Woo, 2005). These two isoforms of BDNF have opposing effect on neurons and have been referred to as "punishment" and "reward" in the pathway (Je et al., 2013). Mature BDNF is released by the post synaptic glutamatergic neurons which then bind to TrkB receptor in the pre synaptic neurons leading to its phosphorylation. This binding enhances axonal branching

and neuronal survival. Pro-BDNF reduces the synaptic plasticity by binding to p75 neurotrophin receptor (p75NTR). Increased pro-BDNF and decreased mBDNF has been reported in the frontal cortex, hippocampus and caudate/putamen of the post mortem brain of HIV+ subjects with cognitive and motor impairment compared to the control (HIV-) and HIV+ non dementia brain. Similar data was observed in a rat cerebellar granular cells extract treated with recombinant HIV-1 gp120IIIB (Alessia Bachis, Avdoshina, Zecca, Parsadanian, & Mocchetti, 2012). Increase in pro BDNF in gp120 IIIB treated cells was accompanied by neurite retraction as compared to the untreated cells (Alessia Bachis et al., 2012; R. L. Nosheny, Bachis, Acquas, & Mocchetti, 2004). Dramatic loss of BDNF in the neuronal processes of a rat acutely injected with gp120 in the striatum was also observed via immunofluorescence (R. L. Nosheny et al., 2004) which shows that gp120 causes neuronal damage. Gp120 is altering pro and mature BDNF ratio by targeting enzymes such as furin and plasminogen (Alessia Bachis et al., 2012). Since protein synthesis of BDNF has been shown to be important for LTP in the hippocampus (Kang & Schuman, 1996) and its alteration has been associated with impaired spatial and working memory formation (Mizuno et al., 2003), this shows that altered BDNF expression with gp120 treatment and in HIVE brain plays an important role in impaired learning and recalling information observed in HIV patients.

Therefore, the accumulation of pro BDNF could be detrimental to the neuronal survival due to an activation of pro apoptotic factor. Neurite retraction observed in gp120 treated neurons could also cause synaptic pruning by inhibiting the synapse and thus prevents neuronal communication leading to altered learning ability. mBDNF protects the neurons from degeneration caused by gp120 in contrast to pro BDNF. Exercise could be

a positive activator of BDNF. Gp120 transgenic mice subjected to voluntary running wheel exercise were able to obtain increased expression of BDNF in the hippocampal area and increased neurogenesis in the dentate gyrus of (M.H. Lee et al., 2013). BDNF treatment has been used to rectify or prevent the toxic effect of gp120 associated with nigrostriatal neuronal degeneration (Mocchetti, Nosheny, Tanda, Ren, & Meyer, 2007; Rachel L. Nosheny et al., 2007). Therefore, mature BDNF has been considered as a therapeutic tool for other neurodegenerative and neuro-psychiatric disorders (Nagahara & Tuszynski, 2011), it could be considered as a therapeutic tool in preventing neuronal degeneration in HIV leading to learning and working memory deficit.

HIV-1 and micro RNA

Micro RNAs are small non-coding RNA molecules that are ~20-22 nucleotide long and are produced by the cleavage of pri-miRNA and pre-miRNA by drosha and dicer in the nucleus and cytoplasm respectively. They regulate the expression of their target genes post-transcriptionally based on host complementarity by binding to the 3'UTR. This binding can either lead to the degradation or, translational repression of the mRNA (Bartel, 2009). One miRNA can have multiple target genes and one gene could be targeted by multiple miRNAs.

Deregulation of the micro RNAs have been reported in several diseases such as cancer, neurodegeneration and HIV. In the case of HIV, it has been shown that HIV-1 can suppress the miRNA silencing pathway to enhance their replication (Triboulet et al., 2007). Additionally, HIV-1 proteins- Tat and Vpr have also been shown to alter miRNA expression and biogenesis (Bennasser, Le, Benkirane, & Jeang, 2005; Coley et al., 2010). miRNA profiling study done on the brain tissue of the HIVE and control brain showed

altered expression of several miRNAs along with deregulation of proteins involved in caspase pathway (Noorbakhsh et al., 2010). Our lab has also shown altered expression of miR-34 in Tat treated and Tat transgenic mice brain (J. R. Chang et al., 2011). Gp120 has shown to regulate miRNAs (miR-21, miR-155 and miR-181b) in human monocyte derived dendritic cells (Masotti et al., 2015) but the miRNAs in the brain have not been reported. In our study we have been able to identify some of the miRNAs related to mitochondrial and neuronal functions being deregulated by HIV-1 gp120 in the neurons.

Hypothesis and Specific Aims

It has been shown that patients who carry the HIV-1 virus accumulate damage to the cells and tissues that are not themselves directly infected by the virus itself (such as- heart, kidneys, bone, and CNS). Importantly, these include neurodegenerative changes leading to loss of neurocognitive functions and HAND. HAND is a serious problem in the clinical aspect of the HIV-1 patients because suppression of infectious virus by cART does not completely block neurodegeneration. Neuropsychological studies disclose cognitive alteration in a substantial proportion (15-50%) of HIV-1 infected patients (Heaton et al., 2011) and analysis of post-mortem brain tissues isolated from HIV-1 patients treated with c-ART show signs of neurodegeneration (Ellis, Langford, & Masliah, 2007). The MRI scans have also shown decrease in their brain volume and density (Mukerjee et al., 2011; Thompson et al., 2005).

In the absence of HIV-1 infection of neurons, a number of mechanisms have been proposed for HAND, including indirect inflammatory effects in the CNS and direct effects of viral proteins shed from activated HIV-1-infected cells (Hill, Mervis, Avidor, Moody, & Brenneman, 1993). Several soluble viral proteins are detectable in the circulation of HIV-1 carriers, and are known to be able to cross the blood brain barrier and bind to or enter neurons. Gp120 protein has been reported to interfere with axonal transport, leading to axon shortening as well as decreased dendritic density (Hill, Mervis, Avidor, Moody, & Brenneman, 1993). Evidence of the viral surface protein gp120 have been reported to bind to surface receptors on neurons, whence they may be internalized by pinocytosis, with reported effects on neurons.

As indicated, several mechanisms of HIV-associated neuronal degeneration have been identified. Their relative contributions to clinical disease in vivo remains to be investigated, and this is a great challenge in the HIV research. Recently, we have obtained data showing the effect of gp120 on CREB protein levels and phosphorylation, in primary human and mouse neurons and in the neuronal cell line SH-SY5Y (data presented here). These findings are important for two reasons:

(1) A correlation between CREB protein, mitochondrial function, and neurodegeneration has been well-established in the literature, suggesting that this may be a significant contributory mechanism in HAND; and
(2) Pharmacological agents are available which can specifically restore CREB protein levels and function, offering an opportunity to test directly the contribution of this mechanism in vivo in mice.

Our hypothesis is that gp120 contributes to neurodegeneration via alteration of the mitochondrial function, mediated by a decrease in CREB protein activity. Decreased CREB activation could then alter the expressions and functions of its downstream targets (PGC-1α, BDNF, COX I-III , ND5 and miR-132) that are involved in mitochondrial function and neuronal communication. Therefore, activation of CREB using pharmacological reagent will rescue the effects of gp120.

Several studies have shown CREB to be a major protein involved in learning and memory. Additionally, CREB function is deregulated in several neurodegenerative diseases and aging. Decreased total and pCREB expressions were observed in the hippocampus and amygdala of the aged mice (Morris & Gold, 2012); and cortex and hippocampus of the aged rats (Chung et al., 2002) which affected memory. Activation of

CREB by either using St. John's Wort or injecting old mice with young mice plasma led to improved learning and memory (Trofimiuk, Holownia, & Braszko, 2010; Villeda et al., 2014). Reduced CREB expression and loss of its phosphorylation have also been shown in Alzheimer's (Saura & Valero, 2011), Parkinson (J. Lee et al., 2005), and Huntington's Disease (Giralt et al., 2013). Therefore, CREB has been considered to be a master regulator of memory. CREB could be regulated by either, Ca2+ and cAMP. Its activity is dependent on its phosphorylation. CREB is an important transcription factor that is involved in intracellular signaling and functions by regulating several key proteins, genes and miRNAs involved in synaptic plasticity and mitochondrial bioenergetics such as: BDNF, PGC-1α, miR132 and DNMTs to name a few.

CREB has several downstream targets that are involved in mitochondrial functioning and neuronal communication. gp120 could be deregulating mitochondria and neuronal communication via CREB inhibition. Therefore, our study by focusing on CREB and its downstream targets, will help identify the mechanisms used by HIV-1 gp120 to deregulate neuronal factors via mitochondrial deregulation and demonstrate the important role of CREB in it. This will also map a molecular pathways involved in gp120 mediated neuronal deregulation by identifying both upstream and downstream targets of CREB.

We propose to test these hypothesis in tissue culture cells and in vivo in mice, and verify the intermediate role of CREB protein using the specific CREB activator rolipram as follows:

Aim 1: Determine the mechanisms used by gp120 leading to the loss of CREB functions.

(A) To investigate the effect of HIV-1 gp120 on CREB expression and function

Differentiated SH-SY5Y, human primary neurons and mouse primary neurons ± 100ηg/mL of gp120 IIIB for 24 hours will be subjected to RT-qPCR and western blot to examine the expression of CREB and/or pCREB. We expect to see decreased CREB and pCREB expression.

(B) To activate CREB pharmacologically by using rolipram.

Differentiated SH-SY5Y cells will be pre-treated with rolipram for 1 hr followed ± 100ηg/mL of gp120 IIIB for 24 hours and the cellular extracts will be subjected to western blot analysis to measure the pCREB expression. We expect to see increased pCREB expression with rolipram treatment.

Aim 2: Impact of CREB functional loss on Mitochondrial Bioenergetics and Synaptic Plasticity ± gp120.

(A) To investigate the effect of gp120 on PGC-1α; miR-132, DNMT3B and synaptic proteins.

Differentiated SH-SY5Y cells will be subjected to ± 100ηg/mL of gp120 IIIB for 24 hours. Western blot and/or RT-qPCR will be performed to measure the expression of PGC-1α, DNMTs and PSD-95. We expect to see decreased expression of these factors.

(B) To investigate the role of HIV-1 gp120 on the mitochondrial shape.

Expression and distribution of mitochondrial fission proteins (Drp-1 and Fis-1) will be measured using the western blot and immunofluorescence. Mitochondrial shape will be measured by labelling mitochondria with pDsRed2-Mito ± gp120 and visualizing under the confocal microscope. We expect to see increased fission in gp120 treated cells.

(C) To investigate the role of miR-499-5p and calcium dependent protein calcineurin in this phenomenon.

Expression of miR-499-5p and Calcineurin will be measured in ± gp120 treated differentiated SH-SY5Y cells and perform RT-qPCR and western blot to measure the expression. We expect the calcineurin expression to increase and miR-499-5p to decrease in gp120 treated cells.

(D) Use of rolipram to restore CREB functions

Differentiated SH-SY5Y cells will be pre-treated with rolipram for 1 hr followed ± 100ηg/mL of gp120 IIIB for 24 hours and the cellular extracts will be subjected to ADP/ATP ratio and mtDNA copy number analysis to measure examine the mitochondrial biogenesis and bioenergetics. We expect rolipram to activate CREB and rescue the effect of gp120.

Aim 3: Intervention using an animal model

(A) Effect of gp120 on learning and working memory on mice

(B) Restoring CREB functions in these mice

8-10 weeks old C57B1/6J male mice will be first injected with either Saline or gp120 followed by either saline or rolipram. There mice will then be subjected to the memory test. We expect mice injected with rolipram to perform better during the memory test.

Outcome of this study will serve to enhance our understanding regarding the progression of HAND, and will link AIDS to aging. Therefore, the outcome of this study could also be directed towards the development of novel therapeutics to delay or minimize the learning and memory in both HIV and aging population.

CHAPTER 2

HIV-1 GP120 DEREGULATES MITOCHONDRIA VIA CREB

Introduction

HIV-1 enters the brain early during the course of infection and begins to evolve as early as 140 days after the initial infection (Sturdevant et al., 2015). The available evidence suggests that HAND is the indirect effect of HIV-1 infection where the viral proteins and the inflammatory factors released by the infected cells cause the neuronal damage. HIV-1 gp120 has been shown as one of the factors released by the HIV-1 infected cells and it has been reported to be involved in causing neuronal deregulation. This 120 kDa envelope protein is important for the viral entry into the target cells. It is also one of the factors released by the infected cells that can then bind to either CXCR4 or CCR5 receptor of the neurons causing its deregulation. Although the ability of gp120 to deregulate neurons has been shown the mechanism leading to it has not been established properly.

One of the major protein that play an important role in memory and learning is CREB. The critical role of CREB in the formation of spatial memory, long term memory and neuronal plasticity has been shown (Silva, Kogan, Frankland, & Kida, 1998). Laboratory of Saul Villeda, has shown that hippocampal CREB is involved in age-related decline of learning and memory by first, subjecting young and old mice to two day radial-arm water maze learning and memory task (RAWM) and calculated the errors made. He also showed decreased pCREB hippocampus of the old mice. Additionally, injecting young mice plasma into an old mice led to increased CREB and pCREB expression and

learning (Figure 5) (Villeda et al., 2014). The role of CREB in several neurodegenerative diseases associated with memory and learning has also been linked (Mantamadiotis et al., 2002; Pugazhenthi, Wang, Pham, Sze, & Eckman, 2011).

In the case of HIV-1, CREB has only been studied mostly with regards to Tat (Zauli et al., 2001). The relation of CREB and gp120 has not yet been established. Therefore, here we will show gp120 mediated deregulation of CREB and its effect on the neuronal and mitochondrial factors. We will also examine the role of CREB in maintaining the mitochondrial integrity by pharmacologically activating CREB and rescuing the effect of gp120 on the mitochondrial biogenesis and bioenergetics. Additionally, we will also show the miRNAs, genes and proteins that are altered in this CREB dependent pathway to understand the pathway better.

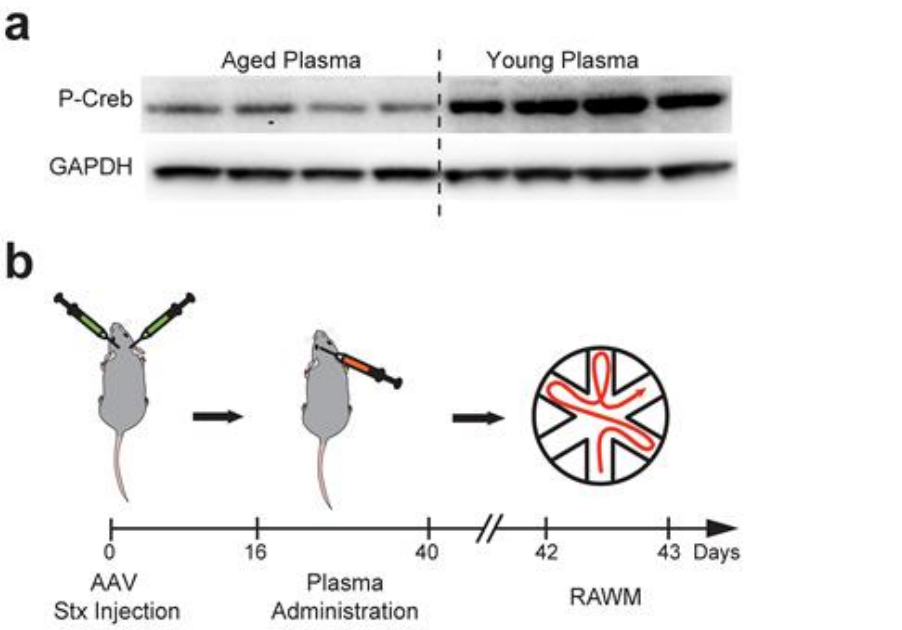
a
Aged Plasma
Young Plasma
P-Creb
GAPDH
b
0
16
40
42
43 Days
AAV
Stx Injection
Plasma
Administration
RAWM
c
GFP
L Hemi1
K-Creb
R Hemi 1
GFP
L Hemi 2
K-Creb
R Hemi 2
GFP
L Hemi 3
K-Creb
R Hemi 3
Creb
P-Creb
GAPDH
d
GFP Aged Plasma
GFP Young Plasma
K-Creb Aged Plasma
K-Creb Young Plasma
Errors
Day 1
Training
Day 2
Testing
Blocks

Figure 5. CREB activity is altered with aging (Villeda et al.,2014) Used with the permission of Dr. Saul Villeda (A) Unpublished data showing decreased pCREB expression in the isolated hippocampi sample of 18 month old mice either injected with old plasma (18 month old) or young plasma (3 month old). (B) Schematic illustrating the chronological order used for AAV delivery, plasma treatment and cognitive testing. Stx, stereotaxic. (C) Western blot analysis of CREB overexpression and pCREB in isolated hippocampi of adult mice that were contralaterally locally infected with AAVs encoding either K-CREB or GFP. Hemi, hemisphere. (D) Number of entry-arm errors before finding platform to test learning.

Materials and Methods

Cell culture

The human neuroblastoma cell line, SH-SY5Y cells were purchased from ATCC (CRL-2266) and grown in Dulbecco modified eagle medium: nutrient type – 12 (DMEM F12) supplemented with 10% Fetal bovine serum (FBS), 1% non-essential amino acid and 1% sodium pyruvate. All cells were incubated at 37˚C supplemented with 5% CO_2. The cells were passaged each time at 85-90% confluency. The cells only within 10 passages from the time purchased from ATCC were used for the experiment. The cells were seeded at the density of 5x10^5 cells/per well for 6 well plates. They were differentiated into neurons with 10µM retinoic acid (RA) treatment for 3-4 days.

Human primary neuronal cells (26 weeks old fetal brain) were generously provided by Dr. Elyseo Eugenin from Rutgers University. The human cortical fetal tissue was used to isolate the mix culture of neurons and astrocytes as described (Eugenin, D'Aversa, Lopez, Calderon, & Berman, 2003). The mixed culture obtained contained 30-40% neurons, 60-70% astrocytes and 2-5% microglia. Neuronal enriched cultures were obtained after 7-10 days of culture in Neurobasal medium supplemented with N2 neuro-survival factor and 5% FBS (Eugenin et al., 2011). The cells were cultured for about 10 days to obtain 70-80% of the neuronal culture before the treatments.

The primary mouse neurons were obtained from E18 (embryonic day 18). The cortex and hippocampus were separated and rinsed in HBSS before digesting them in 0.125% trypsin. The cortex was digested for 20 min (DNase 0.4%) and hippocampus for 15 minutes. The digested tissue were then triturated in DMEM containing 10% FBS

followed by centrifugation at 1000rpm for 10mins. The tissue were then washed twice and re-suspended in DMEM F12 and passed through a strainer to remove the non-dispersed tissue. The cells were then seeded at $7x10^5$ cells/well for 6-well plates and $1.2x10^5$ cells/ chamber for 4 chamber slides and incubated 37°C in an atmosphere of 5% CO_2 in air. DMEM medium was replaced with Neurobasal supplemented with B27, NEAA, GluMax and pen-strep after 2-3 hours of seeding. Half a medium was changed every 3 days.

Treatments

Recombinant HIV-1 gp120IIIB was purchased from NIH AIDS Reagent Program (Catalog # 11784). Samples were treated with 100ηg/mL of gp120 for 24 or 48 hours or specified otherwise. HIV-1 gp120IIIB is T-tropic and works via its interaction with a chemokine receptor CXCR4 which are expressed by the neurons. As mentioned earlier most CNS infections are M tropic but few mixed tropic (R5X4) strains have been identified that can use both co-receptors.

To prevent the interaction of gp120 with CXCR4, its inhibitor AMD3100 (NIH AIDS Research and Reference Reagent Program Cat # 8128) was used at the concentration of 2µM.

Activators of cAMP and CREB such as salidroside (5µM) (Cayman Chemicals) and rolipram (30µM) (Sigma-Aldrich) were used as the pharmacological activators of CREB (cAMP response element binding) protein. Salidroside pre-treatments were done 24 hours before the addition of gp120. Rolipram pre-treatments were done 1 hour before the addition of gp120.

Rotenone (Tocris) is the inhibitor of NADH oxidation. It was used as a positive control for NAD/NADH ratio. Cells were treated with 1µM rotenone for 24 hours.

Ethanol was used as a control to inhibit mitochondrial function. The cells were treated with 200mM of ethanol for 24 hours.

Transfections

RSV CREB plasmid was a gift from Marc Montminy (Addgene plasmid #22394) (Gonzalez & Montminy, 1989). pDsRed2-Mito was purchased from Clontech (Catalog #632421). The SH-SY5Y cells were seeded at 5x10^5/mL in the culture dishes. The day of transfection, the cells were incubated in the OPTI MEM medium for an hour before transfection. For transfection, the following plasmids with the respective concentrations were used: RSV CREB or empty pcDNA with the working concentration of 250ηg/mL and dsMito-Red with 1.5µg/µL using lipofectamine 2000 were prepared in the transfection medium (Opti MEM). The cells were then incubated for 4-6 hours at 37˚C. The transfection medium Opti MEM was replaced by the differentiation medium DMEM F12 with 10 µM retinoic acid after 4-6 hours. The cells were left to differentiate for 4 days followed by the different treatment conditions specified per experiments then subjected to the respective experiments.

Stereotaxic surgery and spatial memory testing

Stereotaxic surgery: Mice were singly housed with *ad-libitum* access to food and water prior to and after surgery. 8-10 weeks old C57B1/6J male mice were anesthetized with isoflurane and received bilateral stereotaxic injections (1 µL volume per injection site) of either saline or gp120 (125 ng/µL) into the hippocampi at rostral (-1.7 mm A/P,

1.2 mm M/L, 2 mm D/V from bregma) and caudal (-2.7 mm A/P, 2 mm M/L, 2.1 mm D/V from bregma) coordinates for a total of 4 intrahippocampal injections per mouse. Mice then received intraperitoneal injections of saline or rolipram (1mg/kg) immediately after surgery and 36 hours after surgery. 72 hours post stereotaxic injection, spatial memory was tested using the object location memory test. All procedures were approved by the Baylor College of Medicine Institutional Animal Care and Use Committee.

Object location memory testing: The object location memory test requires that mice learn and remember the positions of two objects in an arena. Extra-arena spatial cues exist to orient the mice during training and testing phases. For training, two identical flasks were placed at adjacent far corners of the arena, and animals were allowed to explore both flasks in 3 trials of 3 min each with 3 min intervals. The amount of time mice spent exploring each flask was recorded by the experimenter. After a delay of 24 hrs, mice were returned to the arena for the test phase. In this phase, one flask was displaced to the adjacent empty corner. Mice were given 3 minutes to explore both flasks, and the amount of time spent exploring each flask was recorded. An increase in time spent with the displaced object during the test phase relative to the training phase is indicative of intact spatial memory. This experiment was done in the laboratory of our collaborator – Dr. Jeannie Chin, Baylor School of Medicine.

Live cell imaging for the surface area

Images of differentiated (untreated) and gp120 treated SH-SY5Y cells grown in 100 cm^2 dishes were taken every 30 minutes for 44 hours using an EVOS AMD microscope (40x objective) installed inside the incubator. Images were analyzed using ImageJ software. Each image was then analyzed with the compute curvature plugin with

Gaussian convolution sigma parameter set at 1, followed by a conversion to a binary image and finally surface area of the cells analyzed with the measure function. Surface area was expressed as a percentage covered surface per cell.

Synaptophysin

Primary mice neurons (E18) were cultured for 5 days prior being transduced with CellLight Synaptophysin-RFP BacMam 2.0 (Life Technology Catalog# C10610) at MOI of 5. Cells were then cultured for additional 24 hours before gp120 (100 ηg/ml) protein was added. Images were acquired on live cells 24 hours post gp120 treatment using EVOS AMD microscope. Synaptophysin vesicles number and size were quantified using Image J Software - Compute Curvatures and Analyze particles plugins. Images from 10 different fields of three independent experiments were used for statistical analysis.

Western Blot

The whole cell lysate was prepared using Radioimmunoprecipitation assay (RIPA) lysis buffer (25 mM Tris–HCl pH 7.6, 150 mM NaCl, 1 % Triton and 0.1 % SDS) + protease inhibitor and phosphatase inhibitor cocktail. 25µg of the sample were loaded in each well. The cell lysates were vortexed and spun at high speed and spun in 4˚C centrifuge at 13,000 rpm for 10 minutes. Protein concentrations were estimated using a Bradford Assay (Bio-Rad Catalog # 500-0006). Lysates were mixed with 6X loading dye containing β-ME followed by boiling them at 95˚C on a dry bath. 25µg of samples were loaded in each well. The gel was then transferred to a nitrocellulose membrane. The membrane was blocked with 5% BSA for 1 hour at the room temperature. Primary antibodies were prepared in a 5% BSA solution as well and the membranes were incubated for overnight at 4˚C with gentle shaking. Antibodies used to detect the target

proteins: PSD-95 (Santa Cruz), CREB (cell signaling), pCREB (cell signaling), BDNF (Santa Cruz), Kinesin (Santa Cruz), Dynein (Santa Cruz), E2F3 (Cell Signaling), MIRO (Santa Cruz), TRAK (Santa Cruz), PGC-1α (Cell Signaling), ND5 (Cell Signaling), DNMT3a (Santa Cruz) and DNMT3b (Santa Cruz). Species specific secondary antibodies were used from Santa Cruz and the membranes were incubated for 1 hour at the room temperature. Chemo luminescence was used to detect the band signal. Densitometry ratio of the bands were determined using an ImageJ that was normalized to the GAPDH.

RNA extraction

Total RNA was extracted from the sample treated with different conditions using SurePrep TrueTotal RNA purification kit from Fisher Bioreagents as per the instruction from the manufacturer. Nanodrop was used to determine the purity and concentration of the RNA extracted.

miRNA

For micro RNA expression cDNA was synthesized using miRCURY LNA Universal RT microRNA PCR from EXIQON with 100ng of RNA. Primers for miR-34a, miR-132 and miR-134 were purchased from Exiqon. miR-485-5p was detected using cDNA synthesis kit and the primers from Sigma. Results were expressed in relative gene level as compared to the untreated control. U6 was used as an internal control.

mRNA Gene Expression

cDNA was synthesized using SuperScript VILO cDNA synthesis kit (Invitrogen 11754-050). Following primers were purchased from IDT:

BDNF: (F-5'-GAGCAGCTGCCTTGATGGTTACTT)

(R-5'-AAGCCACCTTGTCCTCGGATGTTT)

CREB: (F-5′-GGCAGACAGTTCAAGTCCATG)

(R- 5′-CGCTTTTGGGAATCAGTTACAC)

SIRT1: (F-5′-CAGTGTCATGGTTCCTTTGC

(R- 5′-GTTTCATGATAGCAAGCGGTTC)

COX I: (F- CTG CTA TAG TGG AGG CCG GA)

(R- GGG TGG GAG TAG TTC CCT GC)

COX III: (F- CCA ATG ATG GCG CGA TG)

(R- CTT TTT GGA CAG GTG GTG TGT G)

PGC-1α: (F- CCAAACCAACAACTTTATCTC)

(R- CACTTAAGGTGCGTTCAATAG)

DNMT1: (F- AGA CTA CGC GAG ATT CGA GTC)

(R- TTG GTG GCT GAG TAG TAG AGG)

DNMT3a: (F- GCG GCG AGA GGA CTG GCC)

(R – CGG TCC ACC TGA ATG CCC AA)

DNMT3b: (F- AGG GAG ACA CCA GGC ATC TC)

(R- AGC TTA GCA GCA GAC TGG ACA CC)

GAPDH: (F- 5′-GCCTTCCGTGTTCCTACC)

(R- 5′-CCTCAGTGTAGCCCAAGATG)

Results are expressed in relative gene expression level as compared to the untreated control. GAPDH was used as an internal control.

Immunohistochemistry

Human brain

Frontal lobe brain tissues from HIV-positive patients with varying degrees of dementia, along with non-demented and HIV-negative controls were obtained from the national neuroAIDS tissue consortium (NNTC). The formalin-fixed and paraffin-embedded tissues were sectioned at 5 μm thickness and placed on electromagnetically charged glass slides. Sections were deparaffinized in xylene and re-hydrated through descending grades of alcohol up to water. Non-enzymatic antigen retrieval was performed in citrate buffer for 30 minutes at 95°C in a vacuum oven. Sections were then rinsed with PBS and permeabilized in 0.2% Triton in PBS for 45 minutes at room temperature. Sections were rinsed again with PBS, and a blocking step was performed with normal BSA serum at room temperature in a humidified chamber for 2 hours. Primary antibodies were incubated overnight at 4°C and later for 1 hour at room temperature with fluorescently labeled secondary antibodies. The tissues were

subsequently washed in PBS until finally mounted with DAPI containing medium (Vectashield). Leica EL600 DMI3000 confocal microscope was used for imaging.

Gp120 transgenic mice brain

Imaging for gp120Tg mice brain were done in Dr. Kaul's Lab (Sanford Burnham Presbys Medical Discovery Institute). WT and gp120-tg mice ((express gp120 under GFAP promoter) were provided by Dr. Lennart Mucke (Gladstone Institute of Neurological Disease, University of California) (Toggas et al., 1994). The mice were 9 months of age for both WT and gp120-tg, they were anesthetized with Isoflurane and transcardially perfused with 0.9% saline. The brains were quickly removed and fixed with 4% paraformaldehyde for 48 hours at 4˚C. The brain sections of 30µm thickness were obtained for the histological studies. The slides were permeabilized with 1% Triton X-100 for 30 mins followed by blocking with 10% heat inactivated goat serum in PBS containing 0.5% Tween 20 for 1.5 hours. The sections were then stained with CREB (Cell Signaling) and MAP-2 (Sigma) overnight followed by Alexa Flour 488-labled goat anti-rabbit (Molecular Probes). Nuclear DNA was labeled with H33342. Per animal three sagittal sections were analyzed and each sections five fields were recorded using Zeiss inverted Axiovert 100M fluorescence microscope.

Fluorescence was quantified using ImageJ by selecting ROIs and set measurements by selecting area, integrated density and mean gray value. Corrected total cell fluorescence (CTCF) was measured using the following formula:

CTCF = Integrated Density – Area of selected cell X mean fluorescence of background readings

ADP/ATP ratio

Changes in ADP/ATP ratio was measured by using ADP/ATP ratio assay kit purchased from SIGMA-ALDRICH which is based on luciferin – luciferase assay. The assay involved two steps:

(i) The cells are lysed by a working reagent to release ATP and ADP. ATP immediately reacts with the substrate D luciferin and produce light in the presence of luciferase – measuring the intracellular ATP concentration

(ii) An enzymatic reaction converts ADP to ATP, followed by the reaction of ATP with D-luciferin. The second light intensity measurement is the representation of the total ADP and ATP concentration in the sample.

ATP + D-Luciferin + O2 (Luciferase) → oxyluciferin + AMP + PPi + CO2 + light

The ATP reagents were prepared as per the manual and 90µL/well were added on the samples followed by 1 min incubation at the room temperature. Then, the luminescence was read for the ATP (RLU_A). The samples were then incubated for 10 mins at the room temperature then the luminescence was read again for ATP (RLU_B). This reading is the background generated by the residual ATP signal. Immediately after the second reading 5µL of ADP reagent was added to each well, incubated for 1 min at RT and the luminescence was read (RLU_C).

ADP/ATP ratio was measured using the following formula:

$$\text{ADP/ATP ratio} = \frac{RLU_C - RLU_B}{RLU_A}$$

ATP assay

ATP was measured based on the luciferin – luciferase bioluminescence assay using ATP determination kit from Molecular Probes (A220066) as per manufacturer's protocol. First, the standard curve was measured using different concentration of ATP solution (1nM - 1µM) mixed with the standard solution. The cells treated with different conditions were subjected to the cycle of free and thaw (X3) to lyse the cells and release the ATP. They were then centrifuged at 12000 rpm for 10mins and the 10µL of the supernatants were used for the assay that was mixed with 100µL of the standard solution. The Berthold Detection Luminometer was used to measure the luminescence. The data is expressed as a relative ATP level as compared to the untreated control (Mock).

Luciferin + ATP + O2 (Mg^{2+})(Luciferase) → oxyluciferin + AMP + pyrophosphate + CO2 + light

NAD+/NADH Ratio

Differentiated SH-SY5Y cells subjected to different treatment conditions were first washed with cold PBS then scraped and transferred to a 1.5mL microcentrifuge tubes to be centrifuged at 2,000 rpm for 5 minutes. The cells were then extracted by homogenizing with 400 µL of NADH/NAD extraction buffer. The cells were then vortexed for 10 seconds and centrifuged at 13,000 x g for 10 minutes to remove any insoluble materials. The extracted NAD/NADH supernatants were then transferred into a 96 well plate with the final volume of 50µL. This is used to measure NAD. The second set was prepared by aliquoting 200 µL of the extracted samples into a microcentrifuge tubes and heating them to 60˚C for 30 minutes in a heat block. The samples were then

cooled on ice, spun down and transferred 50µL into the plate. This is used to measure NADH. 100µL of the Master Reaction and 10µL of the NADH Developer were added on each sample. The absorbance was measured at 450 nm (A_{450}) at different time points (half hr, 1 hr and 2 hr) using a Modulus microplate reader. The ratio of NAD/NADH was calculated using a formula below:

$$\text{Ratio} = \frac{NAD_{total} - NADH}{NADH}$$

Where, NAD_{total} = Total amount of NAD (NAD + NADH)

NADH = Amount of NADH

mtDNA copy number

Total genomic DNA was extracted from differentiated and gp120 treated SH-SY5Y cells with different treatment conditions. To measure mtDNA quantitative real time PCR was performed with SYBR green (ROCHE). The primer sequences used for mtDNA were: mt F (CGA AAG GAC AAG AGA AAT AAG G) and mt R (CTG TAA AGT TTT AAG TTT TAT GCG) and β-Globin as an external control β-Globin F (CAA CTT CAT CCA CGT TCA CC) and β-Globin R (GAA GAG CCA AGG ACA GGT AC) purchased from IDT. The copy number was measured as a ratio of mt gene from the D loop over a nuclear gene β Globin.

Mitochondrial membrane potential

Mitochondrial membrane potential was measured using the guava MitoPotential assay which is based on fluorescence. JC-1, a cationic dye, which changes color with the

change in the membrane potential to either green or orange. The polarized mitochondria causes JC-1 to accumulate in the mitochondria forming J-aggregates and fluoresce orange (~590nm) and with the loss of the membrane potential the mitochondria become depolarized thus losing the concentration of the dye and dissociation of the J-aggregates and will fluoresce green (~530nm). The differentiated SH-SY5Y cells with different treatment conditions were seeded at 5 x 10^5 cell/mL. After the treatment the cells were trypsinized and re-suspended in the warm DMEM F-12 medium containing 2µM of JC-1 and incubated them in a 96 well microplate for 30mins. Carbonyl cyanide *m*-chlorophenyl hydrazine (CCCP) was used as a control for the membrane depolarization. Guava easyCyte HT system was used to measure the mitochondrial membrane polarization (MMP) and the data was analyzed with the software provided by Guava easyCyte 2.7.

Mitochondrial Mobility

SH-SY5Y cells were seeded on the glass bottom plate and transfected with pDsRed2-Mito plasmid (Clontech) using lipofectamine 2000 (Invitrogen) to fluorescently label the mitochondria. The transfection media (Opti MEM) was replaced with the differentiation media after 4-6 hours and the cells were left to differentiate for 94 hours. The cells were then subjected for different treatment conditions. The cells were then visualized using Leica EL600 DMI3000 confocal microscope for live cell imaging. The videos were captured for total length of 5 mins with 5 second interval. The area of the cell visualized was focused on the processes and not the cell body. Mitochondrial movement along the processes were represented in the form of kymograph. Image J was used to draw the kymograph by using MultipleKymograph plug in. The vertical straight

line represents the immobile mitochondria whereas, the dotted line along the horizontal axis represents the mobile mitochondria. Percentage of motile mitochondria was measured based on the mitochondria in the processes (mitochondria in the soma were not included). Mitochondria in a field of view were manually classed as moving if they moved >2 μm throughout the movie. Mitochondrial velocity was measured manually by drawing lines using the mouse cursor to track the mitochondrial displacement and recording the total time taken. (V= total displacement/total time taken μm/sec).

Statistical Analysis

Statistical analysis was performed using either Student's t-test or one-way analysis of variance. Data are expressed as the mean of $\pm$ S.D. Results were judged statistically significant if $P<0.05$. (Marked in the figures as *p<0.05, **p<0.01, ***p<0.001 where needed). Data were plotted using GraphPad Prism version (5.0 or 7.0) or Excel.

Results

CREB expression in HIVE and gp120 transgenic mice brain

CREB is a transcription factor and its activity depends on its phosphorylation at S133 (Mayr & Montminy, 2001). It regulates the transcription of its target genes by binding to their CRE binding site. CREB has been shown to play an important role in learning and working memory. Its dysfunction could lead to neurodegeneration (Mantamadiotis et al., 2002; Morris & Gold, 2012). To examine the effect of HIV on CREB, we examined the expression in the human brain and gp120-tg mice brain slides. We observed decreased CREB (Figure 6B) and pCREB S133 (Figure 6A) expression in HIVE brain tissue versus the age matched control. Additionally, HIV-1 gp120-tg mice of 9 month brain also had decreased total CREB expression as shown in Figure 7. About 50-60% decrease in pCREB and CREB has also been reported in the post mortem brain of Alzheimer's disease and Aβ-tg mice (Pugazhenthi, Wang, Pham, Sze, & Eckman, 2011) suggesting the decreased CREB expression could impact the proper brain functioning and alter learning and memory.

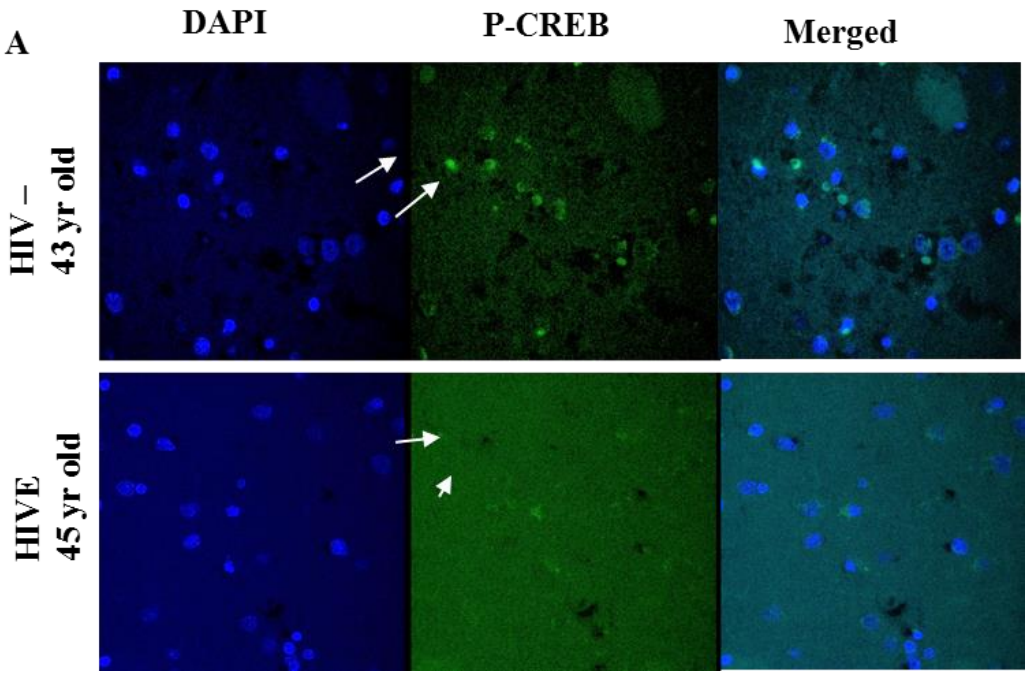
A
DAPI
P-CREB
Merged
HIV –
43 yr old
HIVE
45 yr old

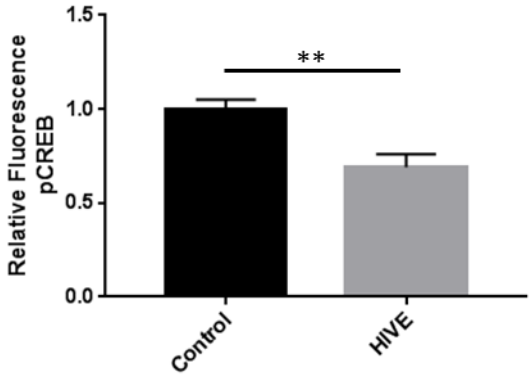
Relative Fluorescence
pCREB
1.5
1.0
0.5
0.0
**
Control
HIVE

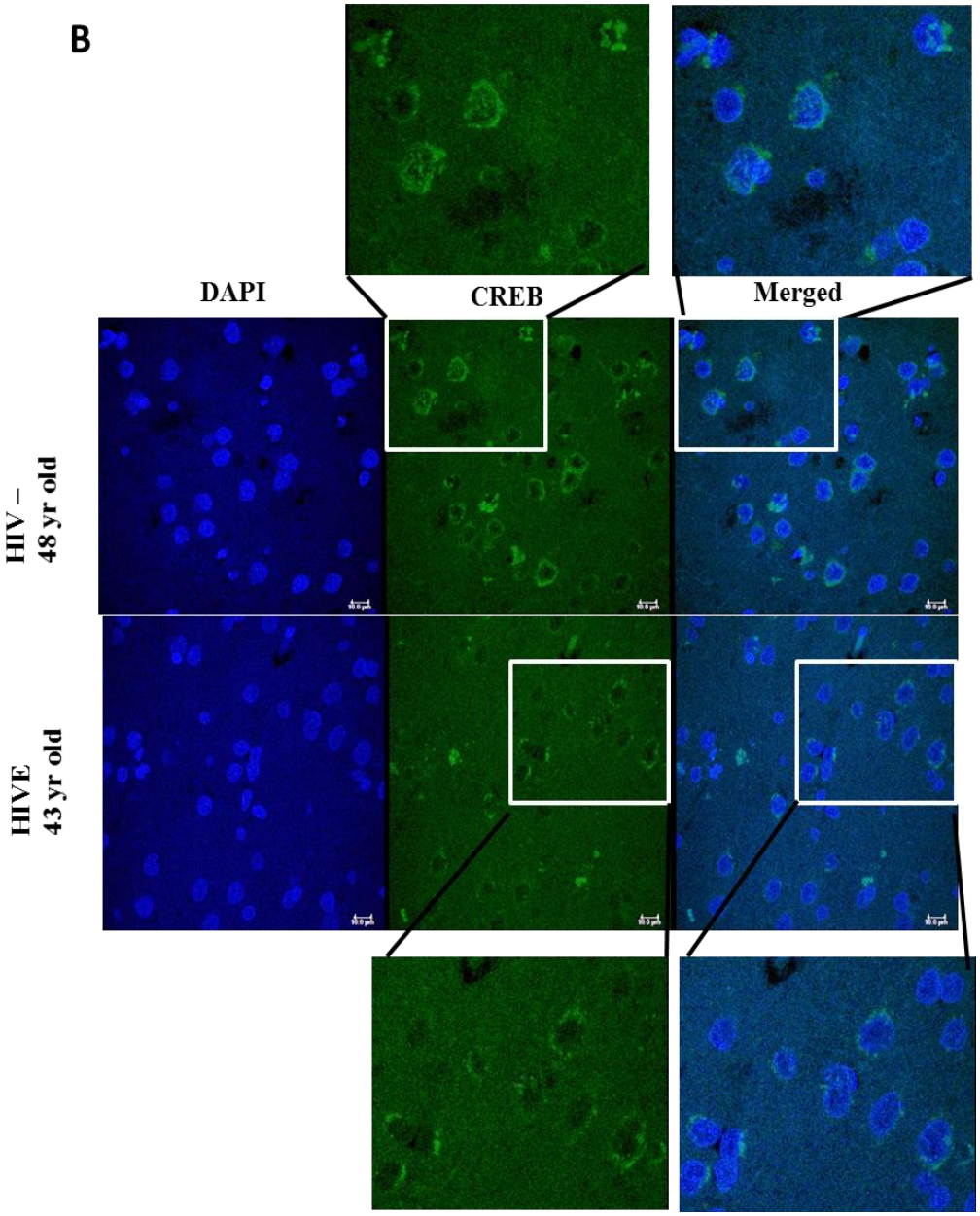
B
DAPI
CREB
Merged
HIV –
48 yr old
HIVE
43 yr old

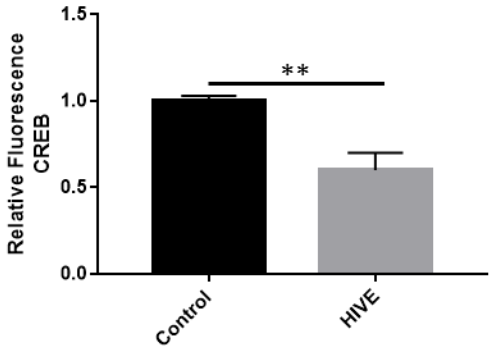
Relative Fluorescence
CREB
1.5
1.0
0.5
0.0
**
Control
HIVE

Figure 6. Altered CREB and phosho-CREB expression in HIVE brain tissue. (A) Distribution and expression of phospho-CREB and quantification of the fluorescence intensity in the brain tissue of HIV- and HIVE as observed via immunohistochemistry assay (B) Distribution and expression of total CREB and quantification of the fluorescence intensity in the brain tissue of the HIV- and HIVE as observed via the immunohistochemistry assay. (Green – Total and phospho-CREB, Blue – DAPI). Images were captured using Leica EL600 DMI3000 confocal microscopy. Fluorescence intensity represents the mean $\pm$ S.D. from 5 separate frames from two slides of each conditions (n=2). Due to limited number of slides that could be obtained from NNTC only 2 slides per proteins were used). The significance was measure using Student's t-test. The results were judged statistically significant if $P<0.05$. (*p<0.05, **p<0.01, ***p<0.001)

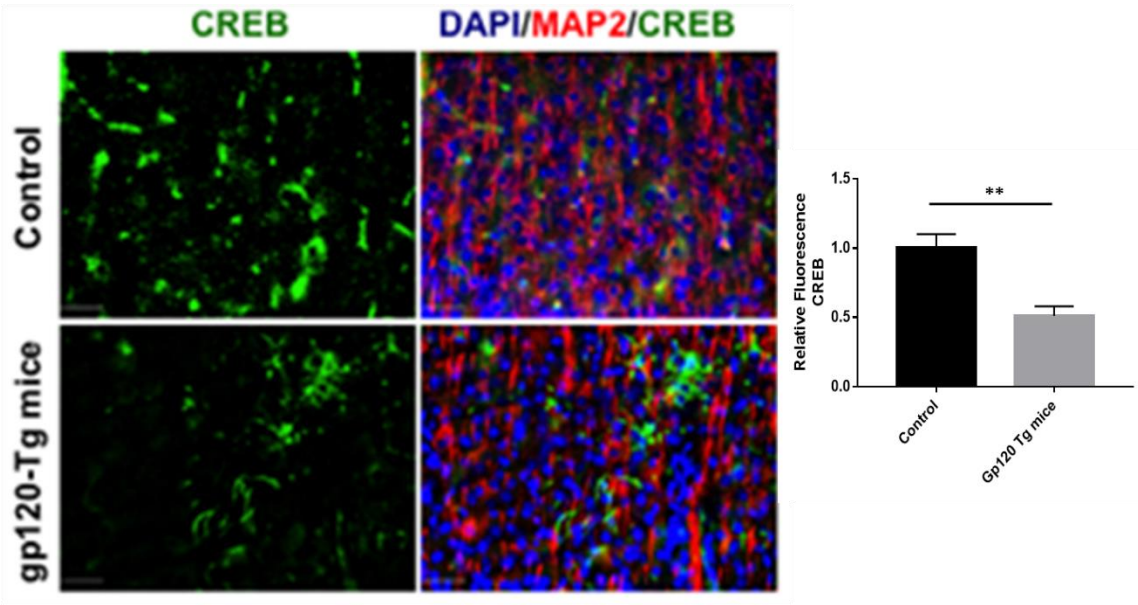

Figure 7. Altered CREB expression in HIV-1 gp120-tg mice brain. The expression of total CREB and the relative fluorescence quantification in the hippocampal brain slides of the 9 month old HIV-1 gp120 transgenic mice and the age matched control mice. (Green – CREB, Red – MAP2, and Blue – DAPI). (Gp120-tg mice brain staining data was done in collaboration with Marcus Kaul at his laboratory). Data represent the mean $\pm$ S.D (n=3). Statistical significance was analyzed using Student's t-test and the results were judged statistically significant if $P<0.05$ (**p<0.01).

Gp120 downregulates CREB in vitro

Next, we investigated the expression level of CREB and pCREB S133 with HIV-1 gp120 treatment in differentiated SH-SY5Y cells and primary human neurons (Figure 8B) and mouse neurons (not shown). Both CREB and pCREB protein expression (Figure 8A) and CREB mRNA (Figure 8B) decreased with gp120 treatment as compared to the untreated control.

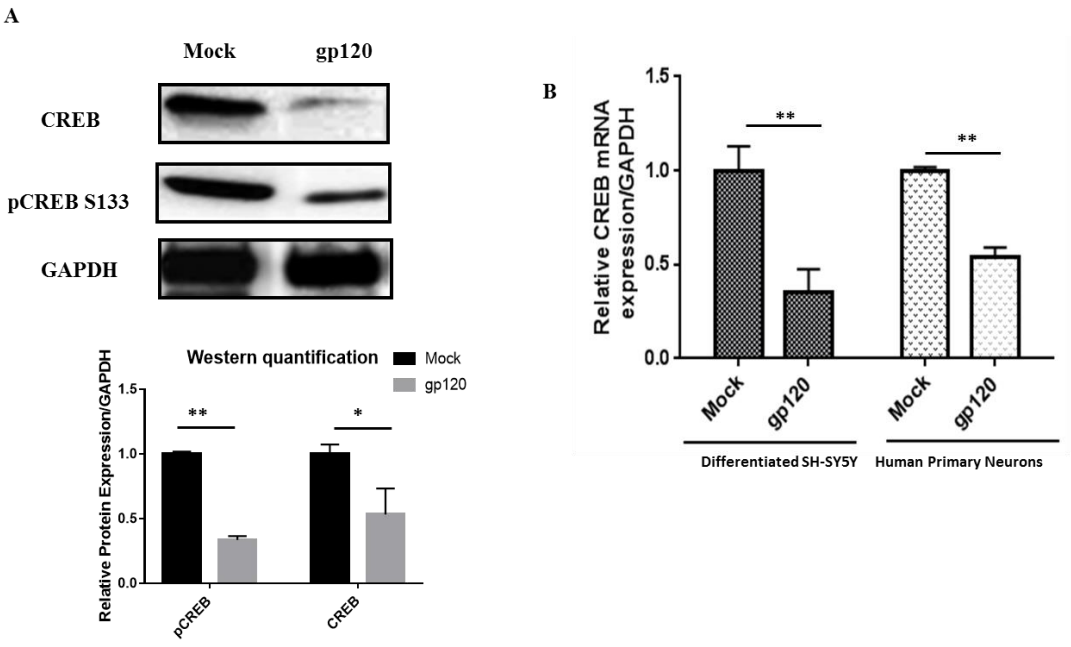

Figure 8. Deregulation of CREB in HIV-1 gp120 treated cells (A) Western blot analysis of the protein expression of total CREB and phospho-CREB and GAPDH was the loading control. Quantitative analysis of the western blot presented along with the bands. (B) Relative mRNA CREB expression normalized to GAPDH as an internal control in differentiated SH-SY5Y cells and human primary neurons. Data represent the mean ± S.D. calculated from three independent experiments (n=3). Results were judged statistically significant using Student's t-test if $P<0.05$. (*p<0.05, **p<0.01, ***p<0.001).

Downstream Targets of CREB

CREB deregulation has been associated with altered synapse formation and neuronal functioning. CREB also has several downstream targets that regulate mitochondrial (PGC-1α, COX I, COX III) and synapse (BDNF, miR-132, DNMTs) activity. In this study we will examine each of these downstream targets to understand gp120 mediated deregulation of CREB and its effect on mitochondrial function and synaptic factors that could alter learning and working memory.

Neuronal Factors

Gp120 leads to alteration of pre and post synaptic factors

Decreased brain density (Mukerjee et al., 2011) and 15% cortical thinning (Thompson et al., 2005) has been observed in the HIV brain based on the MRI scans. This could be due to a loss of dendritic structure or a neuronal size (Freeman et al., 2008). Loss of neuronal processes has been observed in the presence of Tat (Mukerjee et al., 2008) and rodents model of HIV HAND (Gorantla, Poluektova, & Gendelman, 2012). Decreased CREB activity has also been associated with loss of dendritic abnormality (Villeda et., al, 2014). To determine if HIV-1 gp120 affects the neuronal morphology and area, we first examine the total surface area covered by differentiated SH-SY5Y cells before and after HIV-1 gp120IIIB and gp120C treatment.

The total surface area decreased in gp120 IIIB treated cells as compared to untreated (Mock) and gp120C treated cells as shown in Figure 9A. Proper neuronal communication via synapse formation is critical for learning and information processing. Proper synapse formation depends on the integrity of pre and post synaptic factors.

Damaged neuronal dendrites and axons were observed in HIVE brain along with gp120-tg mice as compared to the controls (Ellis, Langford, & Masliah, 2007). Next, we examined the number of synapse formation by counting the number of synaptophysin vesicle formation and PSD95 expression. Synaptophysin (also known as p38) is one of the major protein components of the synaptic vesicles in the pre-synaptic neurons (Eastwood, Burnet, McDonald, Clinton, & Harrison, 1994) and PSD95 (post synaptic density 95) is a scaffold protein present on the dendrites of the post synaptic neurons and has been used as a synaptic markers. In differentiated SH-SY5Y cells, either treated or untreated with gp120, we observed decreased synaptic vesicle formation based on the number of synaptophysin (Figure 9B) and decreased PSD95 expression (Figure 9C). miR-485-5p has been associated with decreased dendritic formation. With gp120 treatment we have observed increased miR-485-5p expression (Figure 13D) suggesting its possible role in altering dendritic formation.

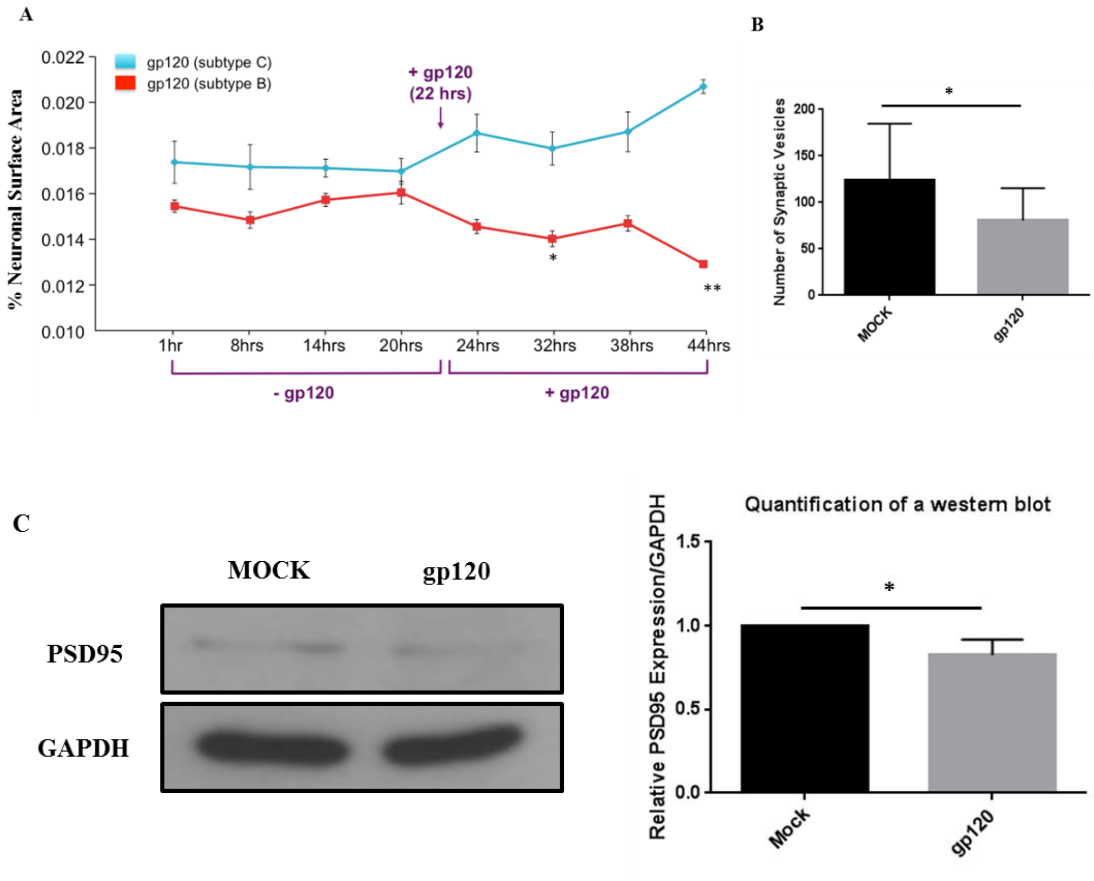

Figure 9. HIV-1 gp120 treatment leads to altered synaptodendritic factors (A) SH-SY5Y cells were seeded at 40% confluency in a culture dish with 10µM retinoic acid for differentiation into neurons. After differentiation, the plates were placed on a live cell imaging station and the bright field contract images were acquired every 30 minutes from the same field. The images were analyzed with Image J software and the surface area covered by the cells was normalized against the total number of the cells in each time point. The experiment was repeated with gp120 supplemented medium added at 20 hour. (B) Synaptophysin was expressed in the cells by incubating the cells with Cell Light Transduction at MOI 5 for 24 hours. The cells were either untreated or treated with gp120 for another 24 hours post transduction. Images of the live cells were acquired after the

treatment using EVOS. Synaptophysin vesicle number and size were calculated using Image J for each condition. The experiment was repeated 3 times and the images from 10 different fields were taken for each set for the statistical significance. (C) Western blot analysis of PSD-95 and the loading control GAPDH along with the quantitative analysis of the western blot data using Image J. Data represent (Mean $\pm$ S.D.) of 3 independent experiments (n=3). Results were judged statistically significant using Student's t-test if $P<0.05$. (*$p<0.05$)

HIV and gp120 leads to altered downstream targets of CREB

BDNF is one of the downstream targets of CREB that is important for synaptic connection. We also observed decreased expression of BDNF at both the protein (Figure 10B) and mRNA level (Figure 10A) in gp120 treated primary human neurons and differentiated SH-SY5Y cells. Similarly, HIVE brain tissue also showed decreased BDNF expression as compared to the control. Along with the expression, BDNF localization was also altered in HIVE brain with less expression and dispersed localization. Control brain had the BDNF expression localized in the peri-nuclear area and HIVE brain has the dispersed expression (Figure 10C). The role of BDNF in regulating HIV-1 co-receptors CCR5 and CXCR4 in a rodent model and SH-SY5Y cells has been reported (Ahmed, Tessarollo, Thiele, & Mocchetti, 2008). BDNF is critical to maintain the synapse between two neurons by binding to its receptor TrkB. Significant decrease in BDNF has been reported in the hippocampus of the AD brain samples (Phillips et al., 1991). Along with BDNF, another important neuronal factor SIRT1 expression also decreased in gp120 treated cells (Figure 11C). Two major regulators of BDNF are SIRT1 via MeCp2 (Zocchi & Sassone-Corsi, 2012) and CREB (Hong, McCord, & Greenberg, 2008). Taken together, these data suggest that HIV-1 gp120 treatment leads to neuronal injury by targeting both pre and post-synaptic factors.

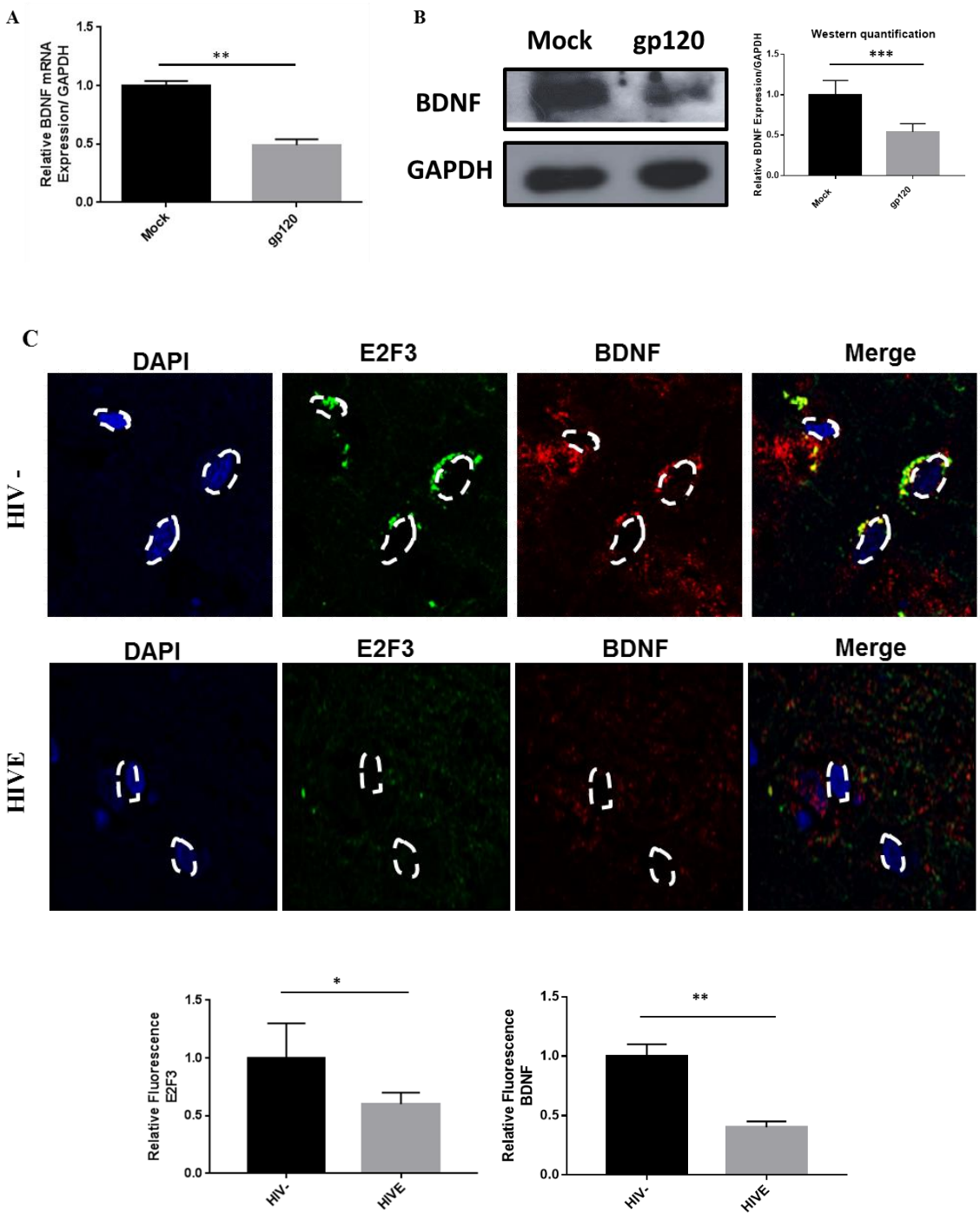

Figure 10. **Deregulation of BDNF expression and distribution in the presence of gp120 and HIVE brain.** (A) Relative mRNA expression of BDNF normalized to GAPDH as an internal control (n=3). (B) Western blot analysis of BDNF and a loading

control GAPDH in mock and gp120 treated human primary neurons and quantitative analysis of the western blot presented along with the bands (n=3). (C) Immunohistochemistry assay showing the expression and distribution of E2F3 (Green) and BDNF (Red) in the human brain tissue of control (HIV-) and HIVE patient along with relative quantification of the fluorescence using ImageJ. The images were obtained using Leica EL600 DMI3000 confocal microscopy. Data represent the mean $\pm$ S.D. The fluorescence quantification represents data calculated from 5 separate fields from 2 slides (n=2 due to limited number of slides that could be obtained from NNTC) of each conditions (HIV- and HIVE). Results were judged statistically significant using Student's t-test if $P<0.05$. (*p<0.05, **p<0.01, ***p<0.001).

The activation of CREB protein also leads to the activation of its downstream miRNA (miR-132), which in turn controls the expression of DNMT3a (Lv et al., 2013). DNA methyltransferase 3a protein (DNMT3a) is responsible for methylation of CRE site. Therefore, we examined whether suppression of CREB expression leads to inhibition of its downstream target- miR-132, which permits activation of DNMT3a protein. Hence, DNMT3a, DNMT3b (Figure 12B and C) expression increased while, miR-132-3p (Figure 12A) expression decreased with HIV-1 gp120 treatment. DNMTs could be involved in methylation of the promoters of the genes involved in mitochondrial and neuronal functioning thus inhibiting their activity.

CREB could be regulated both transcriptionally and post translationally. At the transcription level CREB is regulated by several micro-RNAs upstream. We focused on miR-34a and miR-134. Our lab identified that miR-34a regulates CREB via E2F3 (Bagashev et. al. unpublished). miR-34a expression increased with Tat (J. R. Chang et al., 2011) and Vpr (Mukerjee et al., 2011) treatments as well. HIV-1 gp120 treatment led to increased expression of miR-34a and miR-134 (Figure 11B) in differentiated SH-SY5Y cells, primary human and primary mouse neurons (data not shown). miR-34a is extensively studies in cancer and have entered phase 1 clinical trial for liver cancer (X. J. Li, Ren, & Tang, 2014). E2F3 expression on the other hand decreased in the presence of gp120 (Figure 11A) and in HIVE brain (Figure 10C). These data suggest that gp120 could be targeting CREB via microRNAs. However, it is not known whether the effect of gp120 on these miRNAs are direct or indirect. Altered mRNA and pCREB expression with gp120 treatment suggest that the capability to affect CREB via multiple

mechanisms. In this study we are more interested in the downstream targets of CREB and their effect on the mitochondrial and neuronal functions.

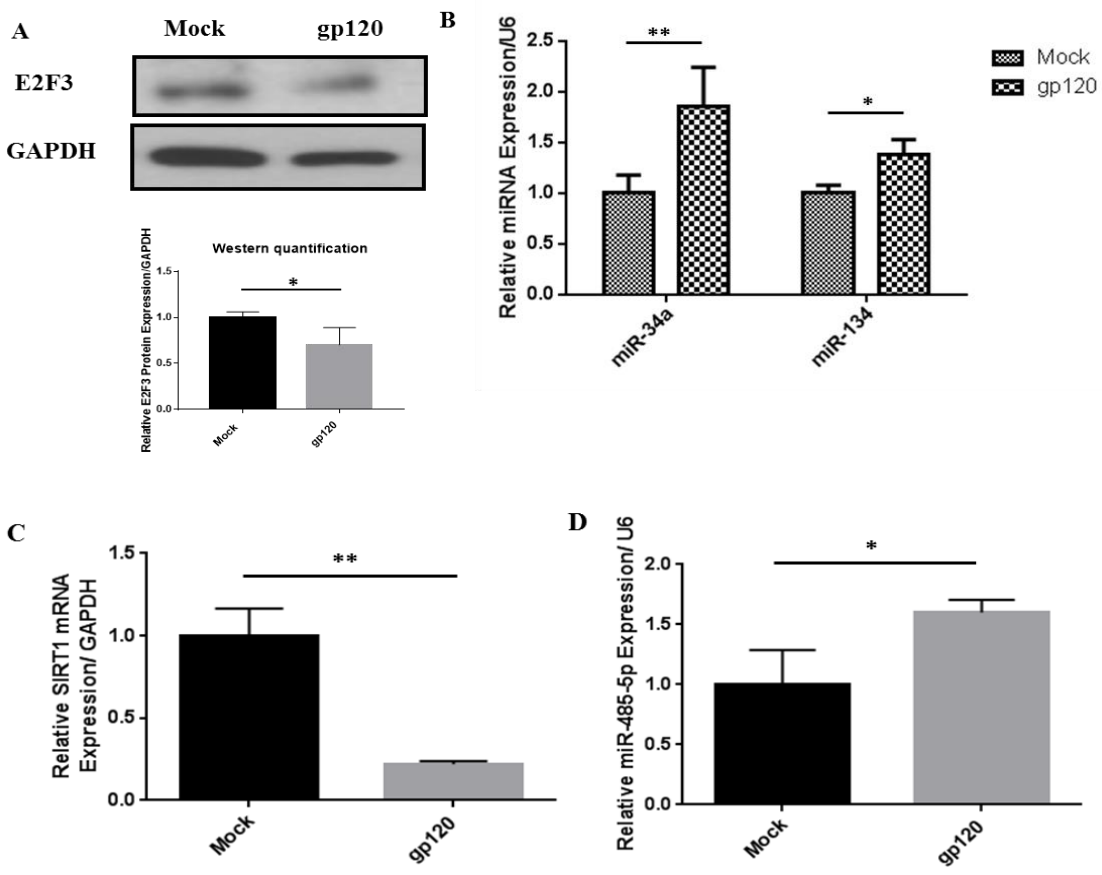

Figure 11. Deregulation of E3F3, SIRT1 and miRNAs (A) Western blot analysis representing a protein expression of E2F3 and GAPDH as a loading control along with the quantitative analysis of the western blot presented along with the bands (n=3). (B) Relative expression of miR-34a and miR-134 relative to the internal control U6 (n=3). (C) Relative mRNA expression of SIRT1 normalized to an internal control GAPDH in untreated mock and gp120 treated SH-SY5Y cells (n=3). (D) Relative expression of miR-485-5p normalized to an internal control U6 in Mock (untreated) and gp120 treated SH-SY5Y cells (n=3). Data presented is the representation of 3 independent experiments (n=3) with mean $\pm$ S.D. Results were judged statistically significant using Student's t-test if $P<0.05$. (*p<0.05, **p<0.01)

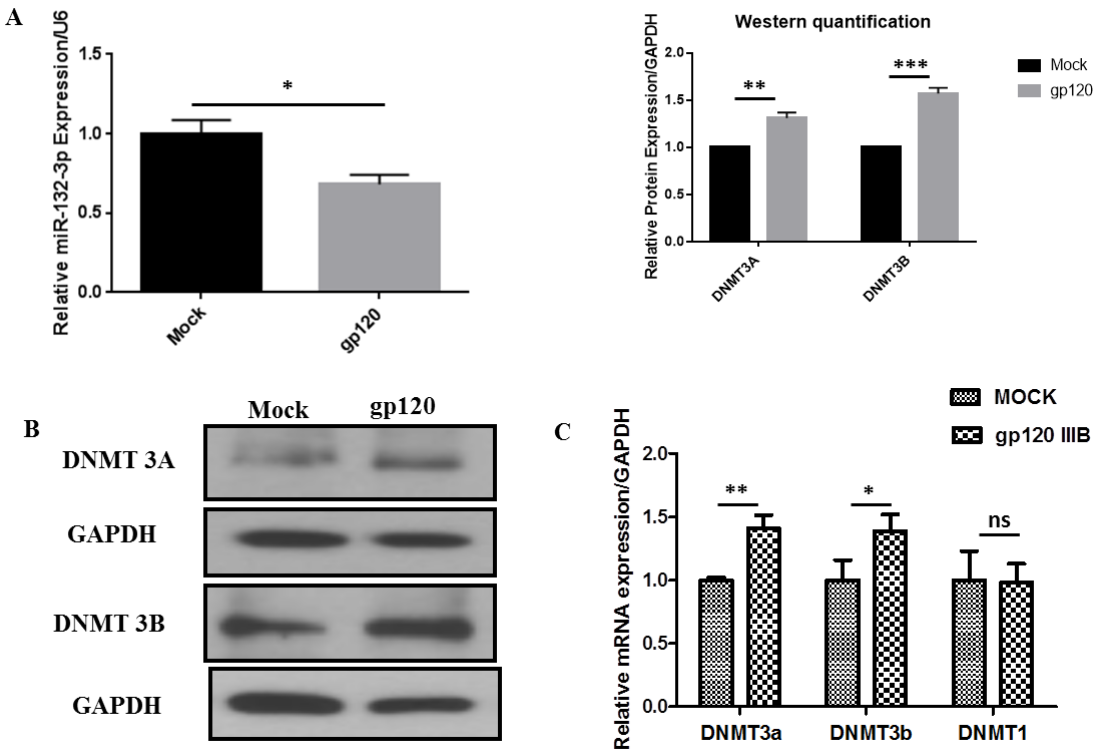

Figure 12. Deregulation of miR-132-3p and DNMTs with gp120 treatment (A) Relative expression of miR-132-3p and U6 as the internal control. (B) Western blot analysis of DNMT3a and DNMT3b with GAPDH as a loading control and the densitometer of the bands (C) Relative mRNA expression levels of DNMT3a, DNMT3b and DNMT1 normalized to GAPDH as an internal control. Data represent the mean $\pm$ S.D. (n=3) of three independent experiments. Results were judged statistically significant using Student's t-test if $P<0.05$. (*p<0.05, **p<0.01, ***p<0.001, ns = not significant)

Mitochondrial factors

Gp120 alters mitochondrial bioenergetics

Mitochondria are the powerhouse of the cell and drive the production of ATP via an electron transport chain and ATPase synthase. Additionally, PGC-1α is regarded as the regulator of the genes that are involved in electron transport chain and mitochondrial bioenergetics (Wu et al., 1999). PGC-1α is also one of the direct targets of CREB (Cheng et al., 2012). Therefore, we checked the expression of several of the genes and proteins involved in mitochondrial electron transport chain and also of PGC-1α. We observed that gp120 treatment on differentiated SH-SY5Y cells lead to decreased expression of PGC-1α and ND5 protein expression (Figure 13A) and also altered the gene expression of PGC-1α, COX I and COX III (Figure 13B). Aberrant ETC gene expression has been linked to altered ATP production (Navarro & Boveris, 2007). To test the integrity of a mitochondrial function, we measured the ATP production using a luciferase assay kit in differentiated SH-SY5Y cells after 24 hours the gp120 treatment. There was a decrease in ATP level in the treated cell as compared to the untreated control (data not shown). We also validated this by measuring ADP/ATP ratio where we see increased ADP/ATP ratio in the presence of gp120 as compared to the untreated control (Figure 13C). ADP/ATP ratio is another method to measure the cellular energy. Increased in the ratio indicates more ADP whereas, decrease in the ratio indicates more ATP. Therefore, an increase in the ADP/ATP ratio in gp120 treated cells indicated less ATP in these cells. The ratio was also measure in the presence of AMD3100, the inhibitor of CXCR4, to examine whether blocking the receptor of gp120 binding site could have a protective effect on the cellular energy production. As shown in figure 13C, blocking CXCR4 did not prevent the effect

of gp120. As mentioned earlier most CNS infections reported are M-tropic (R5) and few are dual tropic (R5X4), here we used T tropic (X4 – CXCR4 dependent gp120). SH-SY5Y cells do express CXCR4 but based on the studies indicating internalization of gp120 with pinocytosis and lipid raft (Berth, Caicedo, Sarma, Morfini, & Brady, 2015; Tanaka et al., 2012), it is possible that the effect of gp120 might not be completely receptor dependent. This explain the partial effect of AMD3100. Additionally, gp120 treatment also caused altered NAD/NADH ratio (Figure 13D) thus indicating its effect on complex I of ETC. Rotenone, the inhibitor of complex I in the electron transport chain, was used as a control. Rotenone led to decreased NAD/NADH ratio as shown in Figure (13D) Loss of mitochondrial bioenergy leads to alteration of mitochondrial distribution (Stojkovic et al., 2001) and loss of neuronal communication (Vos, Lauwers, & Verstreken, 2010), which explains the alteration of working memory and learning deficit.

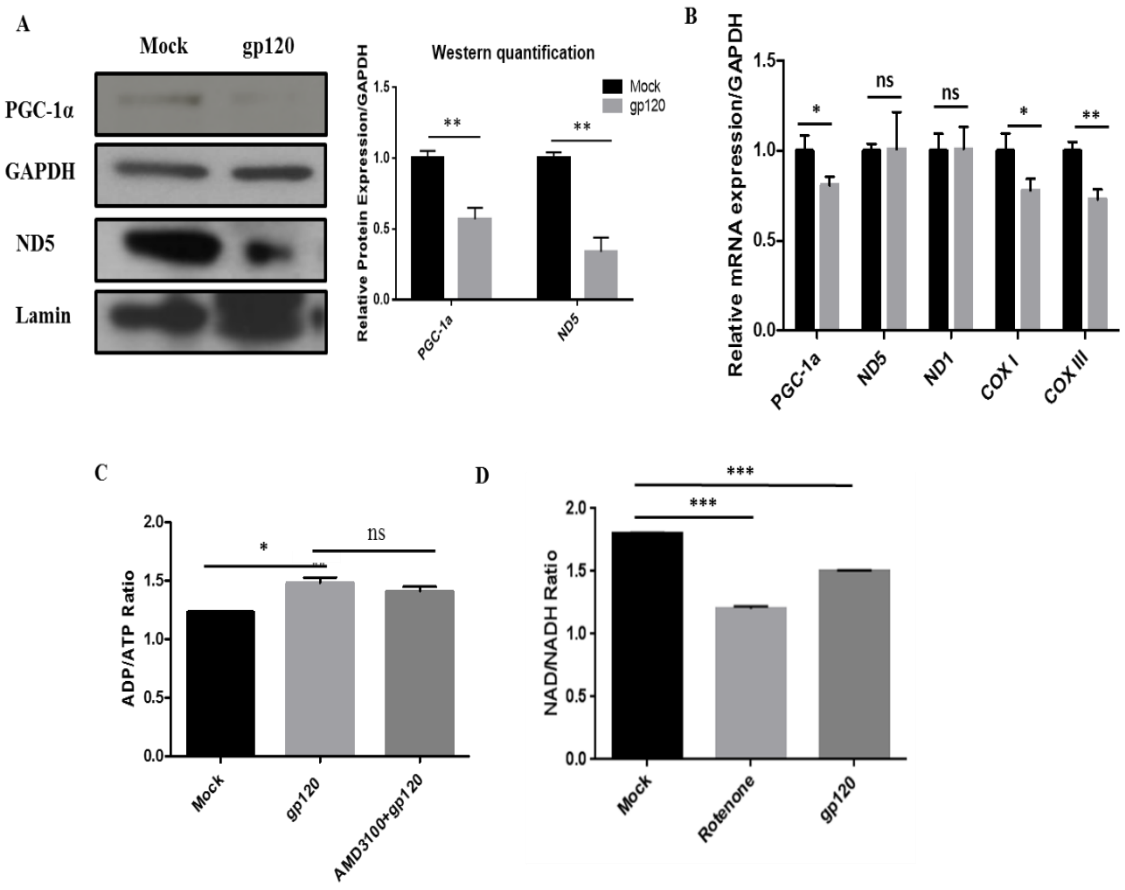

Figure 13. HIV-1 gp120 treatment leads to altered mitochondrial bioenergetics (A) Western blot analysis of PGC-1α and ND5 involved in mitochondrial biogenesis and energetics. GPADH and Lamin were used as the loading controls. Quantitative analysis of the western blot presented along with the bands. (B) Relative mRNA expression of PGC-1α, ND5, ND1, COX1 and COXIII relative to an internal control GAPDH involved in mitochondrial bioenergetics and electron transport chain. (C) Measurement of ADP/ATP ratio in Mock (untreated), gp120 treated and AMD3100+gp120 treated SH-SY5Y cells to determine the effect of gp120 on mitochondrial bioenergetics. AMD3100 pre-treatment was used an inhibitor for CXCR4 to inhibit the effect of gp120. (D) Measurement of NAD/NADH ratio in mock (untreated), gp120 treated and rotenone

treated cells to examine the ETC function. Rotenone is a complex I inhibitor and was used as a positive control. Data presented is the representation of 3 independent experiments (n=3) and the p-values were calculated using Student's t-test (Figure A and B) or one-way ANOVA followed by Dunnett's multiple comparisons test (Figure C and D). Results were judged statistically significant if $P<0.05$. (*p<0.05, **p<0.01, ***p<0.001, ns = not significant)

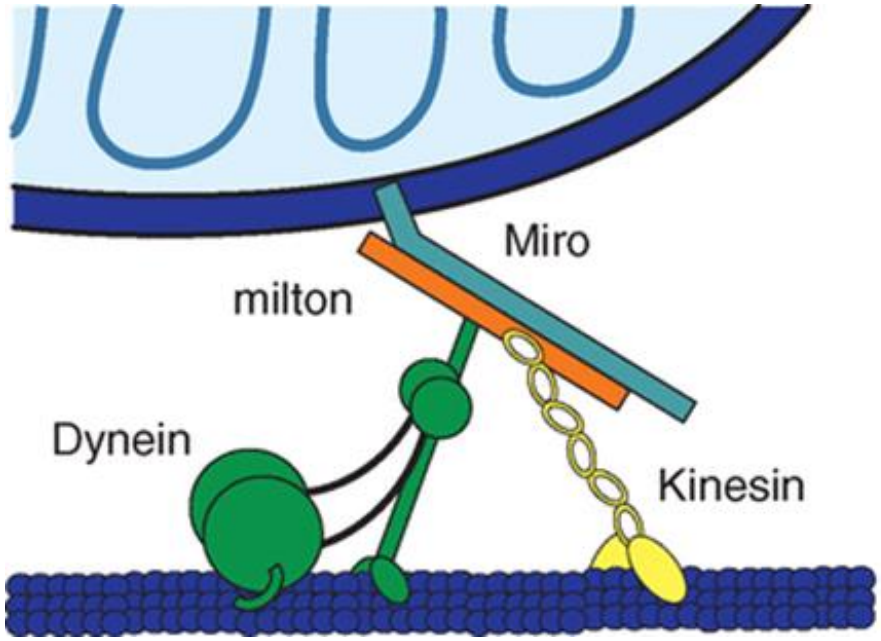

Figure 14. Schematic representation of proteins involved in mitochondrial movement. (Schwarz, 2013)

Gp120 alters motor proteins

Neurons are high energy demanding cells therefore, mitochondrial dynamics is critical for its function. One of the important roles of mitochondria in neurons is their transport along the processes. This complex mechanism of mitochondrial movement is driven by two motor proteins kinesin and dynein that drive the movement in the opposing directions. These motor proteins are linked to mitochondria via the adaptor protein trafficking kinesin protein (TRAK or Milton) and mitochondrial Rho GTPase (MIRO) which is present on the outer mitochondrial membrane (Figure 14). To visualize the mitochondrial movement along the processes, SH-SY5Y cells were first transfected with pDsRed2-Mito plasmid, then differentiated for 72 hours. Then, the cells were subjected to live cell imaging under a confocal microscope with $\pm$ gp120. A kymograph was drawn using ImageJ software using MultipleKymograph plug in from the video taken from the processes with the average length of 85μm to analyze their movement. gp120 treated cells had less mitochondrial movement (Figure 15A), decreased % of mitochondria and velocity (Figure 19B and C) than the mock. These data is the representation of retrograde and anterograde as a composite. Horizontal dotted line moving towards the right side represents the moving mitochondria. The vertical lines represent the immobile mitochondria during the represented time frame. Furthermore, mitochondrial movement is dependent on several motor and microtubule proteins. We observed altered expression of genes and proteins involved in mitochondrial movement such as MIRO, TRAK, KIF-1α (kinesin family member 1) and Dynein with gp120 treatment where all theirs protein expression were decreased (Figure 15B). Therefore, gp120 lead to altered mitochondrial movement by altering proteins and genes involved in the movement.

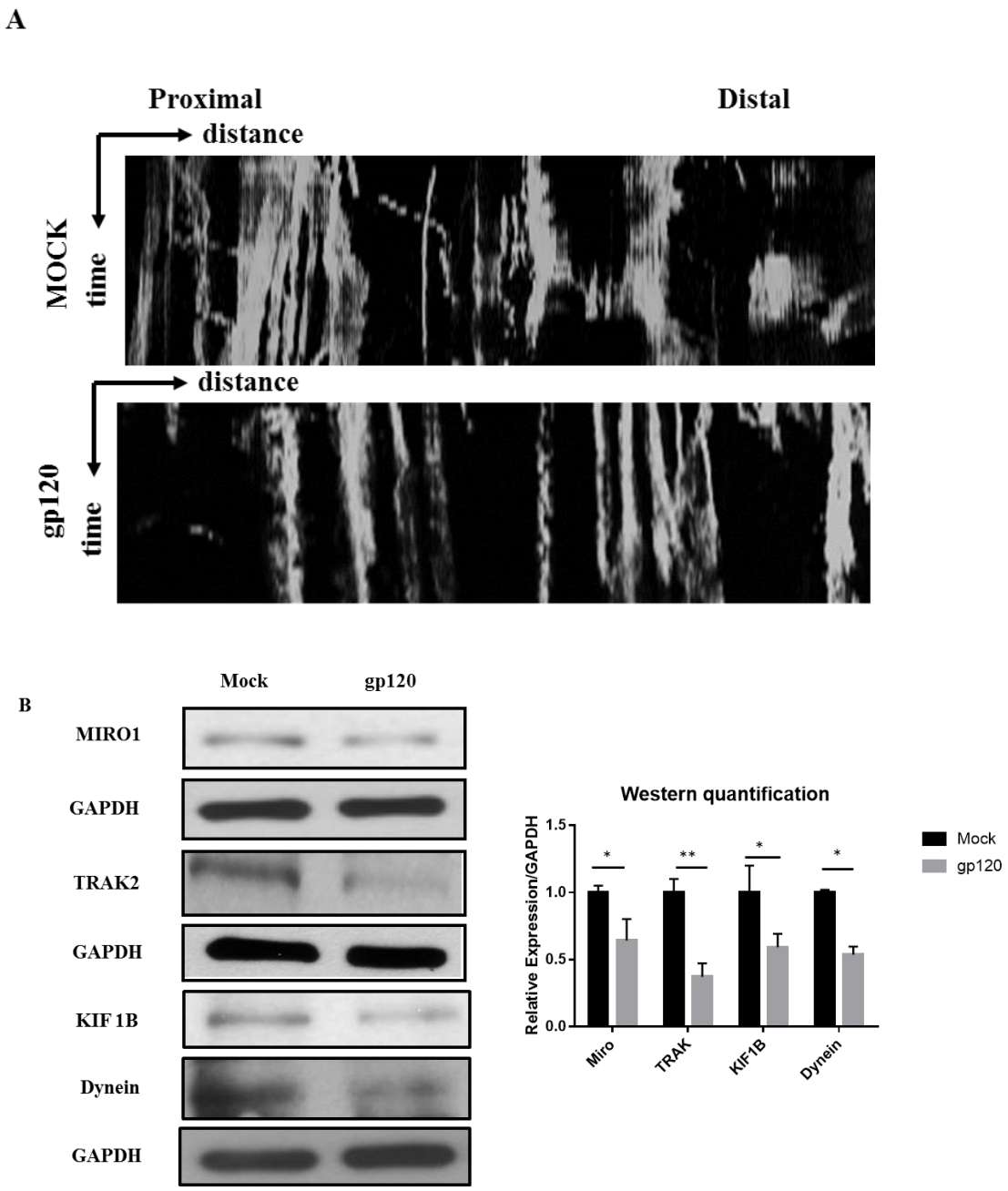

Figure 15. Altered mitochondrial movement and proteins with gp120 IIIB treatment

(A) A kymograph representing the mitochondrial movement in the untreated mock and gp120 treated SH-SY5Y cells. Horizontal axis represents the distance and vertical axis represents the time. Mobile mitochondria are distinguished by the dotted line moving along the horizontal axis. This data is the representation of 15-20 neurites per treatment

conditions repeated three times (n= 60 - 65 total neurites per treatment conditions). (B) Western blot analysis of MIRO1, TRAK2, KIF-1β and Dynein in untreated mock and gp120 treated SH-SY5Y cells showing decrease in the expression of proteins important for mitochondrial movement. GAPDH is used as a loading control. Quantitative analysis of the western blot presented along with the bands (n=3). Data represent the mean $\pm$ S.D. Results were judged statistically significant using Student's t-test if $P<0.05$. (*$p<0.05$, **$p<0.01$)

Mitochondrial membrane potential and mtDNA are altered in the presence of gp120

ROS is the byproduct of ETC and altered ETC leads to increased ROS. We observed increased ROS production with gp120 treatment (Figure 25 data shown in chapter 3). mtDNA is present in close proximity to the ETC in the matrix and are susceptible to ROS production, we measure the mtDNA copy number at different gp120 time point. Therefore, we observed time dependent decrease in mtDNA copy number in the presence of gp120 (Figure 16B). Next, we observed decreased membrane polarization with gp120 treatment in differentiated SH-SY5Y cells and CCCP (carbonyl cyanide m-chlorophenylhydrazone) was used as a control (Figure 16A). Taken together, these data suggest that gp120 is able to alter mitochondrial biogenesis and functions.

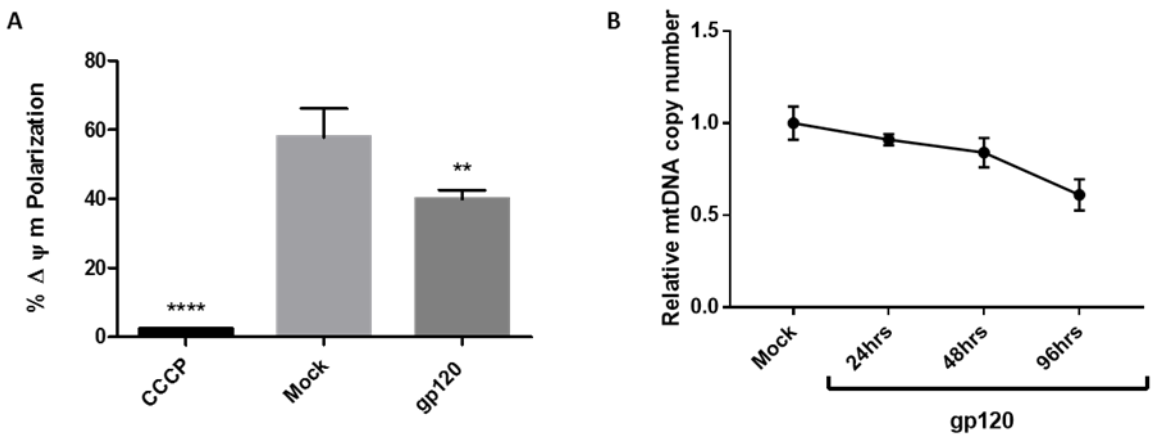

Figure 16. HIV-1 gp120 causes decrease in mitochondrial membrane polarization and mtDNA copy number (A) Mitochondrial membrane potential change was measured using JC-1 dye on differentiated SH-SY5Y cells subjected to different treatment conditions using Guava Flowcytometer. CCCP was used as control to determine the mitochondrial membrane potential collapse. (B) mtDNA copy number was determined by taking the mtDNA/β-Globin ratio for different time points. The data represent Mean ± S.D. of 3 independent experiments (n=3) and the significance were calculated using one way ANOVA followed by Dunnett's multiple comparisons test. The results were considered statistically significant if $P<0.05$. (**p<0.01, ***p<0.001)

Gp120 deregulates mitochondrial function through CREB

Alteration in mitochondrial genome, biogenesis, function and mobility could lead to synaptic damages and impaired transport (Vos et al., 2010). Several of these functions are assured by CREB (J. Lee et al., 2005). CREB also acts as an upstream regulator of the proteins involved in mitochondrial function- PGC-1α (Herzig et al., 2001) and ND5 (J. Lee et al., 2005). In the presence of gp120 we have observed both CREB and mitochondrial deregulation. Therefore, this gave us a rational to examine whether CREB is the major factor triggering the mitochondrial damage. Using the pharmacological activators and overexpression we examined its role on the mitochondrial factors. Here, we first examined the expression level of total and pCREB with salidroside and rolipram, a pharmacological activators of CREB. Rolipram and salidroside were able to overcome the inhibitory effect of gp120 and increased pCREB and CREB expression dramatically (Figure 17A). We also examined the CREB mRNA level by over expressing CREB with RSV CREB transfection (Figure 17B). Previously, we have shown decreased mtDNA in the presence of HIV-1 gp120 (Figure 16B). Therefore, we examined the status of mitochondrial DNA with rolipram and ethanol treatment where mtDNA copy number increased with rolipram but decreased with ethanol treatment (Figure 18A) thus indicating a critical role of CREB in mitochondrial genome integrity. Salidroside and rolipram also enhanced the mitochondrial bioenergetics as seen in Figure 18B, with increased ATP level and improved mitochondrial movement (Figure 19A). With gp120 treatment the percent of motile mitochondria decreased along with the average velocity (μm/sec) were also improved with rolipram treatment in gp120 treated cells (Figure 19B and C). Overexpression of CREB also improved the mtDNA copy number (Figure 18C).

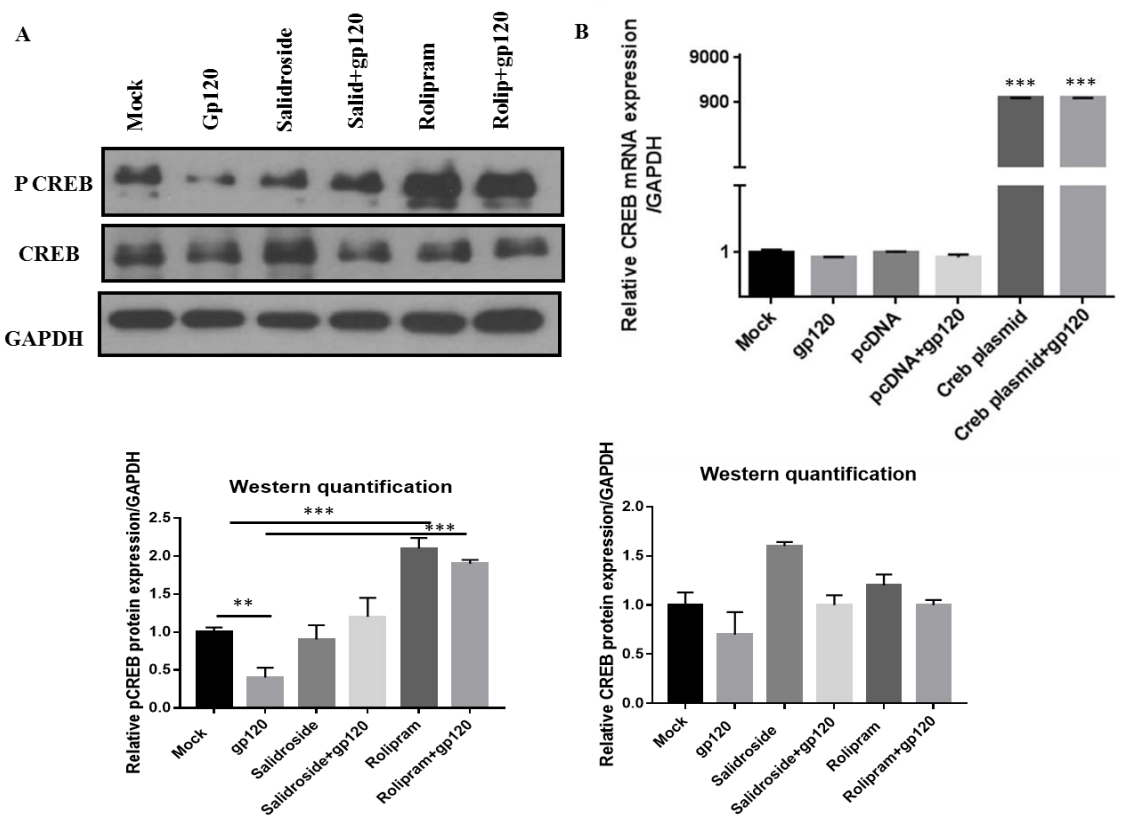

Figure 17. CREB overexpression and activation (A) Western blot analysis of the immunoblot representing the protein expression of the phosphor-CREB and total CREB of the samples subjected to different treatment conditions. GAPDH is represented as the loading control. Salidroside and Rolipram treatment led to increased expression and activation of CREB and also masked the effect of gp120. Quantitative analysis of the western blot presented along with the bands. (B) Relative mRNA expression of CREB normalized to the internal loading control GAPDH representing the effect of RSV CREB plasmid to increase CREB expression. The western quantification data presented depicts Mean $\pm$ S.D. from 3 independent experiments (n=3). Results were judged statistically significant if $P<0.05$ using one-way ANOVA followed by Tukey's multiple comparisons test. (**p<0.01, ***p<0.001)

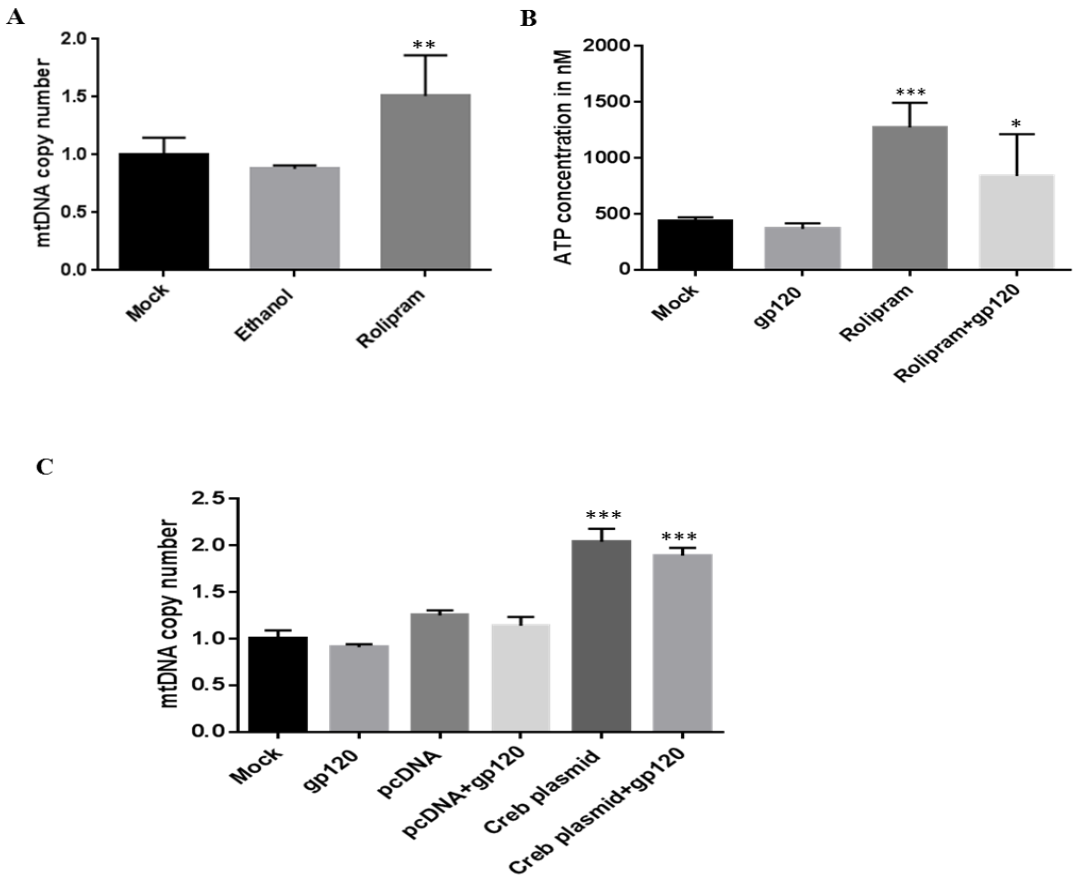

Figure 18. CREB activation reverses the effect of HIV-1 gp120 on the mtDNA and mitochondrial bioenergetics (A) mtDNAcopy number represented by measuring the ratio of mitochondrial genes over the nuclear gene (ratio of mtDNA/β-Globin) of a mock (untreated), ethanol and Rolipram treated. Ethanol is the inhibitor of CREB and rolipram activates CREB by inhibiting PDE-4. (B) ATP level in ηM range is measured using a luciferase assay. Rolipram rescues the effect of gp120. Thus, indicating the role of CREB in mitochondrial function. (C) Overexpression of CREB by transfection was also able to rescue the mitochondrial DNA copy number. The data presented here depicts Mean ± S.D. (n=3). Results were judged statistically significant if $P<0.05$ calculated using one-way ANOVA followed by Tukey's multiple comparisons test (*p<0.05, **p<0.01, ***p<0.001).

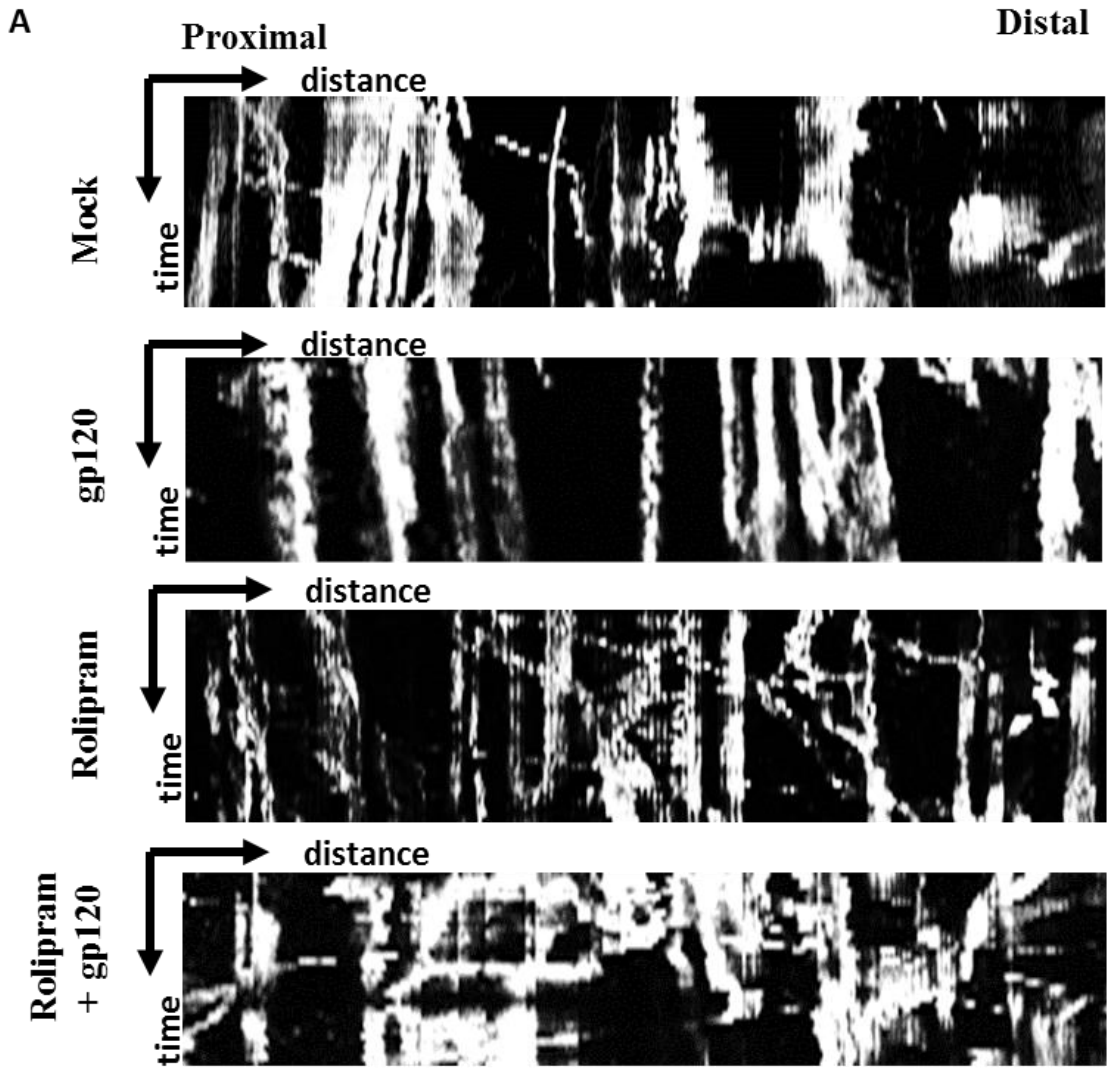
A
Proximal
Distal
distance
time
Mock
gp120
Rolipram
Rolipram + gp120

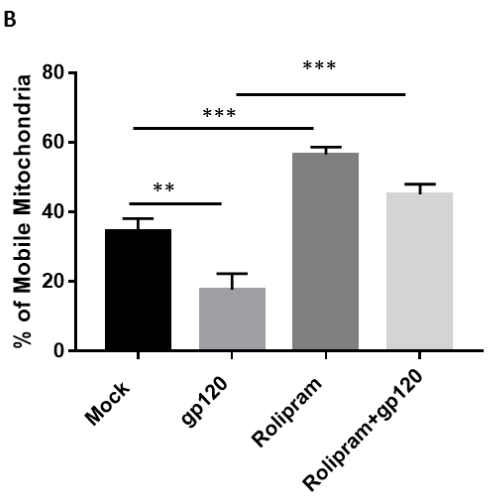
B
% of Mobile Mitochondria
80
60
40
20
0
**
***
***
Mock
gp120
Rolipram
Rolipram+gp120

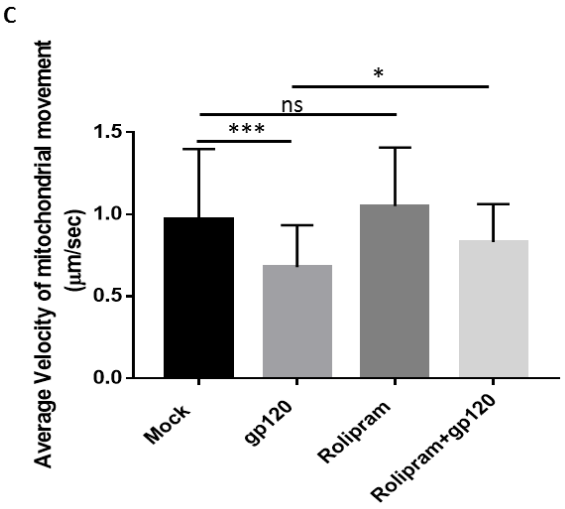
C
Average Velocity of mitochondrial movement (μm/sec)
1.5
1.0
0.5
0.0
***
ns
*
Mock
gp120
Rolipram
Rolipram+gp120

Figure 19. Rolipram treatment improves the mitochondrial movement. (A) Kymographs representing the mitochondrial movement in the untreated mock, gp120 treated, Rolipram treated and Rolipram+gp120 treated SH-SY5Y cells. Horizontal axis represents the distance and vertical axis represents the time. Mobile mitochondria are distinguished by the dotted line moving along the horizontal axis. The mitochondria were tagged using Mito ds-RED transfection and the movement was visualized using Leica EL600 DMI3000 confocal microscopy. Image J was used to create a kymograph. Data is the representation of 12-15 neurites per treatment condition each done in triplicate in 3 independent experiments. (B) Quantification of the percentage of motile mitochondria (Mock n=70, gp120 n=56, rolipram n=81, rolipram+gp120 n=81). (C) Average velocity of the motile mitochondria (n=48 per treatment conditions). Data represent the mean $\pm$ S.D. analyzed using one-way ANOVA followed by Tukey's multiple comparisons test (*$p<0.05$, **$p<0.01$, ***$p<0.001$).

Rolipram rescues the memory impairment in the animal model

Finally, using an animal model we were able to demonstrate the effect of rolipram in reversing the learning disability caused by gp120 treatment. This is a preliminary data obtained from the ongoing experiment done at the laboratory of Dr. Jeannie Chin where 8-10 weeks old C57B1/6J male mice were bilaterally injected with either saline or gp120 via stereotaxic injections followed by either saline or Rolipram. Learning and spatial memory of these mice were tested using object location memory testing. As shown in Figure 20, gp120 treatment led to decrease learning and memory as indicated by decrease in % for exploring the displaced object. This lack of memory was restored with rolipram treatment where these mice spent more time exploring the displaced object as compared to gp120/saline injected mice. Similar behavior was also observed in the mice injected with HIV-1 Vpr and Tat separately (data not shown). This data supports our previous findings in the cellular model that rolipram is able to rescue the effect of gp120.

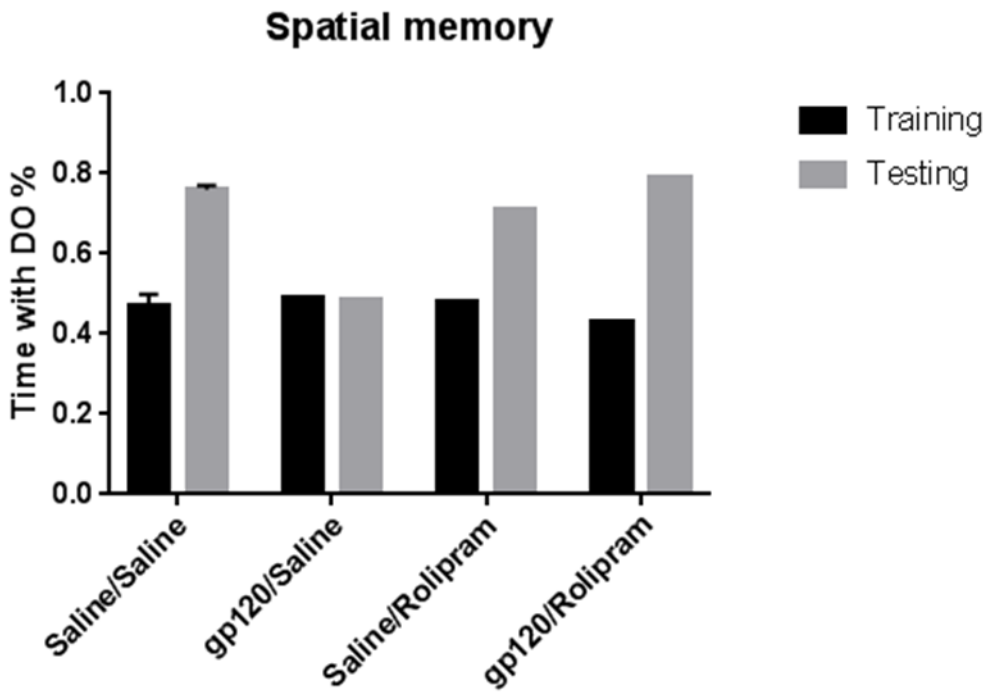

Figure 20. Rolipram rescues the spatial memory in mice injected with gp120 (Done at the laboratory of our collaborator Dr. Jeannie Chin). Black bars represent the training phase and grey bars represent the testing phase. This is an ongoing experiment at the laboratory of Dr. Chin and this histogram summarizes data obtained from one set of experiment done (n=1) with 2 mice per conditions except for Saline/Saline 5 mice were used. S.D. was used only on Saline/Saline due to the number of mice used. S.D. could not be performed on the other treatment conditions due to lack of enough mice used to obtain this preliminary data.

Conclusion and Discussion

In the past four years, our goal was to understand and identify the mechanisms used by HIV-1 leading to learning deficit and impaired working memory. To reach this goal, we focused on the role of CREB protein, a protein described as a key regulatory of the memory. CREB has been shown to be active and functional if it is phosphorylated on serine residue 133. According to the literature, four mechanisms were identified leading to CREB phosphorylation and activation/inhibition (see the scheme – Figure 21).

In this chapter, we presented data to show that expression of CREB protein was altered *in vivo* brain tissues isolated from HIV-1 patients) and *in vitro* (cell line and primary neurons) by HIV-1 gp120 protein (Figures 6, 7, and 8). Finally, we showed that the detrimental effect of gp120 can be reversed in the presence of Rolipram (Figure 17 – 20).

These results gave us the rationale to explore two route, i- determine the mechanisms used by gp120 leading to CREB loss of function, and ii- examine the impact of CREB protein inhibition on its downstream targets mainly PGC-1alpha (involved in mitochondria biogenesis) and BDNF (involved in neuronal communication).

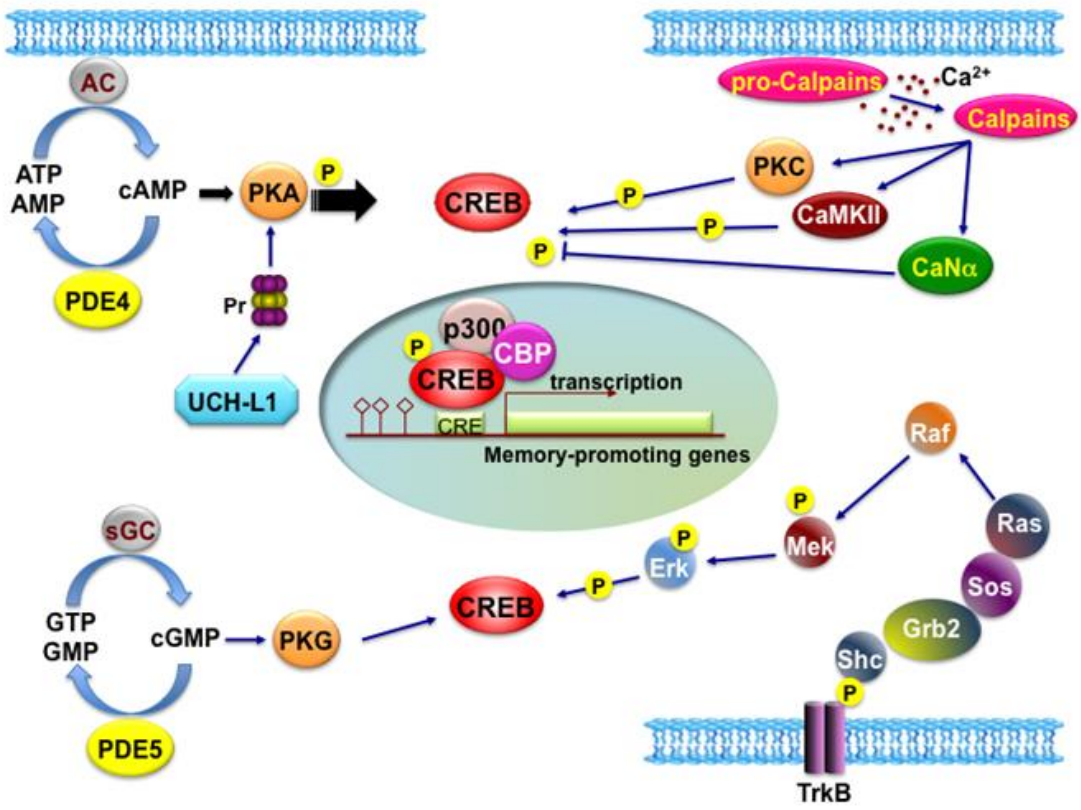

Figure 21. Schematic representation of CREB pathways

CREB upstream effectors

In the first approach, we determined part of the mechanisms used by gp120 leading to CREB dephosphorylation. Since gp120 does not function as transcription factor, we dismissed the idea that gp120 might impact CREB gene directly. Therefore, we thought to examine CREB upstream effectors such as miR-34a and miR-134. The exact mechanism used my gp120 to affect miR-34a and miR-134 are not known but, the effect of miR-34 on CREB regulation was previously shown by several groups including ours where we demonstrated that activation of miR-34a leads to inhibition of CREB functions (J. R. Chang et. al., 2011).

Induction of miR-34a by gp120 was validated using miRNA array, where miR-34 was among the microRNAs that was upregulated in primary human cells and in SH-SY5Y following the addition of gp120 (data not shown). Impact of miR-34 on CREB gene was further shown by (Pigazzi et al., 2013) where they demonstrated that hypomethylation of miR-34 inhibits CREB function. Therefore, we examined the impact of miR-34a on CREB. Using an anti-miR-34, we were also able to demonstrate a link between miR-34a and CREB function (J.R. Chang et.al., 2011). However, one may ask, how miR-34 affects CREB in the absence of any miR-34 site within the CREB gene.

Searching for the miR-34a target, we were able to find miR-34a binding site within its gene (data not shown). Additionally, we also identified E2F3 binding site on the CREB promoter, therefore we confirmed its role as an activator of the CREB promoter (data not shown). Hence, we hypothesized that gp120 upregulates miR-34 which in turn inhibits E2F3 gene and prevents it from binding to the CREB promoter leading to lower expression of CREB protein.

To confirm this hypothesis, we demonstrated decreased expression of the E2F3 protein in brain tissues of HIV-1 patients (Figure 10C). Others and us showed that miR-134 regulates the CREB gene function through a pathway that implicates several factors (calpain, HDAC, cdk5/p25/p35, Sirt1/YY1, miR-134 and CREB) (J. Gao et al., 2010). In general a functional CREB requires a silent miR-134, while an active miR-134 causes CREB protein loss of function. Our data shown in Figure 11B corroborate with this pathway and demonstrated that gp120 is using at least one of the microRNAs to inhibit CREB.

CREB downstream target

In the second approach, we chose to examine whether gp120 affects CREB protein function indirectly by targeting CREB downstream targets. Further, this pathway will allow examining whether by deregulating CREB, this effect can be extended to CREB downstream targets. As shown in our data, we focused mainly on two major targets, PGC-1α and BDNF. The first was chosen because of its capability of controlling mitochondrial and biogenesis which could then affect the mitochondrial bioenergetics and the second because of its effect on neuronal communication and synaptic plasticity.

Effect of CREB on PGC-1α and BDNF is not without a precedent, it has been shown by many group that CREB regulates the promoters of both genes (Cheng et al., 2012) (Tao et al., 1998; Zheng et al., 2012). In one study, rolipram has been shown to contribute to angiogenesis and attenuates neuronal apoptosis through activation of CREB (Hu et al., 2016). Addition of Rolipram was also shown to improve neuronal functions through CREB in an animal model (Zhong et al., 2016). Similarly, salidroside was recently shown to improve learning ability and memory through activation of CREB protein in an animal model (Jin et al., 2016).

Based on that, our data presented in Figures 10A and Figure 13A demonstrated that the addition of gp120 protein decreased PGC-1alpha and BDNF protein expression levels. Interestingly, restoring CREB expression using either, rolipram or, salidroside restored expression levels of CREB thus, improved the downstream effects of these proteins. Hence, we concluded that our data are in accord with published data and that restoring CREB function using chemical reagents will have high impact on neurons.

Note that the relation between PGC-1α and gp120 has never been examined before and our work is the first to describe such a relation. It should be noted that gp120 affects PGC-1α expression and function through two pathways, direct and indirect. The direct pathway is by preventing CREB from activating the PGC-1alpha promoter. While the indirect pathway was confirmed by showing that- by inhibiting CREB, gp120 also decreased expression level of miR-132 (CREB downstream target). Inhibition of miR-132 leads to the activation of DNMT, which in turn methylates the PGC-1alpha gene. This has been demonstrated by other group (Lv et al., 2013) and our data corroborate with their observation. Additionally, we also observed decrease in mtDNA with gp120 treatment thus affecting its biogenesis and PGC-1α is one of the proteins that play an important role in it.

As for the relation between BDNF and gp120, this was amply studied by Mocchetti group where they showed the ability of gp120 to deregulate and inhibit BDNF function (Mochetti et. al., 2007; Bachis et. al., 2012). However, in their studies, they never identified the mechanisms involved. In here, we showed that deregulation of BDNF by gp120 is CREB (Figure 8) and MeCP2 dependent (our lab data – not shown).

To further validate the specificity of our data, we showed that addition of gp120 impacted mitochondrial movement and neurites distribution (Figure 15A and Figure 9A and B). Further, gp120 alters MIRO expression level, a protein involved in mitochondrial movement (Figure 15B). The relation between the two proteins have never been explored and our work pointed at this relation. We also looked at TRAK, Kinesin and Dynein expression levels (Figure 15B). Although we only examined the total protein expression, their functions are also dependent on their phosphorylation status (DeBerg et al., 2013;

Pfister et al., 1996). Furthermore, the ability of gp120 to alter neurites distribution, synaptophysin and PSD95 (Figure 9A-C) expression levels confirmed our hypothesis that inhibition of CREB leads to the deregulation of its downstream targets.

However, one may ask, how to translate the bench work into more significant model. To answer this question, we performed an animal study where gp120 was injected in the hippocampal area of these mice. The mice were subjected to displaced object recognition training known also as spatial memory test. As shown in Figure 20), mice that were injected with gp120 suffered from spatial memory impairment when compared to mice injected with saline. Mice memory was restored when the mice were injected with rolipram immediately after surgery and 34 hrs post gp120 injection. Although the animal study is still in progress this supports our findings from the cellular model. Additional validation using the brain samples from these animals will strengthen our hypothesis. These results wrap and confirm our hypothesis that gp120 is involved in declarative memory impairment and learning deficit which can explain the persistence of HAND. Interestingly, gp120 performs its deleterious effect through CREB pathway (See Figure 22). Our data are the first to link CREB to HAND and to use molecular approach to confirm this link. These results will allow the development of new therapeutic approach based on activation and phosphorylation of CREB to prevent HAND progression.

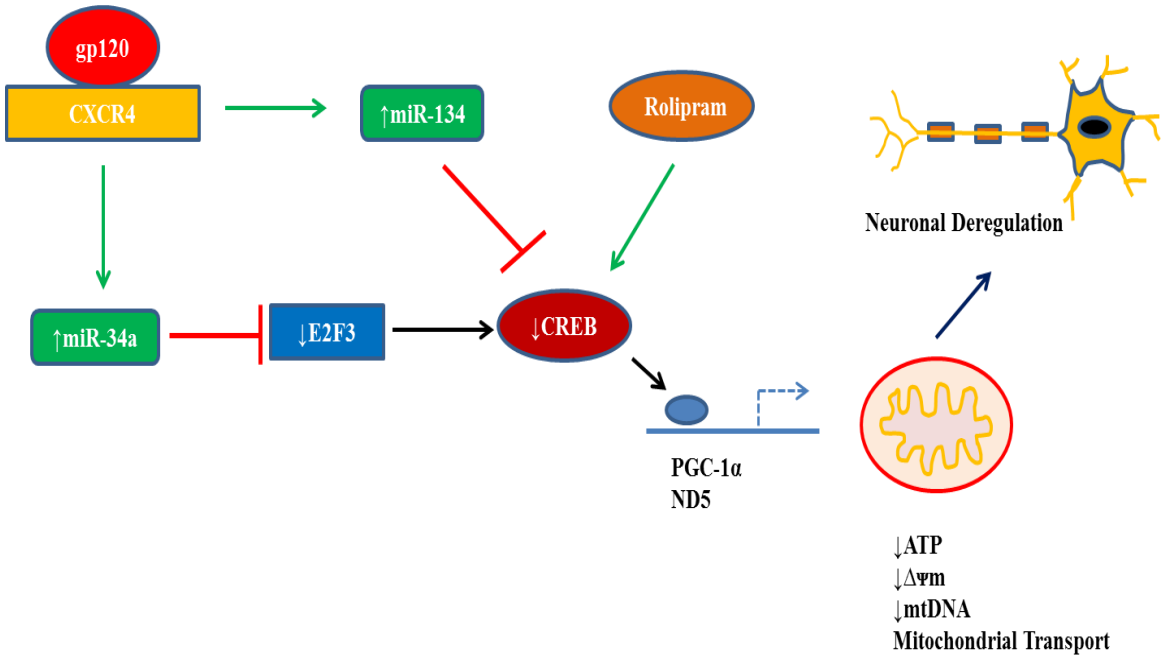

Figure 22. Flow chart representing the possible mechanism used by gp120 to alter mitochondrial and neuronal integrity.

CHAPTER 3

ROLE OF MIR-499-5P AND CALCINEURIN IN GP120 MEDIATED DEREGULATION OF MITOCHONDRIAL SHAPE

Introduction

As mentioned earlier, the goal of my work was to determine the mechanism used by HIV-1 gp120 leading to learning deficit and declarative memory impairment. In Chapter 3, we showed that these mechanisms are CREB-dependent and involve mitochondrial deregulation and axonal transport alteration. To further confirm this observation, especially to further confirm involvement of the Calpain pathway (See Figure 21) in this chapter, we focused on the role of calcineurin and validate our hypothesis regarding mitochondrial deregulation.

Mitochondria are well known as the "power house of the cell" and in neurons mitochondrial integrity is critical. Along with generating ATP, their dynamics to undergo fission and fusion to maintain their shape and activity are also equally important and could be used to decipher the cellular integrity. Under a normal physiological condition, there is a fine balance between fission and fusion machinery but during cellular stress this dynamic is altered. Altered mitochondrial dynamics has been reported in several diseases such as cancer, pulmonary hypertension, patent ductus arteriosus, cardiac myopathies and also in several neurodegenerative diseases like Parkinson's, Alzheimer's and Huntington's (Archer, 2013).

Fission generates fragmented mitochondria and fusion gives rise to elongated mitochondrial network. These dynamics are controlled by fission proteins – Drp-1, Fis-1

and fusion proteins Mfn1, Mfn2 and Opa1 that are guanosine triphosphatases (GTPases) driven (Archer, 2013; Youle & van der Bliek, 2012). Fusion is involved in mixing of mitochondrial contents and rescuing/inhibiting potential stress induced damage and also prevents the loss of mtDNA (Chen & Chan, 2010). Additionally, mitochondrial fusion is required for proper mitochondrial distribution as well as for dendritic spine outgrowth. Furthermore, deletion of Mfn2 has been shown to lead to cerebellar neurodegeneration (Chen, McCaffery, & Chan, 2007). Mitochondrial fission on the other hand is important for cell growth and development. In the case of neurons increased mitochondrial fission has been reported to lead to neurodegeneration. Inhibiting Drp-1 activity has been shown to have neuroprotective effect both in-vitro and in-vivo in a hippocampal neurons (Grohm et al., 2012).

The shape and activity of mitochondria is regulated by several other upstream factors along with the fission and fusion proteins present on their membranes. Recently there has been a tremendous effort to understand the role of mitochondrial dynamics but in the case of HIV it is still poorly understood. In the previous chapter, we were able to demonstrate the effect of gp120 on mitochondrial bioenergetics, in this chapter we will focus on the effect of gp120 on upstream factors such as glutamate excitotoxicity, ROS and miRNAs specifically miR-499-5p, that might lead to altered mitochondrial shape by altering fission and fusion proteins. This chapter also validates our data and hypothesis regarding mitochondrial deregulation leading to the development of HAND and most particularly explains the mechanism of learning deficit and declarative memory impairment.

Materials and Method

Cell culture

The human neuroblastoma cell line, SH-SY5Y cells were purchased from ATCC (CRL-2266) and grown in Dulbecco modified eagle medium: nutrient type – 12 (DMEM F12) supplemented with 10% Fetal bovine serum (FBS), 1% non-essential amino acid and 1% sodium pyruvate. All cells were incubated at 37˚C supplemented with 5% CO_2. The cells were passaged each time at 85-90% confluency. The cells only within 10 passages from the time purchased from ATCC were used for the experiment. The cells were seeded at the density of 5x10^5 cells/per well for 6 well plates. They were differentiated into neurons with 10µM retinoic acid (RA) treatment for 3-4 days.

Treatments

Recombinant HIV-1 gp120IIIB was purchased from NIH AIDS Reagent Program (Catalog # 11784). Samples were treated with 100ηg/mL of gp120 for 24 or 48 hours or specified otherwise. HIV-1 gp120IIIB is T-tropic and works via its interaction with a chemokine receptor CXCR4.

To prevent the interaction of gp120 with CXCR4 inhibitor AMD3100 (NIH AIDS Research and Reference Reagent Program Cat # 8128) was used at the concentration of 2µM.

Transfections

pDsRed2-Mito was purchased from Clontech (Catalog #632421). The has-miR-499-5p mimic (HMI0615) and mimic control were purchased from Sigma. The SH-SY5Y

cells were seeded at 5x10^5/mL in the culture dishes. The day of transfection, the cells were incubated in the OPTI MEM medium for an hour before transfection. For transfection, the following plasmids with the respective concentrations, mimic-499-5p or the mimic control with the working concentration of 2µM and dsMito-Red with 1.5µg/µL using lipofectamine 2000 were prepared in the transfection medium (Opti MEM). The cells were then incubated for 4-6 hours at 37˚C. The transfection medium Opti MEM was replaced by the differentiation medium DMEM F12 with 10 µM retinoic acid after 4-6 hours. The cells were left to differentiate for 4 days followed by the different treatment conditions specified per experiments then subjected to the respective experiments.

Western Blot

The whole cell lysate was prepared using Radioimmunoprecipitation assay (RIPA) lysis buffer (25 mM Tris–HCl pH 7.6, 150 mM NaCl, 1 % Triton and 0.1 % SDS) + protease inhibitor and phosphatase inhibitor cocktail. 25µg of the sample were loaded in each well. The cell lysates were vortexed and spun at high speed and spun in 4˚C centrifuge at 13,000 rpm for 10 minutes. Protein concentrations were estimated using a Bradford Assay (Bio-Rad Catalog # 500-0006). Lysates were mixed with 6X loading dye containing β-ME followed by boiling them at 95˚C on a dry bath. 25µg of samples were loaded in each well. The gel was then transferred to a nitrocellulose membrane. The membrane was blocked with 5% BSA for 1 hour at the room temperature. Primary antibodies were prepared in a 5% BSA solution as well and the membranes were incubated for overnight at 4˚C with gentle shaking. Antibodies used to detect the target proteins: MCU (Santa Cruz), MCUR1 (Santa Cruz), Calcineurin (Cell Signaling), Drp-1 (Novus), phospho Drp-1 at S637 (Cell Signaling), Fis-1 (Santa Cruz) and NMDAR (Cell

Signaling). Species specific secondary antibodies were used from Santa Cruz and the membranes were incubated for 1 hour at the room temperature. Chemo luminescence was used to detect the band signal. Densitometry ratio of the bands were determined using an ImageJ that was normalized to the GAPDH.

RNA extraction

Total RNA was extracted from the sample treated with different conditions using SurePrep TrueTotal RNA purification kit from Fisher Bioreagents as per the instruction from the manufacturer. Nanodrop was used to determine the purity and concentration of the RNA extracted.

miRNA

For micro RNA expression cDNA was synthesized using miRCURY LNA Universal RT microRNA PCR from EXIQON with 100ng of RNA. Primers for miR-499-5p was purchased from Exiqon. U6 was used as an internal control.

mRNA Gene Expression

cDNA was synthesized using SuperScript VILO cDNA synthesis kit (Invitrogen 11754-050). Following primers were purchased from IDT:

DRP-1: (F- ACTTGACCTCCCTACTGGC)

(R- TCCTCTATCCCGTTGACACC)

GAPDH: (F- 5′-GCCTTCCGTGTTCCTACC)

(R- 5′-CCTCAGTGTAGCCCAAGATG)

Immunofluorescence

Cells were fixed with 2% paraformaldehyde for 3 minutes, followed by rinsing with 1X PBS and blocked with 1% BSA for 1 hour. Next, they were incubated in a specific primary antibody (Fis-1 and Drp-1) (1:100 dilutions) overnight at 4˚C followed by incubation in a fluorescein tagged secondary antibody for 1 hour at the room temperature. The cells were then washed and mounted in DAPI containing medium. Leica EL600 DMI3000 confocal microscopy system was used to visualize them.

Immunohistochemistry

Gp120 transgenic mice brain

Imaging for gp120-tg mice brain were done in the laboratory of Dr. Kaul (Sanford Burnham Presbys Medical Discovery Institute). WT and gp120-tg mice (express gp120 under GFAP promoter) were provided by Dr. Lennart Mucke (Gladstone Institute of Neurological Disease, University of California) (Toggas et al., 1994). The mice were 9 months of age for both WT and gp120Tg where they were anesthetized with Isoflurane and transcardially perfused with 0.9% saline. The brains were quickly removed and fixed with 4% paraformaldehyde for 48 hours at 4˚C. The brain sections of 30µm thickness were obtained for the histological studies. The slides were permeabilized with 1% Triton X-100 for 30 mins followed by blocking with 10% heat inactivated goat serum in PBS containing 0.5% Tween 20 for 1.5 hours. The sections were then stained with calcineurin (Cell Signaling) and MAP-2 (Sigma) overnight followed by Alexa Flour 488-labled goat anti-rabbit (Molecular Probes). Nuclear DNA was labeled with H33342. Per animal three sagittal sections were analyzed and each sections five fields were recorded using Zeiss inverted Axiovert 100M fluorescence microscope. Fluorescence was quantified using

ImageJ by selecting ROIs and set measurements by selecting area, integrated density and mean gray value. Corrected total cell fluorescence (CTCF) was measured using the following formula,

CTCF = Integrated Density – Area of selected cell X mean fluorescence of background readings

Glutamate Assay

Glutamate level was measured using the Glutamate Assay Kit from Biovision (Catalog #K629-100) by following the instructions from the manufacturer. Cells treated under different conditions were homogenized in 100µL Assay buffer and centrifuged at 13,000g for 10 minutes to remove any insoluble materials. 10µL of each sample were added on 96 well plates. Then, 40µL of the Assay buffer was added on each plate to bring the volume to 50µL. The reaction mix was prepared as indicated in the protocol and 100µL of it was added to each wells on the standard set and the sample set. The mix was incubated at 37˚C for 30 minutes protected from the light. The signal was measured at OD=450 nM using a Modulus microplate reader. The data is presented in a relative form as compared to the untreated control (Mock).

Calcium measurement

The SH-SY5Y cells were grown on a poly-D-Lysine coated coverslips and differentiated for 72 hours. The cells were untreated (mock) or treated with gp120 for 3 hours which were then exposed to Fura 2AM (fura-2/acetoxymethylester) at 2µM concentration and Rhodamine 123 to detect the cytosolic and the mitochondrial calcium. The Ca^{2+} measurements were taken at 340/380 nm ratios. The cells were treated with

thapsigargin (Tg) at 2µM concentration to deplete ER Ca^{2+} and inhibit SERCA. After the cytosolic Ca^{2+} reached a base line 1mM Ca^{2+} was added to the cells to activate SOCe.

ROS assay

The trafficking of 2,3,4,5,6-pentafluorodihydrotetramethylfosamine (redox sensor red CC-1; Invitrogen) was used to detect reactive oxygen intermediates. Redox Sensor Red CC-1 is oxidized in the presence of O_2^- and H_2O_2. Differentiated SH-SY5Y cells under different treatment conditions were incubated with 5 min with 1 µm of Redox Sensor Red CC-1 (Molecular Probes). 100nM H2O2 treatment was used as a positive control. Culture slides were washed with PBS and visualized with an EVOS microscope. Note that all ROS measurement experiments were performed three times independently. Fluorescence was quantified using ImageJ by selecting ROIs and set measurements by selecting area, integrated density and mean gray value. Corrected total cell fluorescence (CTCF) was measured using the following formula,

CTCF = Integrated Density – Area of selected cell X mean fluorescence of background readings

Statistical Analysis

Statistical analysis was performed using either Student's t-test or, one-way analysis of variance. Data are expressed as the mean of $\pm$ S.D. Results were judged statistically significant if $P<0.05$. (Marked in the figure as *p<0.05, **p<0.01, ***p<0.001 where needed). Data were plotted either using GraphPad Prism version 5.0 or 7.0.

Results

Gp120 treatment leads to increased expression of NMDAR and Glutamate level

Neuronal excitotoxicity has been reported in many neurodegenerative diseases including HIV where there is hyper-activation of the NMDAR leading to increased intracellular calcium. HIV-1 proteins (tat and gp120) has been shown to trigger this mechanism leading to neuronal deregulation (Haughey & Mattson, 2002; Hoke, Morris, & Haughey, 2009). Using differentiated SH-SY5Y cells treated with 100ηg/mL of gp120 for 24 hours, we first looked at the protein expression level of NMDAR. We observed increased NMDAR protein expression with gp120 treatment as compared to the control (Figure 23A). Increased NMDAR expression and activity is often related to glutamate excitotoxicity (Potter, Figuera-Losada, Rojas, & Slusher, 2013) so, next using colorimetric glutamate assay kit we measured the glutamate level in gp120 treated SH-SY5Y cells and untreated control and observed increased glutamate level in gp120 treated cells (Figure 23B). Gp120 regulates neuronal damage through CXCR4 receptor, therefore, to examine if gp120 mediated increased glutamate level could be dampened, we used AMD3100 (CXCR4 antagonist). AMD3100 was able to rescue the effect of gp120 (Figure 20B). As stated in the previous chapter, AMD3100 effect in inhibiting gp120 effect is not consistent therefore suggesting possible receptor dependent and independent mechanism used by this viral protein. Along with NMDAR, gp120 treatment also led to increased calpain expression (Figure 23A), indicating the Ca^{2+} dependent mechanism might be involved. In the case of neurons, increased calpain has been associated with neuronal cell death and neurodegeneration (Chan & Mattson, 1999; Chera et al., 2004).

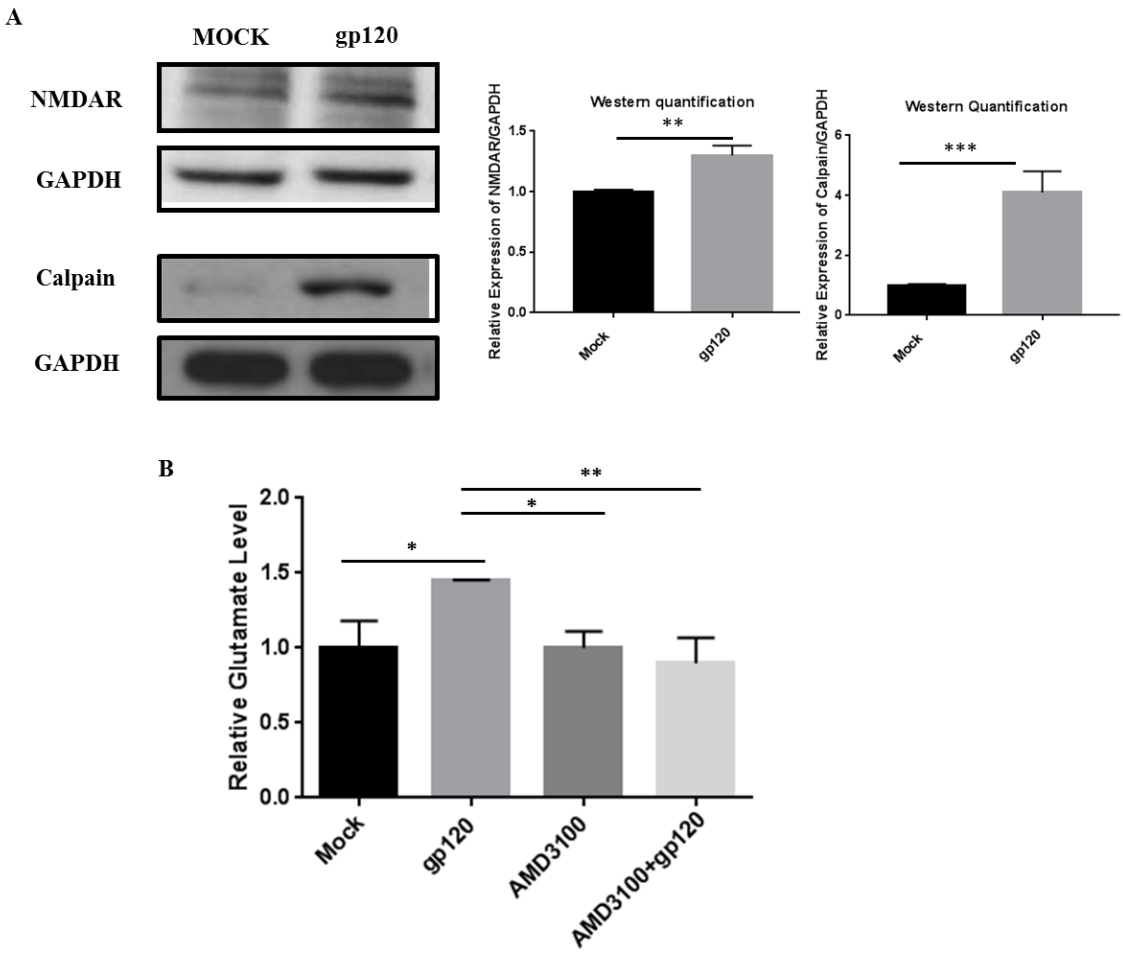

Figure 23. HIV-1 gp120 treatment leads to increased NMDAR expression and glutamate level (A) Western blot representing the protein expression of NMDAR and Calpain. GAPDH represents the loading control. Quantitative analysis of the western blot presented along with the bands represents Mean ± S.D. (n=3). (B) Relative glutamate level measured using a plate reader at O.D. 450 nm for different treatment conditions. The data presented here is the representation of Mean ± S.D. (n=3) of the 3 independent experiments. Results were judged statistically significant using one way ANOVA with Tukey's multiple comparisons test if $P<0.05$ (*p<0.05, **p<0.01, ***p<0.001).

Gp120 caused altered Ca^{2+} homeostasis and MCU complex proteins

NMDAR is an ionic channel that leads to Ca^{2+} entry after being activated by binding of the glutamate. During a normal physiological condition, NMDAR activation is important for synapse formation and neuronal communication. However, during a diseased and a pathological condition, there could be increased NMDAR activity leading to increased Ca^{2+} influx into the cytosol thus deregulating Ca^{2+} homeostasis (Benarroch, 2011). To determine the effect of gp120, the cells either untreated or pre-treated with gp120 for 24 hours were incubated in Fura 2 and rhodamine 123 dye to visualize the cytosolic and mitochondrial Ca^{2+} respectively. Sarcoplasmic/ER Ca^{2+} ATPase inhibitor, Thapsigargin (Tg) was first used to deplete the ER Ca2+ store, followed by SOCE stimulation by the addition of 1mM Ca^{2+}. Here, we observed increased level Ca^{2+} in the cytosol (grey) in the gp120 treated cells as compared to the control (Figure 24A). This increase in Ca^{2+} influx could be involved in calpain/calcineurin pathway which will be discussed in this chapter. Furthermore, increased intracellular calcium in the HIV-1 protein treated neurons (Nath, Padua, & Geiger, 1995); (J. R. Chang et al., 2011) and the immune cells (Weissman et al., 1997) have been reported before by our lab and others, but we also want to investigate its effect on mitochondria. Since, increased Ca^{2+} influx has been linked to mitochondrial damage and cellular deregulation in neurons (Kawamata & Manfredi, 2010). Here, to address the possible factors involved we first decided to examine the status of proteins involved in mitochondrial calcium entry.

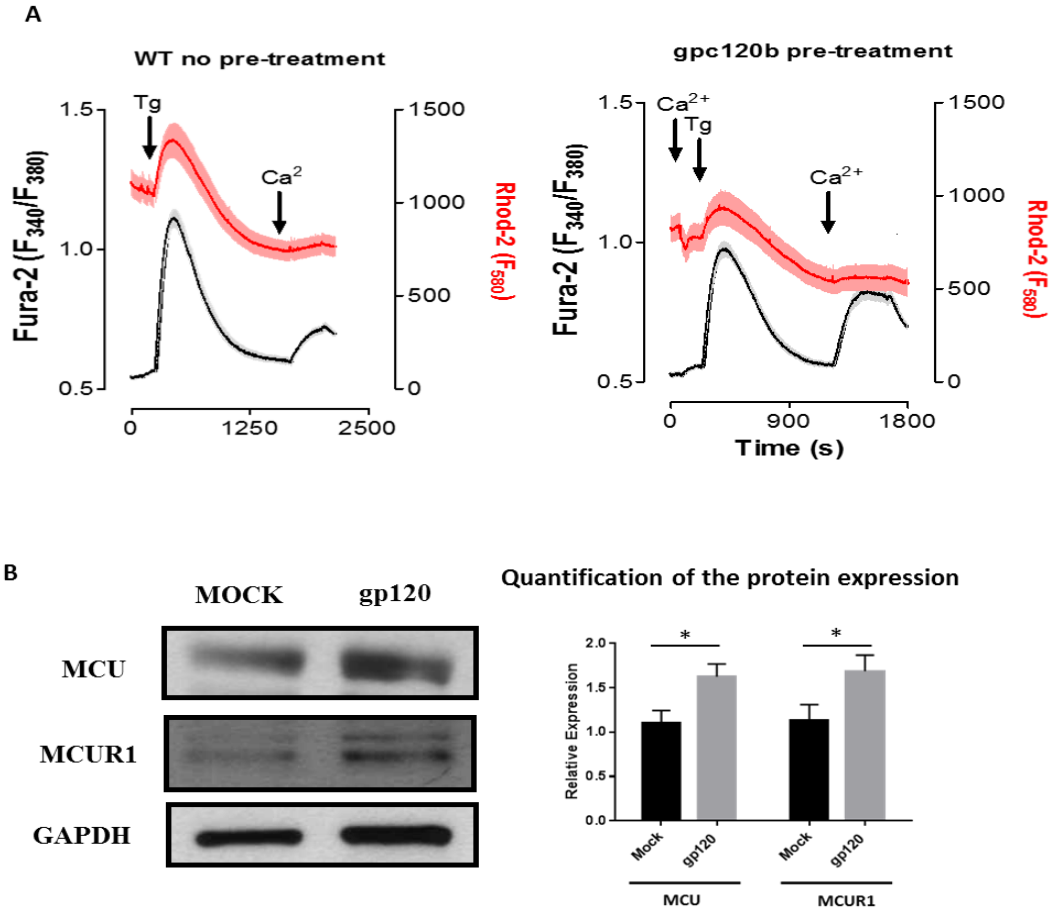

Figure 24. Aberrant Ca^{2+} homeostasis and MCU proteins with gp120 treatment (A) Cytosolic and mitochondrial Ca^{2+} level measured using a ratiometric dye Fura 2AM (Grey) and Rhodamine (Red) for the cytosolic and mitochondrial Ca^{2+}. (B) Western blot analysis of the protein expression of MCU complex proteins (MCU and MCUR1). GAPDH expression was used as a loading control. Quantitative analysis of the western blot presented along with the bands Mean ± S.D. of 3 independent experiments (n=3). Results were judged statistically significant using Student's t-test if $P<0.05$ (*p<0.05). (Calcium measurement was done in collaboration with Dr. Jonathan Soboloff performed by Dr. Robert Hooper.)

Mitochondrial uniporter complex is present in the inner mitochondrial membrane and is involved in Ca^{2+} transport into the mitochondria from the cytosol. It is a multi-protein complex containing MCU, MCUR, MICU, EMRE and SLC25A23 (De Stefani et al., 2015). Here, we looked at MCU and MCUR1 from the complex where, MCU is the pore forming subunit through which the Ca^{2+} enter (Chaudhuri, Sancak, Mootha, & Clapham, 2013) and MCUR1 is the integral membrane protein and binds to MCU and is required for MCU dependent Ca^{2+} entry. MCUR1 knockdown has been shown to alter MCU dependent Ca2+ uptake (Mallilankaraman et al., 2012). Here, we investigated the effect of gp120 treatment on the expression of only these two proteins however exploring the status of other proteins associated could be beneficial to completely understand the impact of gp120 on the complex and mitochondrial Ca^{2+} entry through this mechanism. Differentiated SH-SY5Y cells treated with 100ηg/mL of gp120 IIIB led to increased protein expression of both MCU and MCUR1 as observed via western blot (Figure 24B) suggesting their possible role in gp120 mediated Ca^{2+} entry in the mitochondria and leading to increased mitochondrial Ca^{2+} which could lead to aberrant mitochondrial dysfunction such as increased ROS production and collapse of mitochondrial membrane potential. Although in our study we only looked at MCU and MCUR1 since they are essential for MCU complex assembly (Tomar et al., 2016) but, there are other proteins in the complex that play a role as Ca2+ sensors and regulate the entry such as EMRE and MICU which could be further studied to understand the role of MCU complex and the associated proteins in the case of HIV.

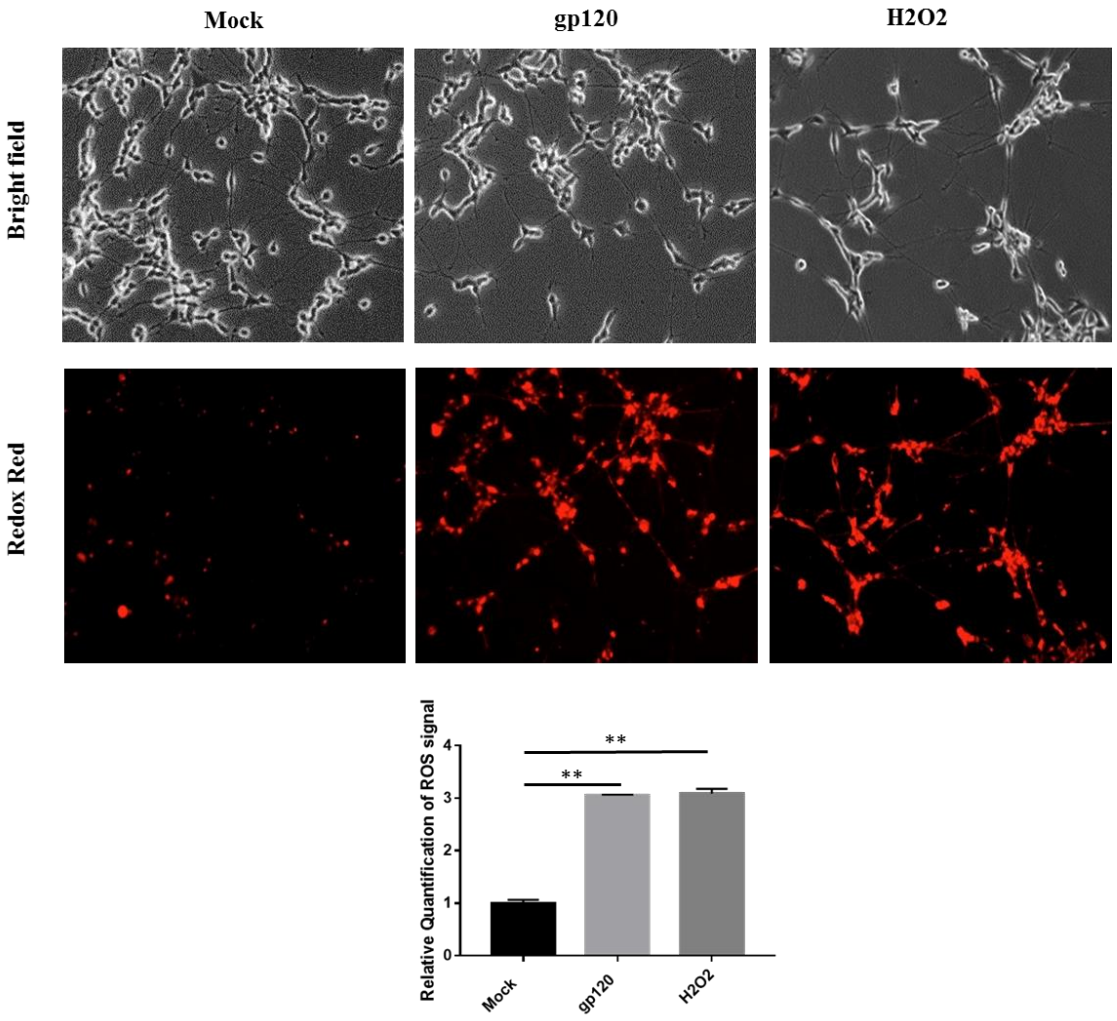

Figure 25. Generation of ROS in HIV-1 gp120 treated cells. ROS production detected using Redox Red Sensor to detect the production of the free radical in the differentiated SH-SY5Y cells subject to different treatment conditions. The production of ROS was determined by analyzing the intensity of Redox Red Sensor signal producing a red signal. The images were captured using EVOS microscope. Data represent the mean $\pm$ S.D. of 3 independent experiments (n=3). Results were judged statistically significant if $P<0.05$. (**p<0.01) using one way ANOVA followed by Tukey's multiple comparisons test.

Increased ROS with gp120 treatment

Intracellular Ca^{2+} is important for ATP production but, it can also lead to mitochondrial dysfunction. Increased intracellular Ca^{2+} and mitochondrial Ca^{2+} have often been associated with increased production of reactive oxygen species and vice versa in diseased conditions forming a loop (Goerlach et al., 2015). To test the role of gp120 in the production of ROS, we took differentiated SH-SY5Y cells treated with different conditions: mock (untreated), gp120 IIIB treated (100ηg/mL for 24 hours) and H2O2 (100ηM for 24 hours). Post treatment their mitochondria were labeled with redox sensitive dye Redox Sensor Red CC1 and visualized under EVOS microscope to observe the co-localization. Only gp120 treated cells exhibit bright red fluorescence, indicative of increased ROS production. These results point to the ability of gp120 to induce ROS in neuronal cell type (Figure 25). Increased oxidative markers have been reported in the HIVE brain (Zhang, Wang, et al., 2012) therefore, our finding with gp120 supports the published data that suggest gp120 could be one of the factors involved in the process.

Gp120 treatment leads to altered mitochondrial morphology

Morphology of the organelle often determines its function and localization. Mitochondria are highly dynamic and often undergo fission and fusion to meet the energy demand of the cells. However, during a stress condition their dynamics are altered. Cells that are stressed and undergoing apoptosis have been shown to have smaller, swollen and fragmented mitochondria as compared to the control with elongated worm like structure (Bottone et al., 2013; A. Lu et al., 2007). Oxidative stress has been reported as one of the

major factors altering mitochondrial morphology (Ahmad et al., 2013). Since gp120 was able to generate mitochondrial ROS next, we wanted to examine whether it has an impact on the mitochondrial shape as well. To investigate the role of gp120 on mitochondrial shape, SH-SY5Y cells were transfected with dsMito-RED to visualize the mitochondria followed by differentiation and either untreated (mock) or treated with gp120 IIIB (100ηg/mL for 24 hours). Post treatment, live mitochondria were visualized under Leica EL600 DMI3000 confocal microscope and the images were captured. As shown in Figure 27, the shape of the mitochondria from an untreated cells- the mitochondria are tubular shaped and longer in shape whereas, in gp120 treated cells- mitochondria are rounded and shorter with a bleb shape. Smaller and rounder mitochondria have been reported in the visual cortex and the hippocampus of the Alzheimer's post mortem brain as compared to the control along with fragmented Golgi bodies and reduced synaptic profile (Baloyannis, 2011). When comparing mitochondrial volume and distribution in Figure 26 (with gp120 treatment), gp120 treated set seem to have less mitochondrial volume. Decreased mitochondrial volume and altered mitochondrial shape (donut vs straight or curved) has also been associated with decreased synaptic vesicles (Ivannikov, Sugimori, & Llinas, 2013) and altered working memory (Hara et al., 2014). Therefore, these observations indicate that gp120 is able to deregulate mitochondrial shape and volume in the neurons.

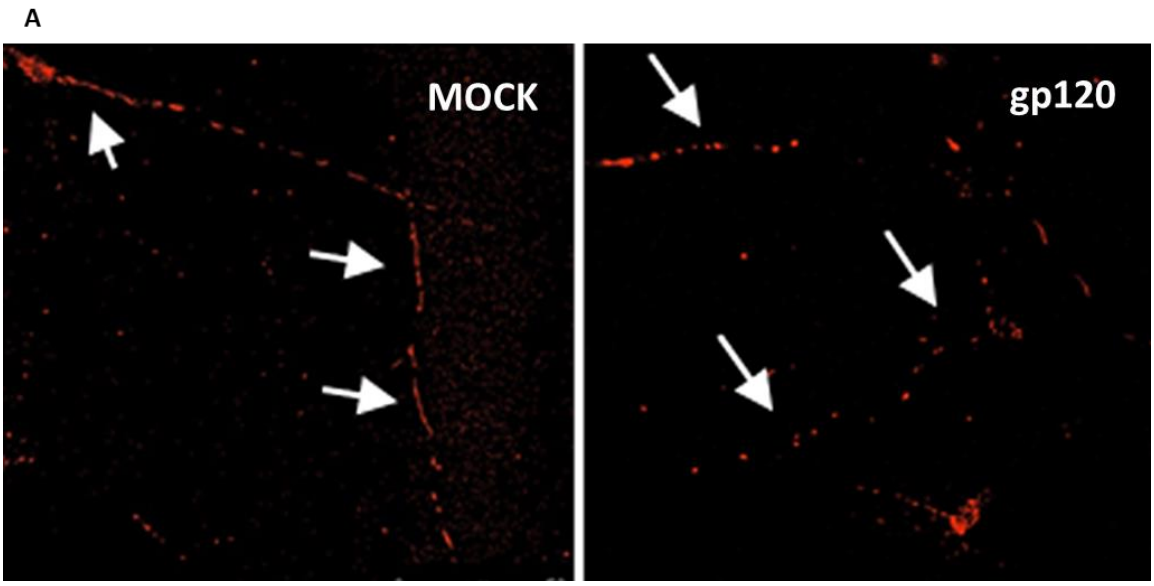

Figure 26. HIV-1 gp120 alters the mitochondrial distribution. A representation of the mitochondrial distribution and density in the neuronal processes of the differentiated SH-SY5Y cells were detected by transfecting the cells prior to differentiation with Mito ds RED. (n=6) of 6 independent experiments obtained from 15 neurites per experiment per treatment conditions. The images were taken post 24 hours of the respective treatment using EVOS microscope.

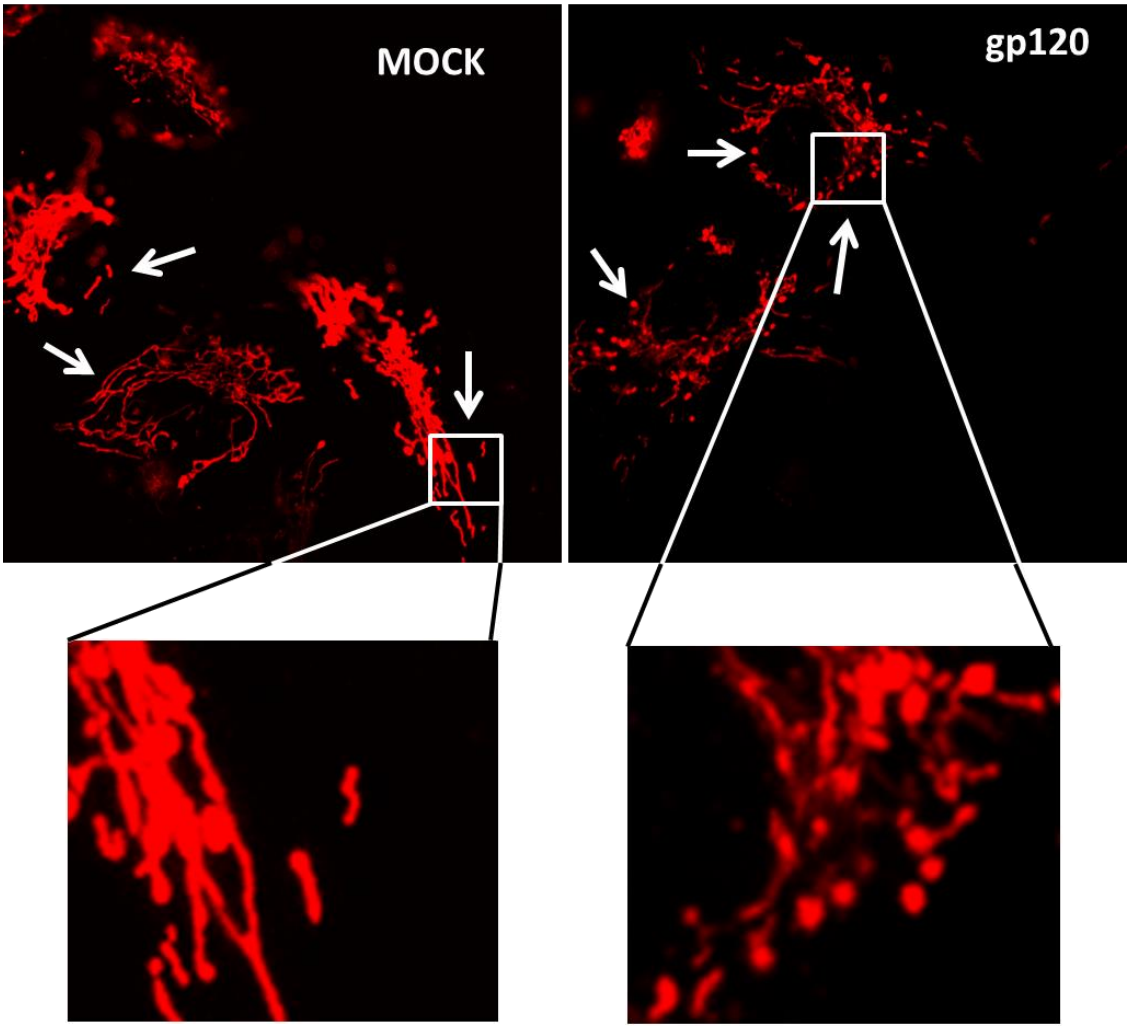

Figure 27. HIV-1 gp120 alters the mitochondrial shape. Mitochondria were labeled by transfecting the SH-SY5Y cells with pDsRed2-Mito prior to differentiation. Followed by differentiation for 3-5 days and subjected them to different conditions (untreated control – Mock and 24 hour gp120 treated. Post treatment the images were captured using a Leica EL600 DMI3000 confocal microscopy 63X lenses. The rod shaped elongated mitochondria are the healthy mitochondria and the rounded mitochondria seen in gp120 treated cells indicate the swelling of mitochondria and possible increased fission. This figure is the representation of 3 independent experiments (n=3) with 10 frames per experiment per treatment conditions.

Gp120 deregulated mitochondrial fission and fusion protein expression

Mitochondrial shape is regulated by several fission and fusion proteins. Since in our previous data we observed smaller and rounder mitochondria, next we examined to see whether the change in the mitochondrial shape is due to the mitochondrial proteins involved in fission and fusion. Therefore, the expression level of mitochondrial fission proteins- Drp-1, p-Drp1 (S637) and Fis-1 with gp120 treatment in differentiated SH-SY5Y cells were tested. As seen in Figure 28, we observed increased expression of these fission proteins Drp-1, p-Drp1 (S637) and Fis-1 with western blot. To visualize the localization and expression of these proteins we also performed immunocytochemistry in the differentiated SH-SY5Y cells transfected with pDsRED Mito and probed with primary antibodies Drp-1 and Fis-1 followed by secondary antibody Alexa 488. Figure 29A and B also shows the increased expression of Drp-1 and Fis-1 and in gp120 treated cells, there is increased co-localization of Drp-1 and Fis-1 with the mitochondria as indicated by the yellowish orange color in gp120 treated cells versus the untreated control. Therefore, these data suggest that gp120 could lead to altered mitochondrial morphology by targeting fission proteins such as Drp-1 and Fis-1.

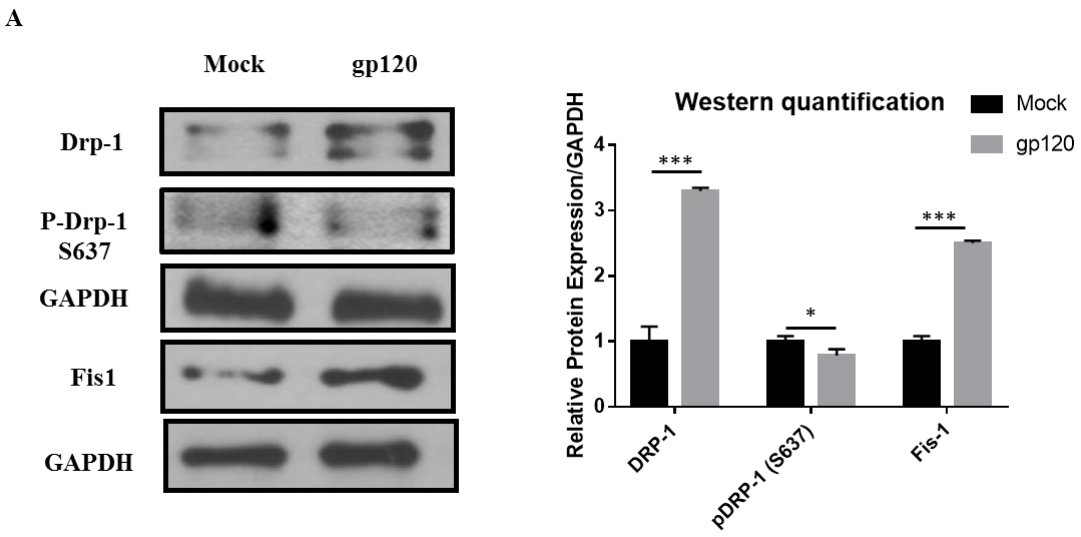

Figure 28. Altered expression of mitochondrial fission proteins with gp120 treatment. The western blot analysis representing the protein expressions of total Drp-1, phosphor-Drp-1 at S637 and Fis-1. GAPDH was used as a loading control. Quantitative analysis of the western blot presented along with the bands. These are the proteins involved in the mitochondrial fission mechanism. Data represent the mean ± S.D. from 3 independent experiments (n=3). Results were judged statistically significant using Student's t-test if $P<0.05$. (*p<0.05, ***p<0.001)

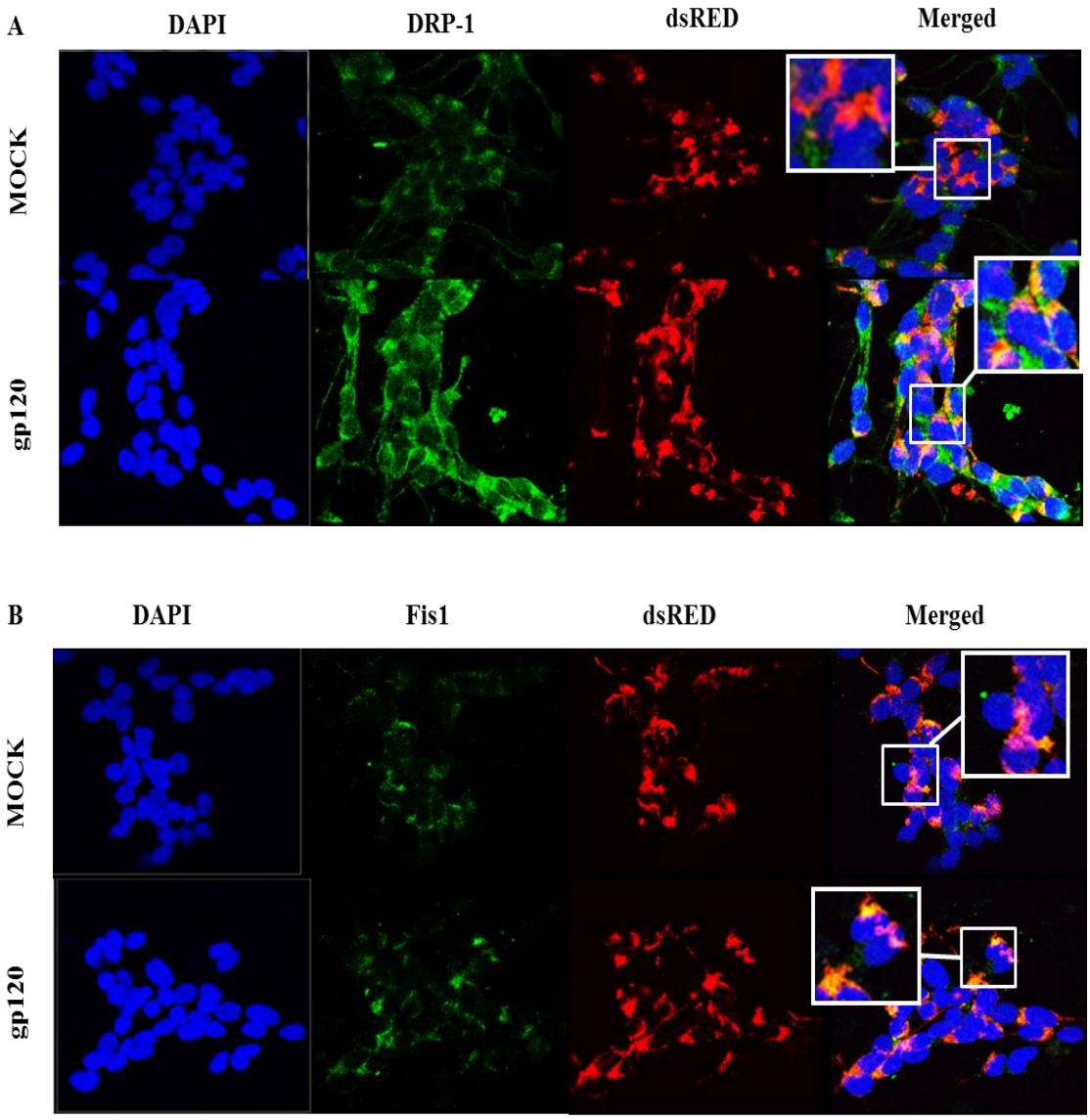

Figure 29. Immunocytochemistry depicting the expression and distribution of Drp-1 and Fis-1. Neuronal SH-SY5Y cells were plated on the glass chamber slides followed by transfection with pDsRed2-Mito to label the mitochondria then differentiated. Differentiated SH-SY5Y cells were subjected to different treatment conditions (either untreated control – Mock or gp120 treatment for 24 hours). Then, these cells were subjected to immunocytochemistry to detect the expression and localization of

mitochondrial fission proteins DRP-1 and FIS-1 in the figures (A) and (B) respectively. Mitochondria are labeled Red, DRP-1 and FIS-1 are green, DAPI (blue) – nuclei. Co-localization of the proteins with mitochondria is indicated by the presence of an orange or yellow signal. This experiment is the representation of 3 independent experiments (n=3) and pictures taken from 10-12 different frames per experiment per treatment conditions.

Gp120 also lead to deregulation of calcineurin and miR-499-5p

Next, we wanted to investigate the upstream regulators of Drp-1 to understand the mechanism used by gp120 is deregulating the fission proteins. Activity of Drp-1 is dependent on its phosphorylation status at two sites S637 and S616 which are regulated by several kinases and phosphatases (Knott, Perkins, Schwarzenbacher, & Bossy-Wetzel, 2008). Calcineurin is a Ca^{2+} dependent phosphatase which can lead to de-phosphorylation of Drp-1 at its conserved site S637 which can cause translocation of Drp-1 from the cytosol to the outer mitochondrial membrane (Cereghetti et al., 2008). Here, in gp120 treated cell extracts, we observe increased calcineurin expression as compared to the untreated samples (Figure 30A). As mentioned earlier, calcineurin is a calcium dependent phosphatase which is activated by increased cytosolic Ca^{2+}, which is triggered by the collapse of the mitochondrial membrane potential (Cereghetti et al., 2008). Previously we have shown increased calcium influx (Figure 24A) and decreased mitochondrial membrane potential (Figure 16A) with gp120 treatment which supports the increased calcineurin expression. Along with the cells treated with gp120, increased calcineurin expression was also observed in the brain slides of gp120-tg mice (Figure 30B).

Calcineurin has been shown to be a direct target of miR-499-5p. This miRNA (miR-499-5p) has been shown to have a protective effect in a cardiomyocytes and regulates mitochondrial fission and fusion by targeting calcineurin and inhibiting its activity along with its downstream target Drp-1 (J.X. Wang et al., 2011). In the brain, miR-499-5p has only been studied regarding neuropsychiatric disorders (Banigan et al., 2013; Smalheiser et al., 2014). This is the first study linking this miRNA to neurodegeneration. Therefore, we examined the level of miR-499-5p in untreated and

gp120 treated differentiated SH-SY5Y cells and primary human neurons where we observed decreased miR-499-5p expression in both cell types, only data with SH-SY5Y cells are shown (Figure 30C). These data suggest that gp120 could be altering mitochondrial shape via miR-499-5p and calcineurin pathway.

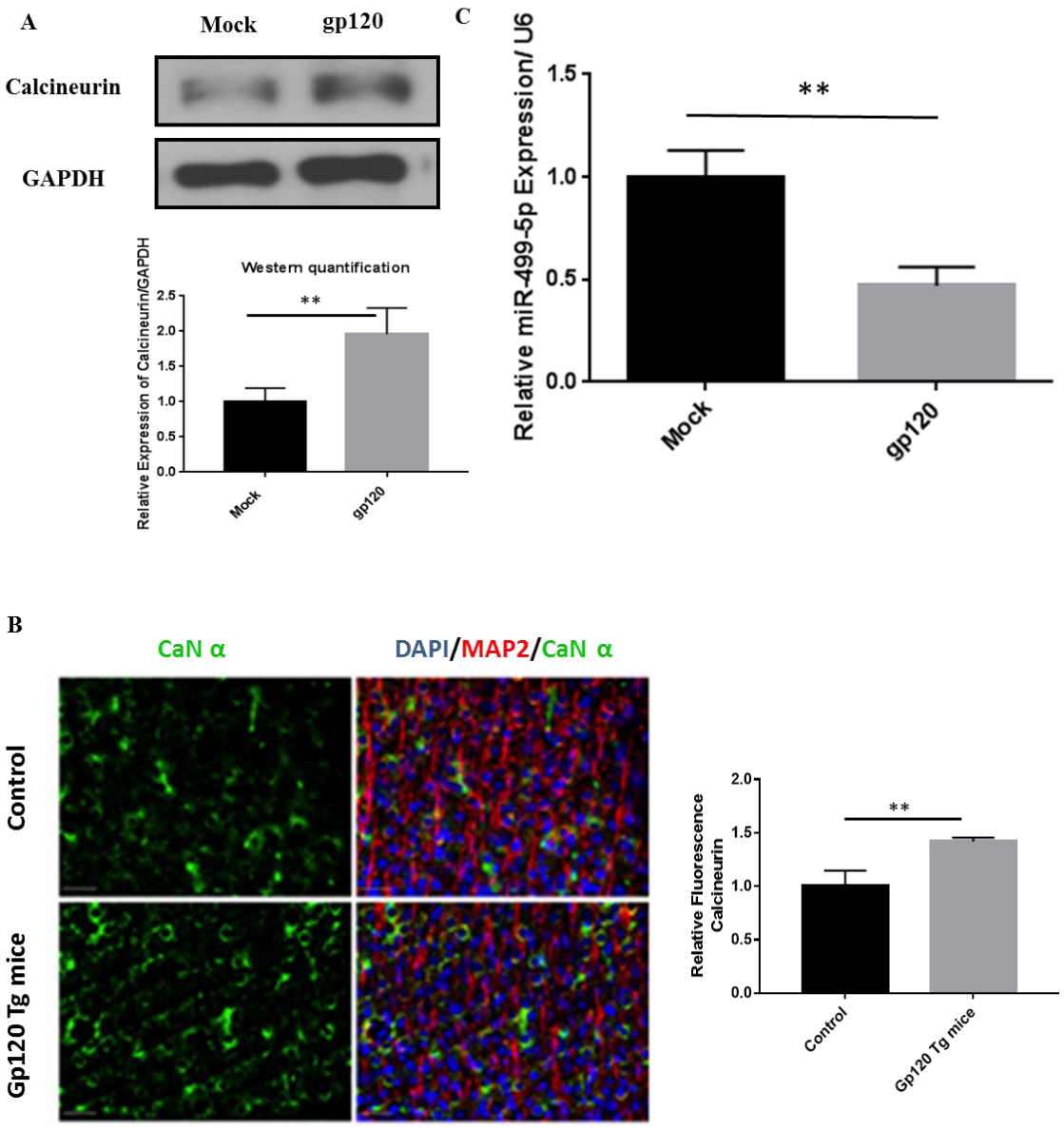

Figure 30. Calcineurin and miR-499-5p expression in the presence of HIV-1 gp120. (A) The whole cell extract subjected to the western blot analysis showing the protein expression of calcineurin in untreated control – Mock and gp120 treated for 24 hours. Quantitative analysis of the western blot presented along with the bands (n=3). (B) The relative expression of miR-499-5p normalized to an internal control U6 (n=3). (C) The immunohistochemistry and the quantitation of the fluorescence of the hippocampal brain

slides of a 9 month old gp120-tg mice and the aged matched control (n=3). Calcineurin – green, MAP-2 – red, and nuclei – blue (DAPI). (Immunohistochemistry on gp120-tg mice brain was done in collaboration with Dr. Marcus Kaul). Data represent the mean $\pm$ S.D. Results were judged statistically significant using Student's t-test if $P<0.05$. (*$p<0.05$, **$p<0.01$, ***$p<0.001$).

Overexpressing miR-499-5p led to downregulation of calcineurin and Drp1 expression

Next, to determine whether gp120 is deregulating Calcineurin and Drp-1 via miR-499-5p, we first overexpressed this micro RNA by transfecting SH-SY5Y cells with mimic-499-5p followed by differentiation and gp120 treatment for 24 hours. Then, the cells were collected and subjected to RT-qPCR to first examine the level of miR-499 (Figure 31A). Then, to observe the effect of miR-499-5p over expression on its downstream targets western blot and RT-qPCR were performed. Over expression of miR-499-5p led to decreased expression of calcineurin (Figure 31B) and Drp-1 (Figure 31C). These data suggest the possible role of miR-499-5p in deregulating mitochondrial dynamics.

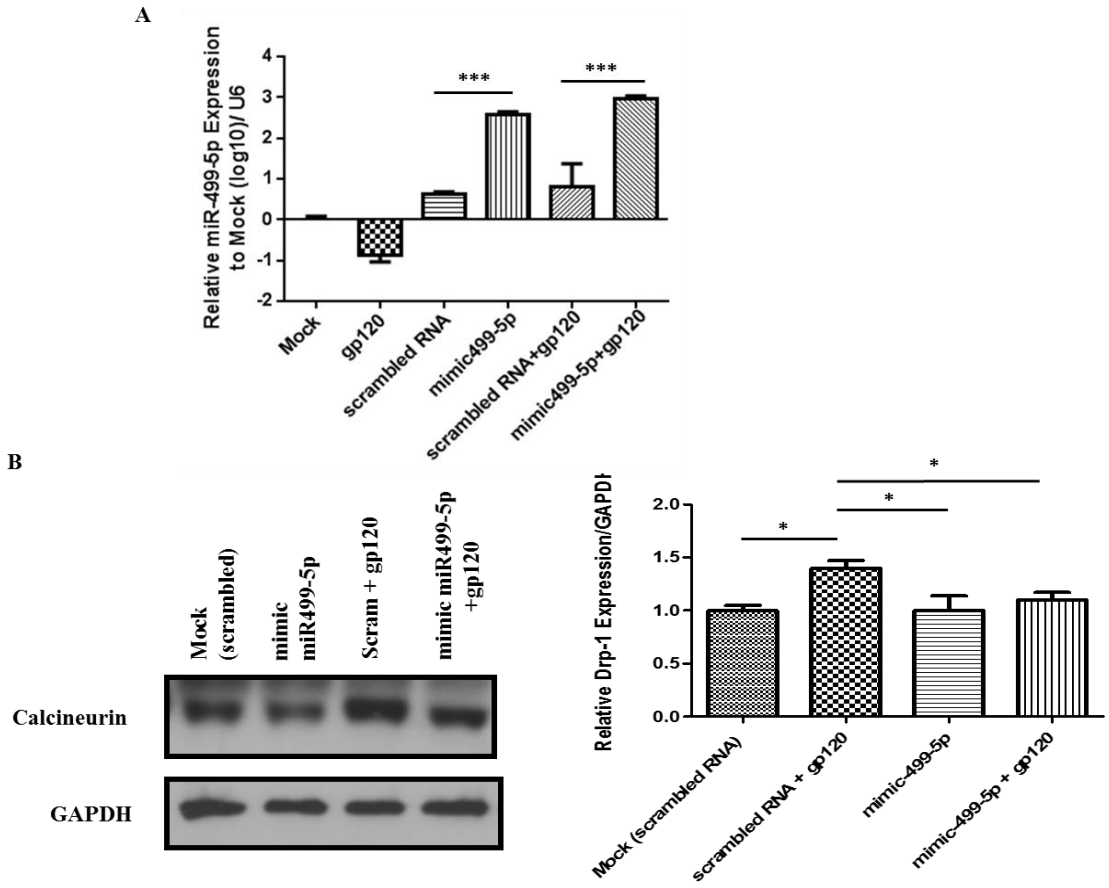

Figure 31. Overexpression of miR-499-5p and its effect on the downstream targets.

(A) Relative expression of miR-499-5p normalized to the untreated Mock (log10) indicating the overexpression of miR-499-5p using a mimic-499-5p and U6 an internal loading control (n=3). (B) Over expression of miR-499-5p led to inhibition in calcineurin expression thus rescuing the effect of gp120 (n=3). (C) Relative DRP-1 expression level normalized to an internal control GAPDH representing the effect of over-expression of miR-499-5p that is upstream of calcineurin led to inhibition of calcineurin and decreased expression of DRP-1 which is downstream of calcineurin (n=3). Data represent the mean ± S.D. of 3 independent experiments. Results were judged statistically significant if $P<0.05$ using one-way ANOVA followed by Tukey's multiple comparisons test. (*p<0.05, ***p<0.001)

Overexpression of miR-499-5p also helped rescue the mitochondrial shape. As indicated in Figure 32, the cells transfected with miR-499-5p has a longer mitochondria. The miR-499-5p transfected cells also prevented the rounding of mitochondria in gp120 treated cells. This indicates the role of miR-499-5p in the mitochondrial shape via calcineurin dependent mechanism.

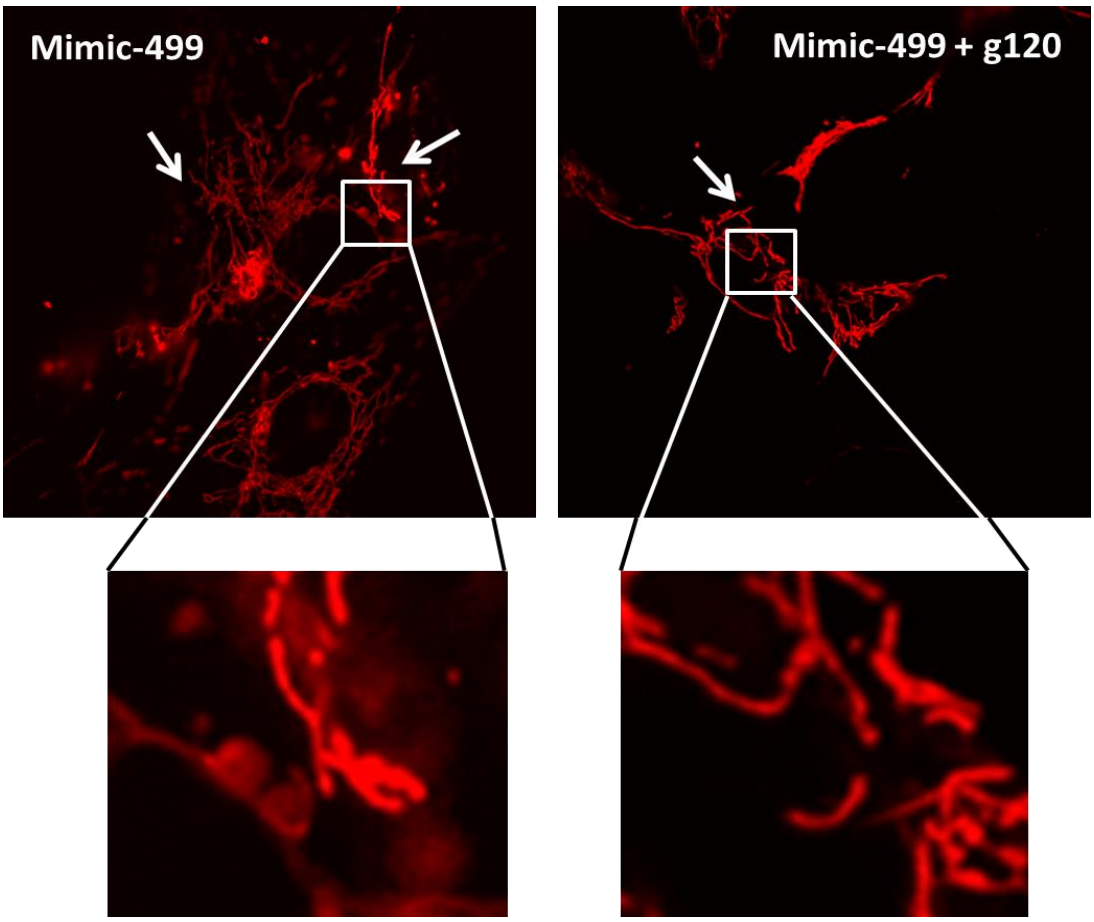

Figure 32. Overexpression of miR-499-5p rescues the mitochondrial shape. Cells transfected with miR-499-5p, the upstream regulator of calcineurin, led to elongated mitochondrial structure and rescued the effect of gp120. These figures are the representation of 3 independent experiments done (n=3) and images captured from 10-12 different frames per treatment condition per experiment.

Conclusion and Discussion

In this chapter, we focused more on the mechanism used by gp120 to alter the mitochondria and validate our data shown in Chapter 3. Further, the results from this chapter confirmed our hypothesis that gp120 is affecting CREB phosphorylation through two possible pathways (PKA and calpain/PKC/calcineurin – See our Model shown in Figure 21). Finally, data in this chapter is aimed to determine whether gp120 is using CREB independent mechanisms to alter mitochondrial shape and movement. We focused on the upstream regulator of calcineurin, miR-499-5p to examine its effect in reversing the gp120 mediated effect with regards to mitochondrial shape.

As shown in our model, addition of gp120 led to intracellular Ca^{2+} increase (Figure 24A) which could then lead to increase mitochondrial ROS production (Figure 25) and activation of calpain pathway. This data is not without a precedent as it has been shown by many labs including ours that addition of viral proteins in general and of gp120 in particular to neurons led to calcium increase (J. R. Chang et al., 2011; Nath et al., 1995; Weissman et al., 1997). Our data corroborate with published data regarding altered calcium homeostasis.

Further, we and others have shown that increased calcium secretion led to reactive oxygen species (ROS) accumulation (Figure 25). Furthermore, our data showed that gp120 treatment led to increased glutamate level (Figure 23B) and NMDAR protein expression (Figure 23A) suggesting the role of gp120 in hyper-activation of NMDAR. Forward trafficking and clustering of NMDAR on a surface has been reported earlier

with gp120 treatment (Xu et al., 2011). Therefore, the increased expression of NMDAR we observed supports the previous findings. NMDAR level and activity could be regulated by the glutamate level. Glutamate level is regulated by astrocytes as well by up taking extracellular glutamate by EAAT2 to minimize the glutamate excitotoxicity. However, in several neurodegeneration and in the HIV brain decreased EAAT2 activity has been reported (Fernandes, Edwards, Ng, & Robinson, 2007; Z. Y. Wang et al., 2003) thus leading to excess glutamate and NMDAR hyperactivity. Our model lacked the co-culture of neurons with astrocytes therefore, the data observed is only for the glutamate from the neurons. Presence of astrocytes could have possible exacerbate the glutamate level. One of the outcomes of NMDAR hyperactivity is the influx of Ca^{2+}. We were also able to show that gp120 treatment could alter Ca^{2+} homeostasis in the cytosol and mitochondria (Figure 24A) which could be the effect of the possible glutamate excitotoxicity triggered by gp120. Increased expression of calpain (Ca^{2+} protein) was also observed (Figure 23A). Additionally, gp120 treatment also led to the increased expression of MCU and MCUR1 proteins (Figure 24B). These proteins belong to the MCU complex that has been shown to be involved in mitochondrial Ca^{2+} entry. These data suggest that this complex might be in involved in HIV-1 induced mitochondrial Ca^{2+} entry. Additional studies need to done to confirm the direct effect of gp120 on the MCU complex activity. Apart from MCU there are other modes of Ca^{2+} entry into the cells such as RyR (ryanodine receptor) and rapid mode uptake (Santo-Domingo & Demaurex, 2010) which were not explored in this study.

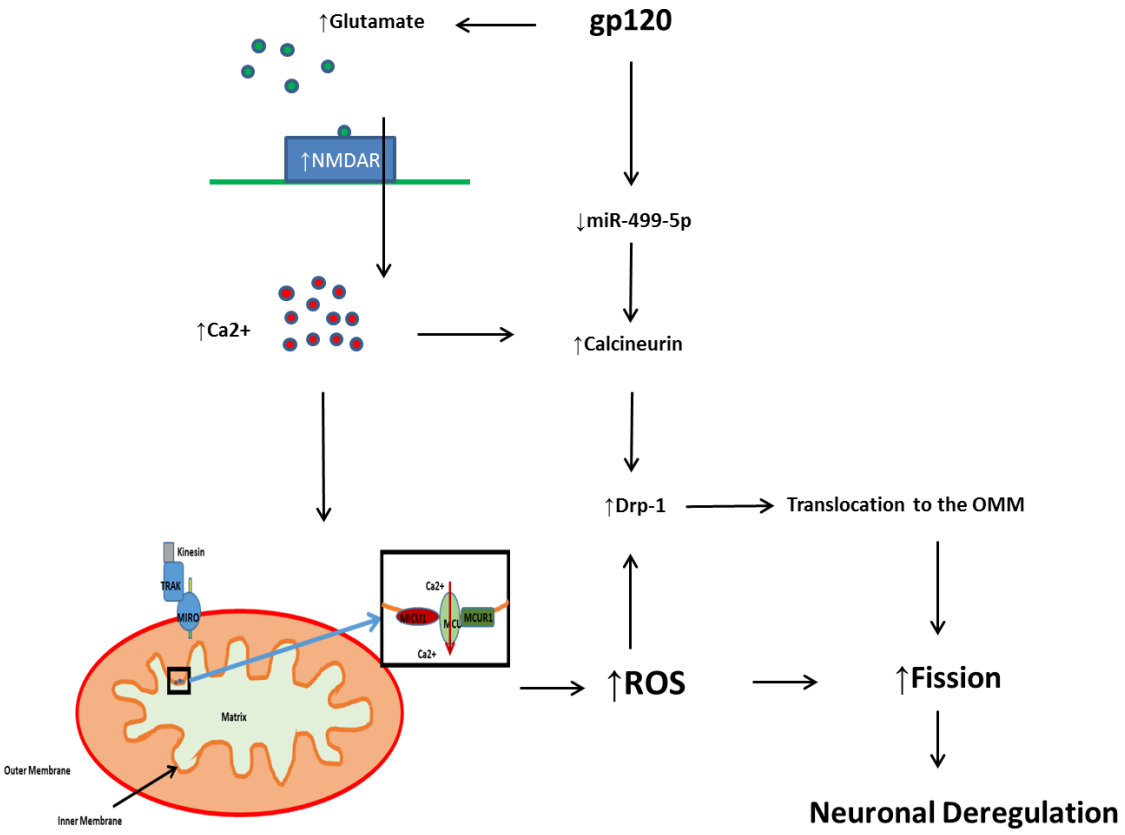

Figure 33. Schematic representation of potential pathway involved in gp-120 mediated mitochondrial shape deregulation

It has been shown that activation of the calcium pathway leads to the activation of calcineurin protein. Therefore, we sought to determine whether addition of gp120 leads to the same results. As shown in Figure 30A, calcineurin expression level increased in gp120-treated neurons as well as in gp120-tg mice brain sample (Figure 30B). As we know that calcineurin is a Ca^{2+} dependent phosphatase and its deregulation can affect the function of Drp1, a protein involved in mitochondrial membrane fission and fusion (Cereghetti et al., 2008). These results were confirmed with the deregulation of Drp1 in gp120-treated neurons (Figure 28 and 29A).

Since calcineurin is a direct target of miR-499-5p, we determined that gp120 addition caused a decrease in miR-499-5p expression (Figure 30C). Furthermore, studies have shown both aberrant fission and fusion to play a role in neuronal damage (Knott et al., 2008; X. Wang et al., 2009). To confirm this observation, we examined the mitochondrial morphology in gp120 treated cells. Interestingly, mitochondria shape changed from tubular filamentous to blebbed, rounded and donut shaped structure (Figure 27) which is the indication of the dying mitochondria often observed in the diseases state (W. H. Gao, Pu, Luo, & Chang, 2001; A. Lu et al., 2007) as compared to the control sample set (untreated). This altered shape could be the outcome of increased mitochondrial ROS generation (Figure 25), decreased mitochondrial membrane potential (Figure 16A) and the altered function of mitochondrial fission and fusion protein activities such as Drp-1, Fis-1, Opa-1 or Mfn-2. Furthermore, decreased ATP, decreased MMP and ROS generation have often been referred to as the vicious cycle (Sanz, Caro, Gomez, & Barja, 2006) where one can affect the other thus leading to a complex mechanism of mitochondrial deregulation ultimately leading to a release of cytochrome c indicating cellular stress (Li et al., 2006).

In addition, we observed increased Drp-1 expression (mRNA and protein) along with another fission protein Fis-1 (Figure 28 and 29) in gp120 treated cells, indicating possible increased fission leading to the above observed phenotype. Drp-1 is a cytosolic protein that after activation could translocate to the mitochondrial outer membrane. Fis-1 was considered to be a Drp-1 tethering protein but this has not been confirmed but it has been shown that Drp-1 binding to the outer mitochondrial membrane is mediated by mitochondrial fission factor (Mff) (Otera et al., 2010). Drp-1 activation is dependent on

its phosphorylation status. Calcineurin has been shown to de-phosphorylate it at S637 which would then lead its translocation to the outer mitochondrial membrane leading to mitochondrial fission (Cereghetti et al., 2008). Reversing the expression of calcineurin and Drp-1 by over-expressing miR-499-5p confirms its role and could possibly consider for a therapeutic approach. Drp-1 phosphorylation is also regulated by other kinases and phosphatases which was not explored in this study. It is not known if the effect of gp120 on miR-499-5p is direct or indirect. Calcineurin-Drp-1 has also been shown to play a role in parkin mediated mitochondrial fission in the case of Parkinson's model which was rescued by inhibiting calcineurin activity. They have also emphasized on the importance of Drp-1 phosphorylation status for the fission activity (Buhlman et al., 2014).

Apart from the phosphorylation status, mitochondrial translocation of Drp-1 is also dependent on the mitochondrial outer membrane proteins such as Miff, MiD49 and Fis-1. In our study we only looked at the expression and localization of Fis-1. Role of Fis-1 in recruiting Drp-1 on the OMM and working together is still under debate but, they are both fission proteins and with gp120 treatment we observe increased expression of both along with the increased co-localization with mitochondria (Figure 29A and B). In the case of HIV-1 there has only been one observation study published regarding the mitochondrial dynamics. Contrary to our finding, this study reported decreased Drp-1 expression in the HIV-1 brain and possible increased fusion (Fields et al., 2016), but the study lacks the mechanisms involved. On the other hand, our study indicates towards increased Drp-1 expression and possible increased mitochondrial fragmentation. This opposing result could be due to the different clades of gp120 used. Although our data lacks the brain samples from the patients, we have been able to use the cellular model to

decipher the key factors involved in the pathway leading to abnormal mitochondrial dynamics. Additionally, our data also corresponds with data regarding other neurodegenerative diseases where they have reported increased fission. Alzheimer's mice model have shown increased expression of fission genes and proteins and decreased fusion genes and proteins in the Alzheimer's mice model leading to shorter and fragmented mitochondria. Same study also reported that this phenomenon precedes decreased synaptic formation observed via decreased PSD95 (Calkins, Manczak, Mao, Shirendeb, & Reddy, 2011). This supports our previous data showing decreased pre and post synaptic proteins with gp120 treatment (Figures 9B and C). To confirm increased fission over fission, additional assays specific to fission and fusion are required. Our study suggest increased fission, there is also a possible autophagy/mitophagy involved that might be involved in aberrant shaped mitochondria with gp120 treatment.

These results confirmed the ability of gp120 to alter the calcium/calpain pathway leading to the activation of calcineurin, a phenomenon that could lead to CREB loss of function especially since calcineurin can dephosphorylate CREB protein (Kim & Seo, 2011). In summary, our results provide some insight on the players that are involved leading to mitochondrial deregulation in the presence of gp120 in a cellular model system. Altered fission and fusion phenomenon could lead to changes in mitochondrial density and bioenergetics. This has been linked to working memory impairment and learning disability in monkeys and mice (Hara et al., 2014; Ivannikov et al., 2013) and could be one of the factors leading to altered working memory and learning deficit in the HIV-1 brain and gp120 could be one of the viral proteins causing these alterations.

Therefore, identifying and targeting the upstream factors leading to these alterations might be a potential therapeutics to prevent the mitochondrial damage.

CHAPTER 4

CONCLUSION AND FUTURE DIRECTIONS

In the cART era with the increasing life expectancy amongst the HIV-1 infected individuals, increase in aging related phenomenon has also increased. HIV-1 associated neurocognitive impairment has been an important issue in the case of HIV-1 infected individuals especially in learning and working memory. Among the numerous factors that could be responsible in this phenomenon, in this study we focused on deciphering the role of gp120. By investigating its effect on important proteins, miRNAs and their targets especially the mitochondrial functions, we have been able to provide a comprehensive understanding of the role played by this viral protein in causing a neuronal dysfunction. In summary, by using neuronal SH-SY5Y cells as a cellular model we were able to identify the proteins and miRNAs whose expressions and functions were altered by gp120. By doing so, we were able to map some potential pathways involved in this complex mechanism that is gp120 driven.

Based on the first part of the study (Chapter 3), we were able to show the important role of CREB in neuronal integrity by focusing on its activity. We also showed several mitochondrial functions that were deregulated by gp120 treatment which were restored with CREB activation using Rolipram. Additionally, we were able to demonstrate the effect of Rolipram using an animal model in which their learning was restored. In the second part of the study (Chapter 4), we examined a CREB independent mechanism used by gp120 to alter mitochondrial shape. Here, we identified calpain/calcineurin pathway which is regulated by miR-499-5p. Overexpressing miR-

499-5p led to inhibition of calcineurin which restored the mitochondrial fragmentation phenotype observed in gp120 treated cells. Our study has helped identify some key pathways used by gp120 and has also opened some areas for further studies that we will explore as follows,

Short-term goal

1. Using brain samples of gp120-tg mice or gp120-injected mice, we will perform immunohistochemistry assay to determine the expression and subcellular localization of CREB/pCREB, PGC-1α, BDNF and PSD-95 proteins in neurons of the hippocampal areas.
2. Examine the O_2 level by using Seahorse XF to further validate the mitochondrial OXPHOS deregulation. Also, further explore the shape and size of mitochondria in gp120-treated neurons in depth to examine the involvement of autophagy/mitophagy in this phenomenon. As a control, the cells will be also treated with Rapamycin as it activates autophagy by inhibiting mTOR. In the case of HIV both autophagy (Killian 2012) and mTOR (Heredia et al., 2015) has been shown to be deregulated. Quantification of fission vs. fusion could also be performed to further understand the role of gp120 in mitochondrial dynamics.

Long-term goal

In our study, we showed that the functions of several cellular factors and pathways are deregulated in the presence of HIV-gp120 protein (CREB, SIRT1 and mitochondrial functions). Interestingly, these same factors and pathways are also shown to be deregulated with aging. These observations led to the conclusion that HIV-1-gp120

promotes neurocognitive disorders similar to the aging population. That could explain the persistence of learning deficit and declarative memory impairments in HIV-1infected patients. Therefore, to further explore this area we propose the following future studies,

- High throughput screening to identify new compounds that can trigger CREB phosphorylation on serine 133 or PDE4 inhibition
- GWAS experiments to determine the factors affected in gp120-treated neurons compared to the Mock untreated
- ChIP-Seq to determine the methylation status of genes affected by the presence of gp120 compared to the mock untreated
- Identification of the senescence-associated secretory phenotype (SASP) affected in gp120-treated cells and restoring their levels. Increased cellular senescence has been associated as the hallmarks of aging and the possible role of senescence-associated secretory phenotype (SASP) has been discussed in brain aging (Chinta et al., 2015).

REFERENCES

Abbott, N. J. (2002). Astrocyte-endothelial interactions and blood-brain barrier permeability. *Journal of Anatomy, 200*(6), 629-638.

Aboul-ela, F., & Varani, G. (1998). Recognition of HIV-1 TAR RNA by Tat protein and Tat-derived peptides. *Theochem-Journal of Molecular Structure, 423*(1-2), 29-39.

Ahmad, T., Aggarwal, K., Pattnaik, B., Mukherjee, S., Sethi, T., Tiwari, B. K., et al. (2013). Computational classification of mitochondrial shapes reflects stress and redox state. *Cell Death & Disease, 4*.

Ahmed, F., MacArthur, L., De Bernardi, M. A., & Mocchetti, I. (2009). Retrograde and anterograde transport of HIV protein gp120 in the nervous system. *Brain Behavior and Immunity, 23*(3), 355-364.

Ahmed, F., Tessarollo, L., Thiele, C., & Mocchetti, I. (2008). Brain-derived neurotrophic factor modulates expression of chemokine receptors in the brain. *Brain Research, 1227*, 1-11.

Amat, R., Planavila, A., Chen, S. L., Iglesias, R., Giralt, M., & Villarroya, F. (2009). SIRT1 Controls the Transcription of the Peroxisome Proliferator-activated Receptor-gamma Co-activator-1 alpha (PGC-1 alpha) Gene in Skeletal Muscle through the PGC-1 alpha Autoregulatory Loop and Interaction with MyoD. *Journal of Biological Chemistry, 284*(33), 21872-21880.

Archer, S. L. (2013). Mitochondrial Dynamics - Mitochondrial Fission and Fusion in Human Diseases. *New England Journal of Medicine, 369*(23), 2236-2251.

Arese, M., Ferrandi, C., Primo, L., Camussi, G., & Bussolino, F. (2001). HIV-1 Tat protein stimulates in vivo vascular permeability and lymphomononuclear cell recruitment. *Journal of Immunology, 166*(2), 1380-1388.

Arrildt, K. T., Joseph, S. B., & Swanstrom, R. (2012). The HIV-1 Env Protein: A Coat of Many Colors. *Current Hiv/Aids Reports, 9*(1), 52-63.

Bachis, A., Aden, S. A., Nosheny, R. L., Andrews, P. M., & Mocchetti, I. (2006). Axonal transport of human immunodeficiency virus type 1 envelope protein glycoprotein

120 is found in association with neuronal apoptosis. *Journal of Neuroscience, 26*(25), 6771-6780.

Bachis, A., Avdoshina, V., Zecca, L., Parsadanian, M., & Mocchetti, I. (2012). Human Immunodeficiency Virus Type 1 Alters Brain-Derived Neurotrophic Factor Processing in Neurons. *Journal of Neuroscience, 32*(28), 9477-9484.

Bachis, A., Major, E. O., & Mocchetti, I. (2003). Brain-derived neurotrophic factor inhibits human immunodeficiency virus-1/gp120-mediated cerebellar granule cell death by preventing gp120 internalization. *Journal of Neuroscience, 23*(13), 5715-5722.

Baloyannis, S. J. (2011). Mitochondria are related to synaptic pathology in Alzheimer's disease. *International journal of Alzheimer's disease, 2011*, 305395-305395.

Banigan, M. G., Kao, P. F., Kozubek, J. A., Winslow, A. R., Medina, J., Costa, J., et al. (2013). Differential Expression of Exosomal microRNAs in Prefrontal Cortices of Schizophrenia and Bipolar Disorder Patients. *Plos One, 8*(1).

Banks, W. A., Akerstrom, V., & Kastin, A. J. (1998). Adsorptive endocytosis mediates the passage of HIV-1 across the blood-brain barrier: evidence for a post-internalization coreceptor. *Journal of Cell Science, 111*, 533-540.

Bartel, D. P. (2009). MicroRNAs: Target Recognition and Regulatory Functions. *Cell, 136*(2), 215-233.

Benarroch, E. E. (2011). NMDA receptors Recent insights and clinical correlations. *Neurology, 76*(20), 1750-1757.

Bennasser, Y., Le, S. Y., Benkirane, M., & Jeang, K. T. (2005). Evidence that HIV-1 encodes an siRNA and a suppressor of RNA silencing. *Immunity, 22*(5), 607-619.

Berth, S., Caicedo, H. H., Sarma, T., Morfini, G., & Brady, S. T. (2015). Internalization and Axonal Transport of the HIV Glycoprotein gp120. *ASN Neuro (American Society of Neuroscience), 7*(1).

Biology of the NMDA Receptor. (2009). *Biology of the Nmda Receptor*, 1-328.

Bissel, S. J., & Wiley, C. A. (2004). Human immunodeficiency virus infection of the brain: Pitfalls in evaluating infected/affected cell populations. *Brain Pathology, 14*(1), 97-108.

Bliss, T. V. P., & Collingridge, G. L. (1993). A synaptic model of memory- long-term potentiation in the hippocampus. *Nature, 361*(6407), 31-39.

Borjabad, A., Morgello, S., Chao, W., Kim, S.-Y., Brooks, A. I., Murray, J., et al. (2011). Significant Effects of Antiretroviral Therapy on Global Gene Expression in Brain Tissues of Patients with HIV-1-Associated Neurocognitive Disorders. *Plos Pathogens, 7*(9).

Bottone, M. G., Santin, G., Aredia, F., Bernocchi, G., Pellicciari, C., & Scovassi, A. I. (2013). Morphological Features of Organelles during Apoptosis: An Overview. *Cells, 2*(2), 294-305.

Brenneman, D. E., McCune, S. K., Mervis, R. F., & Hill, J. M. (1994). Gp120 as an etiologic agent for NeuroAIDS - neurotoxicity and model systems. *Advances in Neuroimmunology, 4*(3), 157-165.

Brightwell, J. J., Smith, C. A., Countryman, R. A., Neve, R. L., & Colombo, P. J. (2005). Hippocampal overexpression of mutant creb blocks long-term, but not short-term memory for a socially transmitted food preference. *Learning & Memory, 12*(1), 12-17.

Brightwell, J. J., Smith, C. A., Neve, R. L., & Colombo, P. J. (2007). Long-term memory for place learning is facilitated by expression of cAMP response element-binding protein in the dorsal hippocampus. *Learning & Memory, 14*(3), 195-199.

Buhlman, L., Damiano, M., Bertolin, G., Ferrando-Miguel, R., Lombes, A., Brice, A., et al. (2014). Functional interplay between Parkin and Drp1 in mitochondrial fission and clearance. *Biochimica Et Biophysica Acta-Molecular Cell Research, 1843*(9), 2012-2026.

Calkins, M. J., Manczak, M., Mao, P., Shirendeb, U., & Reddy, P. H. (2011). Impaired mitochondrial biogenesis, defective axonal transport of mitochondria, abnormal mitochondrial dynamics and synaptic degeneration in a mouse model of Alzheimer's disease. *Human Molecular Genetics, 20*(23), 4515-4529.

Capon, D. J., & Ward, R. H. R. (1991). The CD4-gp120 interaction and AIDS pathogenesis. *Annual Review of Immunology, 9*, 649-678.

Cardoso, S. W., Torres, T. S., Santini-Oliveira, M., Monteiro, L., Marins, S., Veloso, V. G., et al. (2013). Aging with HIV: a practical review. *Brazilian Journal of Infectious Diseases, 17*(4), 464-479.

Catani, M. V., Corasaniti, M. T., Navarra, M., Nistico, G., Finazzi-Agro, A., & Melino, G. (2000). gp120 induces cell death in human neuroblastoma cells through the CXCR4 and CCR5 chemokine receptors. *Journal of Neurochemistry, 74*(6), 2373-2379.

Cereghetti, G. M., Stangherlin, A., de Brito, O. M., Chang, C. R., Blackstone, C., Bernardi, P., et al. (2008). Dephosphorylation by calcineurin regulates translocation of Drp1 to mitochondria. *Proceedings of the National Academy of Sciences of the United States of America, 105*(41), 15803-15808.

Chan, S. L., & Mattson, M. P. (1999). Caspase and calpain substrates: Roles in synaptic plasticity and cell death. *Journal of Neuroscience Research, 58*(1), 167-190.

Chang, D. T. W., Rintoula, G. L., Pandipati, S., & Reynolds, I. J. (2006). Mutant huntingtin aggregates impair mitochondrial movement and trafficking in cortical neurons. *Neurobiology of Disease, 22*(2), 388-400.

Chang, J. R., Mukerjee, R., Bagashev, A., Del Valle, L., Chabrashvili, T., Hawkins, B. J., et al. (2011). HIV-1 Tat Protein Promotes Neuronal Dysfunction through Disruption of MicroRNAs. *Journal of Biological Chemistry, 286*(47), 41125-41134.

Chaudhuri, D., Sancak, Y., Mootha, V. K., & Clapham, D. E. (2013). MCU encodes the pore conducting mitochondrial calcium currents. *Elife, 2*.

Checkley, M. A., Luttge, B. G., & Freed, E. O. (2011). HIV-1 Envelope Glycoprotein Biosynthesis, Trafficking, and Incorporation. *Journal of Molecular Biology, 410*(4), 582-608.

Chen, H., & Chan, D. C. (2010). Physiological functions of mitochondrial fusion. *Mitochondrial Research in Translational Medicine, 1201*, 21-25.

Chen, H., McCaffery, J. M., & Chan, D. C. (2007). Mitochondrial fusion protects against neurodegeneration in the cerebellum. *Cell, 130*(3), 548-562.

Cheng, A., Hou, Y., & Mattson, M. P. (2010). Mitochondria and neuroplasticity. *Asn Neuro, 2*(5), 243-256.

Cheng, A., Wan, R., Yang, J.-L., Kamimura, N., Son, T. G., Ouyang, X., et al. (2012). Involvement of PGC-1 alpha in the formation and maintenance of neuronal dendritic spines. *Nature Communications, 3*.

Chera, H., Schaecher, K. E., Rocchini, A., Imam, S. Z., Sribnick, E. A., Ray, S. K., et al. (2004). Immunofluorescent labeling of increased calpain expression and neuronal death in the spinal cord of 1-methyl-4-phenyl-1,2,3,6-tetrahydropyridine-treated mice. *Brain Research, 1006*(2), 150-156.

Chinta, S. J., Woods, G., Rane, A., Demaria, M., Campisi, J., & Andersen, J. K. (2015). Cellular senescence and the aging brain. *Experimental Gerontology, 68*, 3-7.

Chung, Y. H., Kim, E. J., Shin, C. M., Joo, K. M., Kim, M. J., Woo, H. W., et al. (2002). Age-related changes in CREB binding protein immunoreactivity in the cerebral cortex and hippocampus of rats. *Brain Research, 956*(2), 312-318.

Cohen-Cory, S., Kidane, A. H., Shirkey, N. J., & Marshak, S. (2010). Brain-Derived Neurotrophic Factor and the Development of Structural Neuronal Connectivity. *Developmental Neurobiology, 70*(5), 271-288.

Coley, W., Van Duyne, R., Carpio, L., Guendel, I., Kehn-Hall, K., Chevalier, S., et al. (2010). Absence of DICER in Monocytes and Its Regulation by HIV-1. *Journal of Biological Chemistry, 285*(42), 31930-31943.

Connor, R. I., Sheridan, K. E., Ceradini, D., Choe, S., & Landau, N. R. (1997). Change in coreceptor use correlates with disease progression in HIV-1-infected individuals. *Journal of Experimental Medicine, 185*(4), 621-628.

Das, S. R., & Jameel, S. (2005). Biology of the HIV Nef protein. *Indian Journal of Medical Research, 121*(4), 315-332.

De Rasmo, D., Signorile, A., Roca, E., & Papa, S. (2009). cAMP response element-binding protein (CREB) is imported into mitochondria and promotes protein synthesis. *FEBA Journal, 276*(16), 4325-4333.

De Stefani, D., Patron, M., & Rizzuto, R. (2015). Structure and function of the mitochondrial calcium uniporter complex. *Biochimica Et Biophysica Acta-Molecular Cell Research, 1853*(9), 2006-2011.

DeBerg, H. A., Blehm, B. H., Sheung, J., Thompson, A. R., Bookwalter, C. S., Torabi, S. F., et al. (2013). Motor Domain Phosphorylation Modulates Kinesin-1 Transport. *Journal of Biological Chemistry, 288*(45), 32612-32621.

Deeks, S. G. (2011). HIV Infection, Inflammation, Immunosenescence, and Aging. *Annual Review of Medicine, Vol 62, 2011, 62*, 141-155.

Desplats, P., Dumaop, W., Smith, D., Adame, A., Everall, I., Letendre, S., et al. (2013). Molecular and pathologic insights from latent HIV-1 infection in the human brain. *Neurology, 80*(15), 1415-1423.

Dong, J., & Xiong, H. U. (2006). Human immunodeficiency virus type 1 gp120 inhibits long-term potentiation via chemokine receptor CXCR4 in rat hippocampal slices. *Journal of Neuroscience Research, 83*(3), 489-496.

Donnelly, C., Leisenring, W., Kanki, P., Awerbuch, T., & Sandberg, S. (1993). Comparison of transmission rates of HIV-1 and HIV-2 in a cohort of prostitutes in Senegal. *Bulletin of Mathematical Biology, 55*(4), 731-743.

Dreyer, E. B., Kaiser, P. K., Offermann, J. T., & Lipton, S. A. (1990). HIV-1 coat protein neurotoxicity prevented by calcium-channel antagonists. *Science, 248*(4953), 364-367.

Eastwood, S. L., Burnet, P. W. J., McDonald, B., Clinton, J., & Harrison, P. J. (1994). Synaptophysin gene-expression in human brain - A quantitative in-situ hybridization and immunocytochemical study. *Neuroscience, 59*(4), 881-892.

Ellis, R., Langford, D., & Masliah, E. (2007). HIV and antiretroviral therapy in the brain: neuronal injury and repair. *Nature Reviews Neuroscience, 8*(1), 33-44.

Eugenin, E. A., D'Aversa, T. G., Lopez, L., Calderon, T. M., & Berman, J. W. (2003). MCP-1 (CCL2) protects human neurons and astrocytes from NMDA or HIV-tat-induced apoptosis. *Journal of Neurochemistry, 85*(5), 1299-1311.

Eugenin, E. A., King, J. E., Hazleton, J. E., Major, E. O., Bennett, M. V. L., Zukin, R. S., et al. (2011). Differences in NMDA Receptor Expression During Human Development Determine the Response of Neurons to HIV-Tat-mediated Neurotoxicity. *Neurotoxicity Research, 19*(1), 138-148.

Exner, N., Lutz, A. K., Haass, C., & Winklhofer, K. F. (2012). Mitochondrial dysfunction in Parkinson's disease: molecular mechanisms and pathophysiological consequences. *EMBO Journal, 31*(14), 3038-3062.

Fayard, B., Loeffler, S., Weis, J., Vogelin, E., & Kruttgen, A. (2005). The secreted brain-derived neurotrophic factor precursor pro-BDNF binds to TrkB and p75NTR but not to TrkA or TrkC. *Journal of Neuroscience Research, 80*(1), 18-28.

Federico, A., Cardaioli, E., Da Pozzo, P., Formichi, P., Gallus, G. N., & Radi, E. (2012). Mitochondria, oxidative stress and neurodegeneration. *Journal of the Neurological Sciences, 322*(1-2), 254-262.

Fellows, R. P., Byrd, D. A., & Morgello, S. (2014). Effects of information processing speed on learning, memory, and executive functioning in people living with HIV/AIDS. *Journal of Clinical and Experimental Neuropsychology, 36*(8), 806-817.

Fernandes, S. P., Edwards, T. M., Ng, K. T., & Robinson, S. R. (2007). HIV-1 protein gp120 rapidly impairs memory in chicks by interrupting the glutamate-glutamine cycle. *Neurobiology of Learning and Memory, 87*(1), 1-8.

Ferreira, I. L., Bajouco, L. M., Mota, S. I., Auberson, Y. P., Oliveira, C. R., & Rego, A. C. (2012). Amyloid beta peptide 1-42 disturbs intracellular calcium homeostasis through activation of GluN2B-containing N-methyl-D-aspartate receptors in cortical cultures. *Cell Calcium, 51*(2), 95-106.

Fields, J. A., Serger, E., Campos, S., Divakaruni, A. S., Kim, C., Smith, K., et al. (2016). HIV alters neuronal mitochondrial fission/fusion in the brain during HIV-associated neurocognitive disorders. *Neurobiology of Disease, 86,* 154-169.

Fischer-Smith, T., & Rappaport, J. (2005). Evolving paradigms in the pathogenesis of HIV-1-associated dementia. *Expert Reviews in Molecular Medicine, 7*(27).

Freed, E. O. (1998). HIV-1 Gag proteins: Diverse functions in the virus life cycle. *Virology, 251*(1), 1-15.

Freeman, S. H., Kandel, R., Cruz, L., Rozkalne, A., Newell, K., Frosch, M. P., et al. (2008). Preservation of Neuronal Number Despite Age-Related Cortical Brain Atrophy in Elderly Subjects Without Alzheimer Disease. *Journal of Neuropathology and Experimental Neurology, 67*(12), 1205-1212.

Frisoni, G. B., Fox, N. C., Jack, C. R., Jr., Scheltens, P., & Thompson, P. M. (2010). The clinical use of structural MRI in Alzheimer disease. *Nature Reviews Neurology, 6*(2), 67-77.

Fusco, S., Ripoli, C., Podda, M. V., Ranieri, S. C., Leone, L., Toietta, G., et al. (2012). A role for neuronal cAMP responsive-element binding (CREB)-1 in brain responses to calorie restriction. *Proceedings of the National Academy of Sciences of the United States of America, 109*(2), 621-626.

Gao, J., Wang, W.-Y., Mao, Y.-W., Graeff, J., Guan, J.-S., Pan, L., et al. (2010). A novel pathway regulates memory and plasticity via SIRT1 and miR-134. *Nature, 466*(7310), 1105-U1120.

Gao, W. H., Pu, Y. M., Luo, K. Q., & Chang, D. C. (2001). Temporal relationship between cytochrome c release and mitochondrial swelling during UV-induced apoptosis in living HeLa cells. *Journal of Cell Science, 114*(15), 2855-2862.

Gautier, C. A., Corti, O., & Brice, A. (2014). Mitochondrial dysfunctions in Parkinson's disease. *Revue Neurologique, 170*(5), 339-343.

Gelman, B. B., Chen, T., Lisinicchia, J. G., Soukup, V. M., Carmical, J. R., Starkey, J. M., et al. (2012). The National NeuroAIDS Tissue Consortium Brain Gene Array: Two Types of HIV-Associated Neurocognitive Impairment. *Plos One, 7*(9).

Ghafouri, M., Amini, S., Khalili, K., & Sawaya, B. E. (2006). HIV-1 associated dementia: symptoms and causes. *Retrovirology, 3*.

Giralt, A., Saavedra, A., Carreton, O., Arumi, H., Tyebji, S., Alberch, J., et al. (2013). PDE10 inhibition increases GluA1 and CREB phosphorylation and improves spatial and recognition memories in a Huntington's disease mouse model. *Hippocampus, 23*(8), 684-695.

Glowa, J. R., Panlilio, L. V., Brenneman, D. E., Gozes, I., Fridkin, M., & Hill, J. M. (1992). Learning impairment following intracerebral administration of the HIV envelope protein gp120 or a VIP antagonist. *Brain Research, 570*(1-2), 49-53.

Goerlach, A., Bertram, K., Hudecova, S., & Krizanova, O. (2015). Calcium and ROS: A mutual interplay. *Redox Biology, 6*, 260-271.

Gomes da Silva, M. M. (2012). Neurologic complications of HIV in the HAART era: where are we? *Brazilian Journal of Infectious Diseases, 16*(4), 373-378.

Gonzalez, G. A., & Montminy, M. R. (1989). Cyclic-AMP stimulates somatostatin gene-transcription by phosphorylation of CREB at serine-133. *Cell, 59*(4), 675-680.

Gorantla, S., Poluektova, L., & Gendelman, H. E. (2012). Rodent models for HIV-associated neurocognitive disorders. *Trends in Neurosciences, 35*(3), 197-208.

Gorry, P. R., Bristol, G., Zack, J. A., Ritola, K., Swanstrom, R., Birch, C. J., et al. (2001). Macrophage tropism of human immunodeficiency virus type 1 isolates from brain and lymphoid tissues predicts neurotropism independent of coreceptor specificity. *Journal of Virology, 75*(21), 10073-10089.

Gottlinger, H. G., Sodroski, J. G., & Haseltine, W. A. (1989). Role of capsid precursor processing and myristoylation in morphogenesis and infectivity of human immunodeficiency virus type-1. *Proceedings of the National Academy of Sciences of the United States of America, 86*(15), 5781-5785.

Grohm, J., Kim, S. W., Mamrak, U., Tobaben, S., Cassidy-Stone, A., Nunnari, J., et al. (2012). Inhibition of Drp1 provides neuroprotection in vitro and in vivo. *Cell Death and Differentiation, 19*(9), 1446-1458.

Halliwell, B. (2006). Oxidative stress and neurodegeneration: where are we now? *Journal of Neurochemistry, 97*(6), 1634-1658.

Hara, Y., Yuk, F., Puri, R., Janssen, W. G. M., Rapp, P. R., & Morrison, J. H. (2014). Presynaptic mitochondrial morphology in monkey prefrontal cortex correlates with working memory and is improved with estrogen treatment. *Proceedings of the National Academy of Sciences of the United States of America, 111*(1), 486-491.

Haughey, N. J., & Mattson, T. P. (2002). Calcium dysregulation and neuronal apoptosis by the HIV-1 proteins tat and gp120. *Jaids-Journal of Acquired Immune Deficiency Syndromes, 31*.

Hayakawa, T., Iwai, M., Aoki, S., Takimoto, K., Maruyama, M., Maruyama, W., et al. (2015). SIRT1 Suppresses the Senescence-Associated Secretory Phenotype through Epigenetic Gene Regulation. *Plos One, 10*(1).

Heaton, R. K., Franklin, D. R., Ellis, R. J., McCutchan, J. A., Letendre, S. L., LeBlanc, S., et al. (2011). HIV-associated neurocognitive disorders before and during the era of combination antiretroviral therapy: differences in rates, nature, and predictors. *Journal of Neurovirology, 17*(1), 3-16.

Heinzinger, N. K., Bukrinsky, M. I., Haggerty, S. A., Ragland, A. M., Kewalramani, V., Lee, M. A., et al. (1994). The Vpr protein of human-immunodeficiency-virus type-1 influences nuclear-localization of viral nucleic-acids in nondividing host-cells. *Proceedings of the National Academy of Sciences of the United States of America, 91*(15), 7311-7315.

Herzig, S., Long, F. X., Jhala, U. S., Hedrick, S., Quinn, R., Bauer, A., et al. (2001). CREB regulates hepatic gluconeogenesis through the coactivator PGC-1. *Nature, 413*(6852), 179-183.

Hill, J. M., Mervis, R. F., Avidor, R., Moody, T. W., & Brenneman, D. E. (1993). HIV envelope protein-induced neuronal damage and retardation of behavioral-development in rat neonates. *Brain Research, 603*(2), 222-233.

Hoke, A., Morris, M., & Haughey, N. J. (2009). GPI-1046 protects dorsal root ganglia from gp120-induced axonal injury by modulating store-operated calcium entry. *Journal of the Peripheral Nervous System, 14*(1), 27-35.

Hong, E. J., McCord, A. E., & Greenberg, M. E. (2008). A Biological Function for the Neuronal Activity-Dependent Component of Bdnf Transcription in the Development of Cortical Inhibition. *Neuron, 60*(4), 610-624.

Horch, H. W., & Katz, L. C. (2002). BDNF release from single cells elicits local dendritic growth in nearby neurons. *Nature Neuroscience, 5*(11), 1177-1184.

Hu, S., Cao, Q., Xu, P., Ji, W., Wang, G., & Zhang, Y. (2016). Rolipram stimulates angiogenesis and attenuates neuronal apoptosis through the cAMP/cAMP-responsive element binding protein pathway following ischemic stroke in rats. *Experimental and Therapeutic Medicine, 11*(3), 1005-1010.

Huang, C.-Y., Chiang, S.-F., Lin, T.-Y., Chiou, S.-H., & Chow, K.-C. (2012). HIV-1 Vpr Triggers Mitochondrial Destruction by Impairing Mfn2-Mediated ER-Mitochondria Interaction. *Plos One, 7*(3).

Indo, H. P., Davidson, M., Yen, H.-C., Suenaga, S., Tomita, K., Nishii, T., et al. (2007). Evidence of ROS generation by mitochondria in cells with impaired electron transport chain and mitochondrial DNA damage. *Mitochondrion, 7*(1-2), 106-118.

Ivannikov, M. V., Sugimori, M., & Llinas, R. R. (2013). Synaptic Vesicle Exocytosis in Hippocampal Synaptosomes Correlates Directly with Total Mitochondrial Volume. *Journal of Molecular Neuroscience, 49*(1), 223-230.

Jaeger, S., Kim, D. Y., Hultquist, J. F., Shindo, K., LaRue, R. S., Kwon, E., et al. (2012). Vif hijacks CBF-beta to degrade APOBEC3G and promote HIV-1 infection. *Nature, 481*(7381), 371-375.

Je, H. S., Yang, F., Ji, Y., Potluri, S., Fu, X.-Q., Luo, Z.-G., et al. (2013). ProBDNF and Mature BDNF as Punishment and Reward Signals for Synapse Elimination at Mouse Neuromuscular Junctions. *Journal of Neuroscience, 33*(24), 9957-9962.

Jin, H., Pei, L., Shu, X., Yang, X., Yan, T., Wu, Y., et al. (2016). Therapeutic Intervention of Learning and Memory Decays by Salidroside Stimulation of Neurogenesis in Aging. *Molecular Neurobiology, 53*(2), 851-866.

Joseph, S. B., Arrildt, K. T., Sturdevant, C. B., & Swanstrom, R. (2015). HIV-1 target cells in the CNS. *Journal of Neurovirology, 21*(3), 276-289.

Kang, H. J., & Schuman, E. M. (1996). A requirement for local protein synthesis in neurotrophin-induced hippocampal synaptic plasticity. *Science, 273*(5280), 1402-1406.

Kanki, P. J., Hopper, J. R., & Essex, M. (1987). The origins of HIV-1 and HTLV-4 HIV-2. *Annals of the New York Academy of Sciences, 511*, 370-375.

Kannangai, R., David, S., & Sridharan, G. (2012). Human immunodeficiency virus type-2-A milder, kinder virus: An update. *Indian Journal of Medical Microbiology, 30*(1), 6-15.

Kaul, M., Ma, Q., Medders, K. E., Desai, M. K., & Lipton, S. A. (2007). HIV-1 coreceptors CCR5 and CXCR4 both mediate neuronal cell death but CCR5 paradoxically can also contribute to protection. *Cell Death and Differentiation, 14*(2), 296-305.

Kawamata, H., & Manfredi, G. (2010). Mitochondrial dysfunction and intracellular calcium dysregulation in ALS. *Mechanisms of Ageing and Development, 131*(7-8), 517-526.

Kim, S. S., & Seo, S. R. (2011). The Regulator of Calcineurin 1 (RCAN1/DSCR1) Activates the cAMP Response Element-binding Protein (CREB) Pathway. *Journal of Biological Chemistry, 286*(43), 37841-37848.

Knott, A. B., Perkins, G., Schwarzenbacher, R., & Bossy-Wetzel, E. (2008). Mitochondrial fragmentation in neurodegeneration. *Nature Reviews Neuroscience, 9*(7), 505-518.

Lee, J., Kim, C. H., Simon, D. K., Aminova, L. R., Andreyev, A. Y., Kushnareva, Y. E., et al. (2005). Mitochondrial cyclic AMP response element-binding protein (CREB) mediates mitochondrial gene expression and neuronal survival. *Journal of Biological Chemistry, 280*(49), 40398-40401.

Lee, M.-H., Amin, N. D., Venkatesan, A., Wang, T., Tyagi, R., Pant, H. C., et al. (2013). Impaired neurogenesis and neurite outgrowth in an HIV-gp120 transgenic model is reversed by exercise via BDNF production and Cdk5 regulation. *Journal of Neurovirology, 19*(5), 418-431.

Levin, A., Hayouka, Z., Friedler, A., & Loyter, A. (2010). Transportin 3 and importin alpha are required for effective nuclear import of HIV-1 integrase in virus-infected cells. *Nucleus-Austin, 1*(5), 422-431.

Li, Q., Sato, E. F., Kira, Y., Nishikawa, M., Utsumi, K., & Inoue, M. (2006). A possible cooperation of SOD1 and cytochrome c in mitochondria-dependent apoptosis. *Free Radical Biology and Medicine, 40*(1), 173-181.

Li, X. J., Ren, Z. J., & Tang, J. H. (2014). MicroRNA-34a: a potential therapeutic target in human cancer. *Cell Death & Disease, 5*, E1327.

Lu, A., Frink, M., Choudhry, M. A., Hubbard, W. J., Rue, L. W., III, Bland, K. I., et al. (2007). Mitochondria play an important role in 17 beta-estradiol attenuation of H2O2-induced rat endothelial cell apoptosis. *American Journal of Physiology-Endocrinology and Metabolism, 292*(2), E585-E593.

Lu, B., Pang, P. T., & Woo, N. H. (2005). The yin and yang of neurotrophin action. *Nature Reviews Neuroscience, 6*(8), 603-614.

Lv, J., Xin, Y., Zhou, W., & Qiu, Z. (2013). The Epigenetic Switches for Neural Development and Psychiatric Disorders. *Journal of Genetics and Genomics, 40*(7), 339-346.

Malim, M. H., Hauber, J., Le, S. Y., Maizel, J. V., & Cullen, B. R. (1989). The HIV-1 rev trans-activator acts through a structured target sequence to activate nuclear export of unspliced viral messenger-RNA. *Nature, 338*(6212), 254-257.

Mallilankaraman, K., Cardenas, C., Doonan, P. J., Chandramoorthy, H. C., Irrinki, K. M., Golenar, T., et al. (2012). MCUR1 is an essential component of mitochondrial Ca2+ uptake that regulates cellular metabolism. *Nature Cell Biology, 14*(12), 1336-1343.

Mantamadiotis, T., Lemberger, T., Bleckmann, S. C., Kern, H., Kretz, O., Villalba, A. M., et al. (2002). Disruption of CREB function in brain leads to neurodegeneration. *Nature Genetics, 31*(1), 47-54.

Masotti, A., Donninelli, G., Da Sacco, L., Varano, B., Del Corno, M., & Gessani, S. (2015). HIV-1 gp120 influences the expression of microRNAs in human monocyte-derived dendritic cells via STAT3 activation. *Bmc Genomics, 16*.

Mattson, M. P., Gleichmann, M., & Cheng, A. (2008). Mitochondria in Neuroplasticity and Neurological Disorders. *Neuron, 60*(5), 748-766.

Mayr, B., & Montminy, M. (2001). Transcriptional regulation by the phosphorylation-dependent factor CREB. *Nature Reviews Molecular Cell Biology, 2*(8), 599-609.

Mefford, M. E., Gorry, P. R., Kunstman, K., Wolinsky, S. M., & Gabuzda, D. (2008). Bioinformatic prediction programs underestimate the frequency of CXCR4 usage by R5X4 HIV type 1 in brain and other tissues. *Aids Research and Human Retroviruses, 24*(9), 1215-1220.

Meyer, B. E., & Malim, M. H. (1994). The HIV-1 Rev transactivator shuttles between the nucleus and the cytoplasm. *Genes & Development, 8*(13), 1538-1547.

Miller, M. D., Warmerdam, M. T., Gaston, I., Greene, W. C., & Feinberg, M. B. (1994). The human immunodeficiency virus-1 Nef gene-product - a positive factor for viral-infection and replication in primary lymphocytes and macrophages. *Journal of Experimental Medicine, 179*(1), 101-113.

Mizuno, M., Yamada, K., Takei, N., Tran, M. H., He, J., Nakajima, A., et al. (2003). Phosphatidylinositol 3-kinase: a molecule mediating BDNF-dependent spatial memory formation. *Molecular Psychiatry, 8*(2), 217-224.

Mocchetti, I., Bachis, A., & Avdoshina, V. (2012). Neurotoxicity of Human Immunodeficiency Virus-1: Viral Proteins and Axonal Transport. *Neurotoxicity Research, 21*(1), 79-89.

Mocchetti, I., Nosheny, R. L., Tanda, G., Ren, K., & Meyer, E. M. (2007). Brain-derived neurotrophic factor prevents human immunodeficiency virus type 1 protein gp120 neurotoxicity in the rat nigrostriatal system. *Neuroprotective Agents: Eighth International Neuroprotection Society Meeting, 1122*, 144-154.

Morris, K. A., & Gold, P. E. (2012). Age-related impairments in memory and in CREB and pCREB expression in hippocampus and amygdala following inhibitory avoidance training. *Mechanisms of Ageing and Development, 133*(5), 291-299.

Moses, A. V., & Nelson, J. A. (1994). HIV-infection of human brain capillary endothelial-cells - implications for AIDS dementia. *Advances in Neuroimmunology, 4*(3), 239-247.

Mukerjee, R., Chang, J. R., Del Valle, L., Bagashev, A., Gayed, M. M., Lyde, R. B., et al. (2011). Deregulation of microRNAs by HIV-1 Vpr Protein Leads to the

Development of Neurocognitive Disorders. *Journal of Biological Chemistry, 286*(40), 34976-34985.

Mukerjee, R., Deshmane, S. L., Fan, S., Del Valle, L., White, M. K., Khalili, K., et al. (2008). Involvement of the p53 and p73 transcription factors in neuroAIDS. *Cell Cycle, 7*(17), 2682-2690.

Nagahara, A. H., & Tuszynski, M. H. (2011). Potential therapeutic uses of BDNF in neurological and psychiatric disorders. *Nature Reviews Drug Discovery, 10*(3), 209-219.

Nasi, M., Pinti, M., De Biasi, S., Gibellini, L., Ferraro, D., Mussini, C., et al. (2014). Aging with HIV infection: A journey to the center of inflammAIDS, immunosenescence and neuroHIV. *Immunology Letters, 162*(1), 329-333.

Nath, A., Padua, R. A., & Geiger, J. D. (1995). HIV-1 coat protein gp120-induced increases in levels of intrasynaptosomal calcium. *Brain Research, 678*(1-2), 200-206.

Navarro, A., & Boveris, A. (2007). The mitochondrial energy transduction system and the aging process. *American Journal of Physiology-Cell Physiology, 292*(2), C670-C686.

Nguyen, D., Alavi, M. V., Kim, K. Y., Kang, T., Scott, R. T., Noh, Y. H., et al. (2011). A new vicious cycle involving glutamate excitotoxicity, oxidative stress and mitochondrial dynamics. *Cell Death & Disease, 2*,e240.

Noorbakhsh, F., Ramachandran, R., Barsby, N., Ellestad, K. K., LeBlanc, A., Dickie, P., et al. (2010). MicroRNA profiling reveals new aspects of HIV neurodegeneration: caspase-6 regulates astrocyte survival. *Faseb Journal, 24*(6), 1799-1812.

Nosheny, R. L., Ahmed, F., Yakovlev, A., Meyer, E. M., Ren, K., Tessarollo, L., et al. (2007). Brain-derived neurotrophic factor prevents the nigrostriatal degeneration induced by human immunodeficiency virus-1 glycoprotein 120 in vivo. *European Journal of Neuroscience, 25*(8), 2275-2284.

Nosheny, R. L., Bachis, A., Acquas, E., & Mocchetti, I. (2004). Human immunodeficiency virus type 1 glycoprotein gp120 reduces the levels of brain-derived neurotrophic factor in vivo: potential implication for neuronal cell death. *European Journal of Neuroscience, 20*(11), 2857-2864.

Ohagen, A., Devitt, A., Kunstman, K. J., Gorry, P. R., Rose, P. P., Korber, B., et al. (2003). Genetic and functional analysis of full-length human immunodeficiency virus type 1 env genes derived from brain and blood of patients with AIDS. *Journal of Virology, 77*(22), 12336-12345.

Opella, S. J., Park, S. H., Lee, S., Jones, D., Nevzorov, A., Mesleh, M., et al. (2005). Structure and function of Vpu from HIV-1. *Viral Membrane Proteins: Structure, Function, and Drug Design, 1*, 147-163.

Otera, H., Wang, C., Cleland, M. M., Setoguchi, K., Yokota, S., Youle, R. J., et al. (2010). Mff is an essential factor for mitochondrial recruitment of Drp1 during mitochondrial fission in mammalian cells. *Journal of Cell Biology, 191*(6), 1141-1158.

Ou, L.-C., & Gean, P.-W. (2007). Transcriptional regulation of brain-derived neurotrophic factor in the amygdala during consolidation of fear memory. *Molecular Pharmacology, 72*(2), 350-358.

Ou, X., Lee, M. R., Huang, X., Messina-Graham, S., & Broxmeyer, H. E. (2014). SIRT1 Positively Regulates Autophagy and Mitochondria Function in Embryonic Stem Cells Under Oxidative Stress. *Stem Cells, 32*(5), 1183-1194.

Peterson, C. M., Johannsen, D. L., & Ravussin, E. (2012). Skeletal muscle mitochondria and aging: a review. *Journal of aging research, 2012*, 194821-194821.

Pfister, K. K., Salata, M. W., Dillman, J. F., Vaughan, K. T., Vallee, R. B., Torre, E., et al. (1996). Differential expression and phosphorylation of the 74-kDa intermediate chains of cytoplasmic dynein in cultured neurons and glia. *Journal of Biological Chemistry, 271*(3), 1687-1694.

Phillips, H. S., Hains, J. M., Armanini, M., Laramee, G. R., Johnson, S. A., & Winslow, J. W. (1991). BDNF MESSENGER-RNA IS DECREASED IN THE HIPPOCAMPUS OF INDIVIDUALS WITH ALZHEIMERS-DISEASE. *Neuron, 7*(5), 695-702

Pigazzi, M., Manara, E., Bresolin, S., Tregnago, C., Beghin, A., Baron, E., et al. (2013). MicroRNA-34b promoter hypermethylation induces CREB overexpression and contributes to myeloid transformation. *Haematologica, 98*(4), 602-610.

Potter, M. C., Figuera-Losada, M., Rojas, C., & Slusher, B. S. (2013). Targeting the Glutamatergic System for the Treatment of HIV-Associated Neurocognitive Disorders. *Journal of Neuroimmune Pharmacology, 8*(3), 594-607.

Price, T. O., Ercal, N., Nakaoke, R., & Banks, W. A. (2005). HIV-1 viral proteins gp120 and Tat induce oxidative stress in brain endothelial cells. *Brain Research, 1045*(1-2), 57-63.

Pugazhenthi, S., Wang, M., Pham, S., Sze, C.-I., & Eckman, C. B. (2011). Downregulation of CREB expression in Alzheimer's brain and in A beta-treated rat hippocampal neurons. *Molecular Neurodegeneration, 6(60).*

Qiu, J., Tan, Y.-W., Hagenston, A. M., Martel, M.-A., Kneisel, N., Skehel, P. A., et al. (2013). Mitochondrial calcium uniporter Mcu controls excitotoxicity and is transcriptionally repressed by neuroprotective nuclear calcium signals. *Nature Communications, 4(2034).*

Quintanilla, R. A., & Johnson, G. V. W. (2009). Role of mitochondrial dysfunction in the pathogenesis of Huntington's disease. *Brain Research Bulletin, 80*(4-5), 242-247.

Rambaut, A., Posada, D., Crandall, K. A., & Holmes, E. C. (2004). The causes and consequences of HIV evolution. *Nature Reviews Genetics, 5*(1), 52-61.

Roggero, R., Robert-Hebmann, V., Harrington, S., Roland, J., Vergne, L., Jaleco, S., et al. (2001). Binding of human immunodeficiency virus type 1 gp120 to CXCR4 induces mitochondrial transmembrane depolarization and cytochrome c-mediated apoptosis independently of Fas signaling. *Journal of Virology, 75*(16), 7637-7650.

Rosas, H. D., Salat, D. H., Lee, S. Y., Zaleta, A. K., Pappu, V., Fischl, B., et al. (2008). Cerebral cortex and the clinical expression of Huntington's disease: complexity and heterogeneity. *Brain, 131*, 1057-1068.

Rouaux, C., Panteleeva, I., Rene, F., de Aguilar, J.-L. G., Echaniz-Laguna, A., Dupuis, L., et al. (2007). Sodium valproate exerts neuroprotective effects in vivo through CREB-binding protein-dependent mechanisms but does not improve survival in an amyotrophic lateral sclerosis mouse model. *Journal of Neuroscience, 27*(21), 5535-5545.

Saha, R. N., & Pahan, K. (2007). Differential regulation of Mn-superoxide dismutase in neurons and astroglia by HIV-1 gp120: Implications for HIV-associated dementia. *Free Radical Biology and Medicine, 42*(12), 1866-1878.

Samikkannu, T., Ranjith, D., Rao, K. V. K., Atluri, V. S. R., Pimentel, E., El-Hage, N., et al. (2015). HIV-1 gp120 and morphine induced oxidative stress: role in cell cycle regulation. *Frontiers in Microbiology, 6(614).*

Santo-Domingo, J., & Demaurex, N. (2010). Calcium uptake mechanisms of mitochondria. *Biochimica Et Biophysica Acta-Bioenergetics, 1797*(6-7), 907-912.

Sanz, A., Caro, P., Gomez, J., & Barja, G. (2006). Testing the vicious cycle theory of mitochondrial ROS production: effects of H2O2 and cumene hydroperoxide treatment on heart mitochondria. *Journal of Bioenergetics and Biomembranes, 38*(2), 121-127.

Saura, C. A., & Valero, J. (2011). The role of CREB signaling in Alzheimer's disease and other cognitive disorders. *Reviews in the Neurosciences, 22*(2), 153-169.

Schwarz, T. L. (2013). Mitochondrial Trafficking in Neurons. *Cold Spring Harbor Perspectives in Biology, 5*(6).

Segura, B., Cesar Baggio, H., Josep Marti, M., Valldeoriola, F., Compta, Y., Isabel Garcia-Diaz, A., et al. (2014). Cortical Thinning Associated With Mild Cognitive Impairment in Parkinson's Disease. *Movement Disorders, 29*(12), 1495-1503.

Sheng, B., Wang, X., Su, B., Lee, H.-g., Casadesus, G., Perry, G., et al. (2012). Impaired mitochondrial biogenesis contributes to mitochondrial dysfunction in Alzheimer's disease. *Journal of Neurochemistry, 120*(3), 419-429.

Shi, P., Gal, J., Kwinter, D. M., Liu, X., & Zhu, H. (2010). Mitochondrial dysfunction in amyotrophic lateral sclerosis. *Biochimica Et Biophysica Acta-Molecular Basis of Disease, 1802*(1), 45-51.

Siliciano, J. D., & Siliciano, R. F. (2010). Biomarkers of HIV replication. *Current Opinion in Hiv and Aids, 5*(6), 491-497.

Silva, A. J., Kogan, J. H., Frankland, P. W., & Kida, S. (1998). CREB and memory. *Annual Review of Neuroscience, 21*, 127-148.

Smalheiser, N. R., Lugli, G., Zhang, H., Rizavi, H., Cook, E. H., & Dwivedi, Y. (2014). Expression of microRNAs and Other Small RNAs in Prefrontal Cortex in Schizophrenia, Bipolar Disorder and Depressed Subjects. *Plos One*, *9*(1).

Sohal, R. S., & Forster, M. J. (2014). Caloric restriction and the aging process: a critique. *Free Radical Biology and Medicine, 73*, 366-382.

Stojkovic, M., Machado, S. A., Stojkovic, P., Zakhartchenko, V., Hutzler, P., Goncalves, P. B., et al. (2001). Mitochondrial distribution and adenosine triphosphate content of bovine oocytes before and after in vitro maturation: Correlation with morphological criteria and developmental capacity after in vitro fertilization and culture. *Biology of Reproduction, 64*(3), 904-909.

Stokin, G. B., Lillo, C., Falzone, T. L., Brusch, R. G., Rockenstein, E., Mount, S. L., et al. (2005). Axonopathy and transport deficits early in the pathogenesis of Alzheimer's disease. *Science, 307*(5713), 1282-1288.

Strazza, M., Pirrone, V., Wigdahl, B., & Nonnemacher, M. R. (2011). Breaking down the barrier: The effects of HIV-1 on the blood-brain barrier. *Brain Research, 1399*, 96-115.

Sturdevant, C. B., Joseph, S. B., Schnell, G., Price, R. W., Swanstrom, R., & Spudich, S. (2015). Compartmentalized Replication of R5 T Cell-Tropic HIV-1 in the Central Nervous System Early in the Course of Infection. *Plos Pathogens*, *11*(3).

Suedhof, T. C. (2012). Calcium Control of Neurotransmitter Release. *Cold Spring Harbor Perspectives in Biology, 4*(1).

Tanaka, G., Nakase, I., Fukuda, Y., Masuda, R., Oishi, S., Shimura, K., et al. (2012). CXCR4 Stimulates Macropinocytosis: Implications for Cellular Uptake of Arginine-Rich Cell-Penetrating Peptides and HIV. *Chemistry & Biology, 19*(11), 1437-1446.

Tao, X., Finkbeiner, S., Arnold, D. B., Shaywitz, A. J., & Greenberg, M. E. (1998). Ca2+ influx regulates BDNF transcription by a CREB family transcription factor-dependent mechanism. *Neuron, 20*(4), 709-726.

Taube, R., Fujinaga, K., Wimmer, J., Barboric, M., & Peterlin, B. M. (1999). Tat transactivation: A model for the regulation of eukaryotic transcriptional elongation. *Virology, 264*(2), 245-253.

Thayer, D. A., Jan, Y. N., & Jan, L. Y. (2013). Increased neuronal activity fragments the Golgi complex. *Proceedings of the National Academy of Sciences of the United States of America, 110*(4), 1482-1487.

Thomas, S., Mayer, L., & Sperber, K. (2009). Mitochondria Influence Fas Expression in GP120-Induced Apoptosis of Neuronal Cells. *International Journal of Neuroscience, 119*(2), 157-165.

Thompson, P. M., Dutton, R. A., Hayashi, K. M., Toga, A. W., Lopez, O. L., Aizenstein, H. J., et al. (2005). Thinning of the cerebral cortex visualized in HIV/AIDS reflects CD4(+) T lymphocyte decline. *Proceedings of the National Academy of Sciences of the United States of America, 102*(43), 15647-15652.

Toggas, S. M., Masliah, E., Rockenstein, E. M., Rall, G. F., Abraham, C. R., & Mucke, L. (1994). Central-nervous-system damage produced by expression of the HIV-1 coat protein gp120 in transgenic mice. *Nature, 367*(6459), 188-193.

Tomar, D., Dong, Z., Shanmughapriya, S., Koch, D. A., Thomas, T., Hoffman, N. E., et al. (2016). MCUR1 Is a Scaffold Factor for the MCU Complex Function and Promotes Mitochondrial Bioenergetics. *Cell reports, 15*(8), 1673-1685.

Triboulet, R., Mari, B., Lin, Y.-L., Chable-Bessia, C., Bennasser, Y., Lebrigand, K., et al. (2007). Suppression of microRNA-silencing pathway by HIV-1 during virus replication. *Science, 315*(5818), 1579-1582.

Trofimiuk, E., Holownia, A., & Braszko, J. J. (2010). Activation of CREB by St. John's Wort May Diminish Deletorious Effects of Aging on Spatial Memory. *Archives of Pharmacal Research, 33*(3), 469-477.

Valcour, V., Sithinamsuwan, P., Letendre, S., & Ances, B. (2011). Pathogenesis of HIV in the central nervous system. *Current HIV/AIDS reports, 8*(1), 54-61.

Villeda, S. A., Plambeck, K. E., Middeldorp, J., Castellano, J. M., Mosher, K. I., Luo, J., et al. (2014). Young blood reverses age-related impairments in cognitive function and synaptic plasticity in mice. *Nature Medicine, 20*(6), 659-663.

Viviani, B., Gardoni, F., Bartesaghi, S., Corsini, E., Facchi, A., Galli, C. L., et al. (2006). Interleukin-1 beta released by gp120 drives neural death through tyrosine phosphorylation and trafficking of NMDA receptors. *Journal of Biological Chemistry, 281*(40), 30212-30222.

Vos, M., Lauwers, E., & Verstreken, P. (2010). Synaptic mitochondria in synaptic transmission and organization of vesicle pools in health and disease. *Frontiers in synaptic neuroscience, 2*, 139-139.

Wang, J.X., Jiao, J.Q., Li, Q., Long, B., Wang, K., Liu, J.P., et al. (2011). miR-499 regulates mitochondrial dynamics by targeting calcineurin and dynamin-related protein-1. *Nature Medicine, 17*(1), 71-78.

Wang, X., Su, B., Lee, H.-g., Li, X., Perry, G., Smith, M. A., et al. (2009). Impaired Balance of Mitochondrial Fission and Fusion in Alzheimer's Disease. *Journal of Neuroscience, 29*(28), 9090-9103.

Wang, Z. Y., Pekarskaya, O., Bencheikh, M., Chao, W., Gelbard, H. A., Ghorpade, A., et al. (2003). Reduced expression of glutamate transporter EAAT2 and impaired glutamate transport in human primary astrocytes exposed to HIV-1 or gp120. *Virology, 312*(1), 60-73.

Warmus, B. A., Sekar, D. R., McCutchen, E., Schellenberg, G. D., Roberts, R. C., McMahon, L. L., et al. (2014). Tau-Mediated NMDA Receptor Impairment Underlies Dysfunction of a Selectively Vulnerable Network in a Mouse Model of Frontotemporal Dementia. *Journal of Neuroscience, 34*(49), 16482-16495.

Weissman, D., Rabin, R. L., Arthos, J., Rubbert, A., Dybul, M., Swofford, R., et al. (1997). Macrophage-tropic HIV and SIV envelope proteins induce a signal through the CCR5 chemokine receptor. *Nature, 389*(6654), 981-985.

Whitney, J. B., Hill, A. L., Sanisetty, S., Penaloza-MacMaster, P., Liu, J., Shetty, M., et al. (2014). Rapid seeding of the viral reservoir prior to SIV viraemia in rhesus monkeys. *Nature, 512*(7512), 74-77.

Wilen, C. B., Tilton, J. C., & Doms, R. W. (2012). HIV: Cell Binding and Entry. *Cold Spring Harbor Perspectives in Medicine, 2*(8).

Williams, D. W., Calderon, T. M., Lopez, L., Carvallo-Torres, L., Gaskill, P. J., Eugenin, E. A., et al. (2013). Mechanisms of HIV Entry into the CNS: Increased Sensitivity of HIV Infected CD14(+)CD16(+) Monocytes to CCL2 and Key Roles of CCR2, JAM-A, and ALCAM in Diapedesis. *Plos One, 8*(7).

Wolinsky, S. M., Korber, B. T. M., Neumann, A. U., Daniels, M., Kunstman, K. J., Whetsell, A. J., et al. (1996). Adaptive evolution of human immunodeficiency virus-type 1 during the natural course of infection. *Science, 272*(5261), 537-542.

Woods, S. P., Moore, D. J., Weber, E., & Grant, I. (2009). Cognitive Neuropsychology of HIV-Associated Neurocognitive Disorders. *Neuropsychology Review, 19*(2), 152-168.

Wu, Z. D., Puigserver, P., Andersson, U., Zhang, C. Y., Adelmant, G., Mootha, V., et al. (1999). Mechanisms controlling mitochondrial biogenesis and respiration through the thermogenic coactivator PGC-1. *Cell, 98*(1), 115-124.

Wyatt, R., Kwong, P. D., Desjardins, E., Sweet, R. W., Robinson, J., Hendrickson, W. A., et al. (1998). The antigenic structure of the HIV gp120 envelope glycoprotein. *Nature, 393*(6686), 705-711.

Xiang, S.-H., Finzi, A., Pacheco, B., Alexander, K., Yuan, W., Rizzuto, C., et al. (2010). A V3 Loop-Dependent gp120 Element Disrupted by CD4 Binding Stabilizes the Human Immunodeficiency Virus Envelope Glycoprotein Trimer. *Journal of Virology, 84*(7), 3147-3161.

Xu, H., Bae, M., Tovar-y-Romo, L. B., Patel, N., Bandaru, V. V. R., Pomerantz, D., et al. (2011). The Human Immunodeficiency Virus Coat Protein gp120 Promotes Forward Trafficking and Surface Clustering of NMDA Receptors in Membrane Microdomains. *Journal of Neuroscience, 31*(47), 17074-17090.

Yin, J. C. P., & Tully, T. (1996). CREB and the formation of long-term memory. *Current Opinion in Neurobiology, 6*(2), 264-268.

Youle, R. J., & van der Bliek, A. M. (2012). Mitochondrial Fission, Fusion, and Stress. *Science, 337*(6098), 1062-1065.

Yuan, Y., Yokoyama, M., Maeda, Y., Terasawa, H., Harada, S., Sato, H., et al. (2013). Structure and Dynamics of the gp120 V3 Loop That Confers Noncompetitive Resistance in R5 HIV-1(JR-FL) to Maraviroc. *Plos One, 8*(6).

Zauli, G., Milani, D., Mirandola, P., Mazzoni, M., Secchiero, P., Miscia, S., et al. (2001). HIV-1 Tat protein down-regulates CREB transcription factor expression in PC12 neuronal cells through a phosphatidylinositol 3-kinase/AKT/cyclic nucleoside phosphodiesterase pathway. *Faseb Journal, 15*(2), 483-491.

Zhang, Y., Shi, Y., Qiao, L., Sun, Y., Ding, W., Zhang, H., et al. (2012). Sigma-1 receptor agonists provide neuroprotection against gp120 via a change in bcl-2 expression in mouse neuronal cultures. *Brain Research, 1431,* 13-22.

Zhang, Y., Wang, M., Li, H., Zhang, H., Shi, Y., Wei, F., et al. (2012). Accumulation of nuclear and mitochondrial DNA damage in the frontal cortex cells of patients with HIV-associated neurocognitive disorders. *Brain Research, 1458*, 1-11.

Zheng, F., Zhou, X., Moon, C., & Wang, H. (2012). Regulation of brain-derived neurotrophic factor expression in neurons. *International journal of physiology, pathophysiology and pharmacology*, *4*(4), 188-200.

Zhong, Y., Zhu, Y., He, T., Li, W., Yan, H., & Miao, Y. (2016). Rolipram-induced improvement of cognitive function correlates with changes in hippocampal CREB phosphorylation, BDNF and Arc protein levels. *Neuroscience Letters, 610*, 171-176.

Zhou, Z., Hong, E. J., Cohen, S., Zhao, W.N., Ho, H.Y., Schmidt, L., et al. (2006). Brain-specific phosphorylation of MeCP2 regulates activity-dependent Bdnf transcription, dendritic growth, and spine maturation. *Neuron, 52*(2), 255-269.

Zocchi, L., & Sassone-Corsi, P. (2012). SIRT1-mediated deacetylation of MeCP2 contributes to BDNF expression. *Epigenetics, 7*(7), 695-700.